Russian Chemical Reviews **69** (3) 231 – 260 (2000) © 2000 Russian Academy of Sciences and Turpion Ltd

DOI 10.1070/RC2000v069n03ABEH000549

Heterophase mechanisms of thermal oxidation of polymers. New horizons

Yu A Mikheev, G E Zaikov

Contents

I.	Introduction	231
II.	The influence of the thermomechanical state of a polymer on the oxidation kinetics	232
III.	The microreactor model and kinetic regimes of oxidation	235
IV.	Kinetic model of oxidation of polyolefins	236
V.	Oxidation of molten polystyrene	243
VI.	Oxidation of molten poly(ethylene oxide)	245
VII.	Characteristic features of initiated oxidation of polymers	248
VIII.	The model of oxidation of thermofluctuationally active objects	253
IX.	Cross-linking of polyolefin macromolecules	257
X.	Oxidation of fibrillised polyolefins	258
XI.	Conclusion	259

Abstract. Based on the results of kinetic analysis of numerous experimental data, advantages of heterogeneous and heterophase mechanisms of autooxidation of non-crystalline polymers over homogeneous liquid-phase mechanisms are demonstrated. The supermolecular organisation of polymer chains according to the pattern of spongy micelles incorporating non-uniform porous areas is chosen as the model structure. It is established that, depending on the physical state of the polymer, the oxidation kinetics correspond either to a mechanism in which reaction chains are distributed over non-uniform nanophases or to a mechanism in which they are mainly located in one nanophase. The kinetic equations obtained for the macroscopic stages of oxidation take into account the dependence of the chemical reactivity of reactants on the thermomechanical mobility of the molecular sponge. It is demonstrated that the fine structure of molecular spongy micelles plays a crucial role in the chemical physics of polymers. The bibliography includes 94 references.

I. Introduction

Oxidation of block polymers is often considered within the framework of homogeneous oxidation schemes designed for liquid hydrocarbons.[1–13] This is formally based on the view, accepted long ago, that a non-crystalline polymer is an amorphous homogeneous material. The evident physical difference between polymeric and liquid phases is attributed in its simplified form to the functioning of unstable structures continuously formed and degraded and having rather long lifetimes and low rates of the relaxation response to an external action.

Meanwhile, the kinetics of polymer oxidation usually do not fit in the framework of homogeneous reactions. In fact, when analysing the mechanisms of several macroscopic stages (for example, induction period[5] and self-accelerated stage[4–6,8–15]) in terms of homogeneous schemes, researchers were forced either to change the essence of these schemes or to use mathematical simplifications.[1–17] The results were often at variance with experimental data.

The contradictions caused by the use of the homogeneous reaction model could not fail to cast doubt[16] upon the validity of the mechanisms of inhibited oxidation and 'critical' concentrations of antioxidants discussed in the literature.[4,6–8] Nevertheless, the generally accepted view of the liquid-phase homogeneous structure of a non-crystalline polymeric matrix delayed for a long period the development of an adequate oxidation mechanism, even after the dependence of the reaction rate on the thermomechanical state of the polymeric matrix had been established.[4–6,18–26] Instead of diverging from the old-fashioned homogeneous model, the researchers spent effort on the improvement of this model. This was done by invoking ideas of polychromatism of kinetic parameters[5–7] and by assuming the presence of so-called 'disordered areas'[4,5] and 'rigid cages'[8] in the matrix being oxidised.

The kinetic 'polychromatism' assumes that reactions which are elementary in homogeneous media cannot be characterised by a single rate constant when they occur in polymers. It is postulated that the reactivity of particles depends on their closest environment. However, the physical grounds for this dependence usually remain unknown.

The ideas of the molecular-segment 'disordered areas' and 'rigid cages' make the views on a polymer process somewhat more detailed. It cannot be ruled out that the schemes based on each concept would describe different particular situations. They are unable to serve as the common ground for the simulation of reactions in a non-crystalline polymeric matrix because they assume *a priori* that the 'areas' and 'cages' arise in an essentially homogeneous medium.

The same is true for the known theoretical approach resorting to the model of propagation of infectious diseases.[14] This approach is based on the statements that oxidation of a partially crystalline polymer develops through multiplication of 'pest-holes', which successively involves amorphous regions dispersed inside the crystalline phase, and that the 'infection' is transmitted by monomeric oxidation products acting as initiators.

Yu A Mikheev, G E Zaikov N M Emanuel Institute of Biochemical Physics, Russian Academy of Sciences, ul. Kosygina 4, 117977 Moscow, Russian Federation. Fax (7-095) 137 41 01. Tel. (7-095) 939 73 62 (Yu A Mikheev). E-mail: chembio@glas.apc.org (G E Zaikov)

Received 2 August 1999
Uspekhi Khimii **69** (3) 249 – 282 (2000); translated by Z P Bobkova

Since the above approaches are modifications of the same homogeneous reaction model, none of them discloses the physical reasons for, for example, the fact that oxidation of polymer samples in different physical states often follows the same kinetics. Thus the temperature dependence of the rate constant of non-inhibited oxidation of low-density polyethylene (LDPE) in the induction period is described by an Arrhenius equation in the temperature range of 40–200 °C; this implies the absence of changes in the oxidation mechanism on passing from the solid state to the molten state ($T_m \sim 115$ °C).[27]

The inapplicability of homogeneous schemes (both the classical and modified ones) to the description of the oxidation of polymers is also indicated by the fact that the same polymer often behaves (in the reaction) in different ways depending on the method used to prepare the sample. In addition, the macroscopic stages of polymer oxidation are described by kinetic laws different in kind.

The reasons for these specific kinetic features are hidden in the supermolecular organisation of polymer chains in spongy micelles incorporating non-homogeneous porous areas, *i.e.* in the real heterogeneity of the 'amorphous' polymer phase.[15, 16, 28, 29] The molecular-chain sponge is actually a system of connected pendula (oscillators), the oscillations of which can become cooperated; this makes the units of macromolecules move apart to form nanopores with different widths.

It was emphasised in a series of studies[15, 16, 18–22] that the initiating activity of admixed initiators and polymeric hydroperoxides and the routes of transformation of free radicals depend on which particular site in the nanoporous structural zone of the molecular spongy matrix contains the reactants. Due to the high degree of heterogeneity and the high elasticity with respect to mechanical treatment, typical of this matrix, stretching of polymer chains and the amplitudes of beating of nanopores of each size can vary over wide limits.

Therefore, the kinetics of oxidation of samples existing in different thermomechanical states, depending on the preparation method, can be different in kind, although the chemical structure of the polymeric molecules remains the same.

II. The influence of the thermomechanical state of a polymer on the oxidation kinetics

1. Characteristic features of the process under structural relaxation conditions

The thermomechanical state of a polymer subjected to oxidation largely depends on the character of thermal and mechanical treatment of the polymer sample prior to the reaction. Oxidation of polymer samples can be described by qualitatively different kinetics depending on the previous history of the samples.

This refers, for example, to samples of isotactic polypropylene (IPP), studied by Pudov *et al.*[1, 2, 30] and Monakhova *et al.*[24, 31]

The data on accumulation of polymeric hydroperoxide (POOH) in IPP samples obtained by Pudov *et al.*[1, 2, 30] (Fig. 1) differ from the results of Monakhova *et al.*[24, 31] (Fig. 2) by a longer period of accumulation and a lower rate of decomposition of POOH.

The plots for the oxygen absorption rate *vs.* the concentration of accumulated POOH also follow different patterns in these two cases. Pudov *et al.*[1, 2, 30] attribute this plot to one macroscopic stage and describe it as a sum of two terms close in magnitude

$$v = a\,[\mathrm{POOH}]^{0.5} + b\,[\mathrm{POOH}],$$

where a and b are constants. On the contrary, the curves shown in Fig. 2[24, 31] actually represent three macroscopic stages of oxidation, characterised by different types of variation of v *vs.* [POOH]. In fact, successive transitions from a more or less extensive induction period to a short self-accelerated process and then to a stage with a virtually constant rate of oxygen absorption can be distinguished in curves *3* and *4*. At the third stage of oxidation, the concentration of POOH first increases and then starts to decrease.

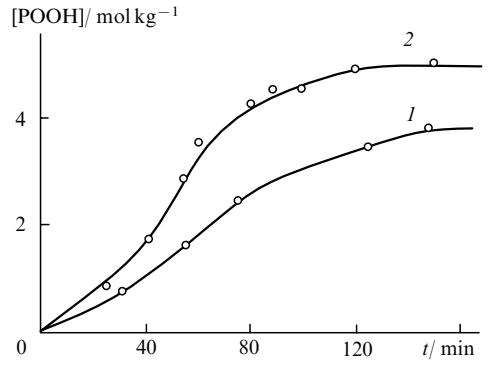


Figure 1. Variation in the concentration of hydroperoxide in films pressed from non-melted IPP powder during oxidation at 130 °C and oxygen pressures of 26.7 (*1*) and 53.3 kPa (*2*).[1, 2, 30]

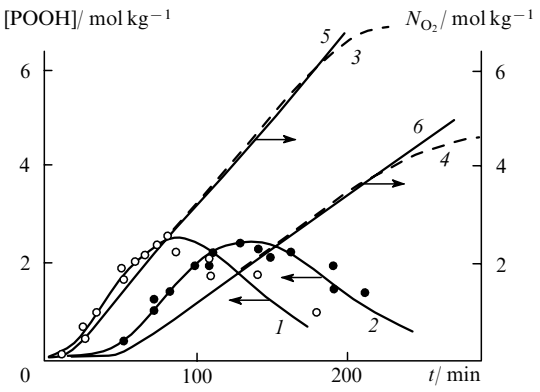


Figure 2. Calculated curves for hydroperoxide accumulation (*1*, *2*) and experimental (*3*, *4*) and calculated (*5*, *6*) curves for the oxygen absorption during oxidation at 130 °C and P_{O_2} = 40 kPa of IPP films prepared from the melt and containing small (*1*, *3*, *5*) and large (*2*, *4*, *6*) spherulites.[24, 31] The dots correspond to experimental concentrations of POOH.

These kinetic differences are apparently due to nonequivalent methods used to prepare the samples in question. In one study[30] films were prepared by short-term (2–3 min) pressing of the IPP powder at 125–130 °C without bringing the crystals to melting, while in the other studies[24, 31] the initial IPP was first melted at 220 °C and then the melt was cooled to give films with small spherulites. On additional heating, large spherulites were formed but the degree of crystallinity did not change.

It is obvious that pressed films employed by Pudov *et al.*[1, 2, 30] were characterised by enhanced internal mechanical stress, caused by deformation of the framework of non-melted crystallites and by biaxial orientational stretching of polymer chains which fill the space between the crystallites. Comparison of curves *1*, *2* in Fig. 1 with the corresponding curves in Fig. 2 leads to the conclusion that in the concentration range of 0–0.2 mol kg^{-1}, accumulation of POOH in the films prepared by pressing occurs at almost the same rate as in the films with small spherulites. However, the yield of POOH in the subsequent oxidation stages is much higher in the former type of films. This indicates that the reaction rate increases in samples with internal stresses. Apparently, at a certain stage of the process, efficient stress relaxation occurs in 'stressed' films, which is accompanied by the appearance of local centres of thixotropic excitation of the matrix.[32] In these centres, the frequency and amplitude of beats of macromolecular units increase; this changes the dimensions of nanopores and, consequently, increases the rate of generation of free radicals.[15–22, 33, 34]

The IPP films prepared by cooling a melt[24, 31] differed from those made of a pressed conglomerate of non-melted particles by the presence of a much more equilibrated (as regards the thermomechanical state) framework of crystallites. The residual internal

stress in the crystallites is much lower. They are distributed more uniformly in the material and do not bring about any thermomechanical excitation of the matrix or substantial shear deformations during oxidation.

The increase in the induction period associated with enlargement of spherulites due to recrystallisation (see Fig. 2, curve *2*) can be explained by assuming that some of the units of macromolecules are incorporated into crystallites and thus induce orientational drawing of the polymer chains in the intercrystallite regions. The stretched polymer chains are fixed rather firmly on the crystallite framework; this accounts for the extension of the induction period.

A similar effect is involved in the oxidation of highly crystalline films of IPP, high-density polyethylene (HDPE) and polymethylpentene subjected to uniaxial orientational drawing. The greater the degree of drawing, the greater the increase in the induction period of oxidation.[5, 35]

The rate of oxidation of LDPE is affected by orientational drawing in a different way. The low degree of crystallinity of this polymer does not ensure sufficient resistance to the internal stress and the fast relaxation increases the oxidation rate from the very beginning of the process.[35]

Thus, despite the identical treatment of the polyolefin films (orientational drawing), the rates of the initial stage of their oxidation differ depending on the strength of the supermolecular framework.

Yet another specific feature of oxidation of uniaxially stretched IPP films is that the molecular mass of the polymer increases substantially at the initial oxidation stages, whereas in the case of isotropic films, fast destruction of macromolecules is observed.[5] Calculations have shown[35] that the influence of drawing is due to the change in the physical structure of the IPP matrix subjected to oxidation rather than to the change in the solubility and the oxygen diffusion coefficient.

It should be noted that the draw ratio also influences the parameters of the self-accelerated stage of oxidation. This stage becomes longer for high draw ratios;[5, 26, 35] in some cases, the rate of oxygen absorption increases according to the law $\upsilon \sim \exp(\Phi t)$ rather than in proportion with time.[26]

The state of the spongy molecular matrix can change due to different types of treatment and thus influence the oxidation kinetics. Thus, it has been reported[20] that previous heat treatment of a non-stabilised commercial sample of IPP *in vacuo* decreases the rate of its high-temperature oxidation by increasing the induction period; however, the rate of low-temperature (20 °C) oxidation substantially increases (possibly, due to the structural relaxation under the influence of absorbed moisture[29]).

Simultaneously, a new specific feature appears which cannot be interpreted within the framework of the homogeneous reaction model, namely, different induction periods are observed for identical contents of POOH in the polymer and, conversely, identical induction periods correspond to hydroperoxide concentrations that differ by an order of magnitude.[20]

Note that these regularities (observed in the kinetic regime of oxygen absorption) reflect a general feature of heterogeneous micro- and nanoporous materials associated with the lability of their physical structure. In many cases, this lability is undesirable because it accounts for the poor reproducibility of the useful properties of materials.[36] The molecular sponge, which is an important structural material of a non-crystalline polymer matrix, exhibits clear-cut susceptibility to thermomechanical treatment and has a fairly labile structure. Owing to these properties of the molecular sponge, non-crystalline polymers differ fundamentally from homogeneous fluids, in which reaction rates do not change upon shear mechanical treatment (stirring). Moreover, parameters of elementary chemical steps proceeding in homogeneous media are usually unambiguous.

2. Specific features of oxidation in the steady state of the polymer matrix

The notion of structural steady state as applied to a polymer being oxidised is somewhat arbitrary. Oxidation is inevitably associated with the formation of oxygen-containing groups in macromolecules and with rupture or cross-linking of polymer chains. These processes change the initial balance of elastic forces in the spongy molecular matrix and cause more or less fast structural evolution. However, if the chemico-mechanical perturbation is relatively slight and the matrix quickly returns to the thermomechanical equilibrium, this process can be regarded as being structurally stationary.

The structurally steady-state oxidation includes several macroscopic stages which obey different kinetic laws. Thus the induction period is characterised by a low rate of oxygen consumption (υ_1). This period ends after a small amount of oxygen, usually less than 0.1 mol kg^{-1}, has been absorbed. The υ_1 value does not depend on the concentration of hydroperoxide accumulated during the induction period but increases with an increase in the pressure of oxygen without, however, reaching a limiting value[20]

$$\upsilon_1 = \frac{a_1 P_{O_2}}{(b + P_{O_2})^{1/2}},$$

where a_1 and b are constants.

The induction period is followed by a short stage of self-accelerated oxygen absorption. The reaction rate at this stage (υ_2) is most often proportional to the oxidation time. In this case, reaction chains are initiated upon dissociation of POOH and are terminated upon recombination of macroperoxyls.

As oxidation develops, the increase in the rate of oxygen absorption becomes less pronounced. After some period, the rate reaches a maximum and no longer depends on the POOH concentration. Whereas in the first stage (υ_1), the rate of oxygen absorption does not reach any limiting value upon an increase in the pressure of oxygen, in the third stage (υ_3) this rate does have a limit. It is significant that the third stage of oxidation is established earlier than the maximum hydroperoxide concentration has been attained and continues even after the POOH concentration has considerably diminished. This pattern (which can be seen, for example, in Fig. 2) is typical of reactions having the zero order with respect to hydroperoxide.[20–22] This distinguishes high-molecular-mass block polymers from their solutions.

The difference between the kinetics of oxidation of block and dissolved LDPE is demonstrated in Fig. 3 (data of Ref. 37). Although curves *1′–3′* are qualitatively similar, the kinetics of accumulation of POOH in the two systems are substantially different. It can be seen that the variation of the hydroperoxide concentration in the melt is described by a curve with a sharp maximum (curve *1′*), while that in solution is described by monotonic curves with relatively low limiting values (curves *2′*, *3′*).

According to a study by Iring *et al.*,[37] oxidation of LDPE in solutions can be described by a kinetic equation for liquid-phase oxidation

$$\frac{d[POOH]}{dt} = \alpha \upsilon - k[POOH], \qquad (1)$$

where α is the yield of POOH, υ is the rate of oxygen absorption and k is the rate constant for the decomposition of POOH. The reaction reaches a steady-state regime at those degrees of conversion at which the consumption of the CH groups is still insignificant and the following conditions hold:

$$\left(\frac{d[POOH]}{dt}\right)_{lim} = 0, \quad \alpha \upsilon_{lim} = k[POOH]_{lim} \rightarrow \text{const}.$$

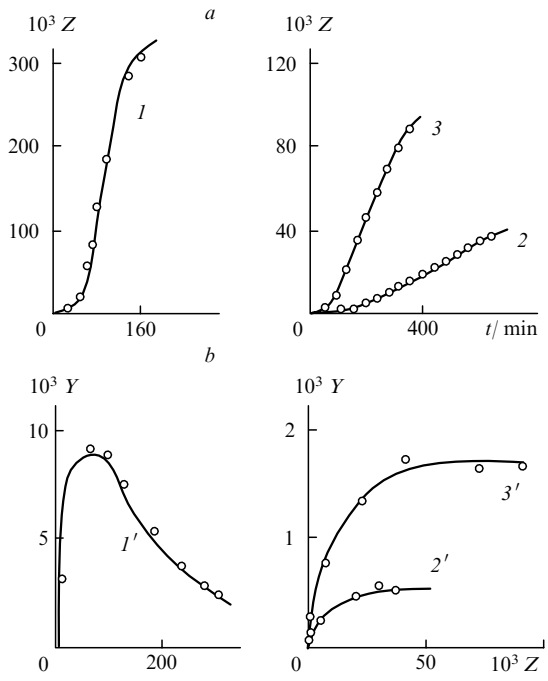


Figure 3. Amount of absorbed oxygen (Z, moles of O_2 per mole of molecular units) *vs.* oxidation time (*a*) and amount of accumulated hydroperoxide (Y, moles of POOH per mole of molecular units) *vs.* amount of absorbed oxygen (*b*) during the oxidation of a melt (*1*, *1′*) and a solution of LDPE (the LDPE concentration is 0.56 mol litre^{-1}) in trichlorobenzene (*2*, *2′*, *3*, *3′*).[37]
Temperature/ °C: *1*, *1′*, *2*, *2′* — 160, *3*, *3′* — 170.
Pressure of O_2/ kPa: *1*, *1′* — 100; *2*, *2′*, *3*, *3′* — 75.

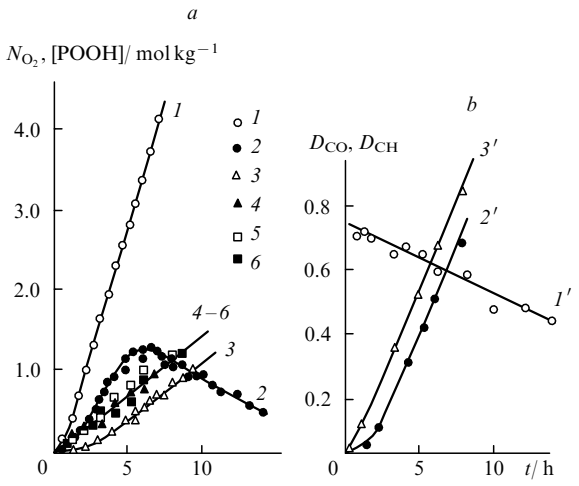


Figure 4. Curves for oxidation of molten poly(ethylene oxide) at 90 (*1*, *2*, *1′–3′*) and 80 °C (*3–6*);
(*a*) oxygen absorption (*1*) and hydroperoxide accumulation (*2–6*); (*b*) variation of the optical density of the CH (*1′*) and CO (*2′*, *3′*) absorption bands in the IR spectra. Concentration of dibenzoyl peroxide /mol kg^{-1}: 0 (*1–3*, *1′*, *2′*), 0.06 (*3′*), 0.0165 (*4*), 0.039 (*5*) and 0.12 (*6*). The IR spectra were recorded using chloroform solutions of the polymer (10 mg ml^{-1}) (data from Refs 15, 18).

Oxidation in the melt also reaches a steady-state regime at a relatively low consumption of CH groups (Fig. 3, curve *1*); however, the pattern of variation of the POOH concentration (Fig. 3, curve *1′*) differs from that for the liquid-phase reaction.

Oxidation of high-molecular-mass block polyolefins in the steady-state regime is characterised by the following features.[15,20–22]

(1) hydroperoxide is not the only molecular product of the reaction (other oxygen-containing compounds are also formed);

(2) decomposition of POOH is due to its reaction with an oxidation product and is not accompanied by the formation of free radicals;

(3) oxidation has the zero order with respect to hydroperoxide.

It should be emphasised that the zero order with respect to hydroperoxide in the steady state has been repeatedly found by numerous researchers; however, this fact has not received adequate attention (apparently, in the heyday of the theory of liquid-phase oxidation of hydrocarbons, researchers have not yet faced the problem of structure-kinetic modelling). Since this finding was undoubtedly significant, it was specially verified in relation to the oxidation of molten polyethylene oxide (PEO),[15,18,19] a high-elasticity copolymer of ethylene with propylene and solid-like IPP.[21] These experiments confirmed simultaneously yet another fact which had been repeatedly described previously — admixed initiators present in polymers accelerate the attainment of the highest reaction rate but do not influence the rate itself over a broad range of concentrations.

Figure 4 presents experimental results on the oxidation of a PEO melt in air.[15] It can be seen that the constant rate v_3 is established earlier (curve *1*) than the maximum POOH concentration is attained (curve *2*). The curves for the consumption of the polymer CH groups (curve *1′*) and for the accumulation of aldehyde reaction products (curve *2′*) also indicate that constant oxidation rates are rapidly attained and that they do not depend on the content of POOH in the melt.

The introduction of a foreign initiator, dibenzoyl peroxide (BP) in concentrations of up to 0.12 mol kg^{-1}, into the PEO melt eliminates the self-accelerated stage but does not influence the steady-state rates of accumulation of aldehyde (curve *3′* in Fig. 4 is parallel to the straight section in curve *2′*) and hydroperoxide (curves *4–6* are parallel to the straight section in curve *3*).

The fact that the steady-state rate of oxidation does not depend on the content of a foreign initiator indicates that the polymeric matrix has some structural filter ('bottle-neck'), which restricts the transfer of free radicals from areas in which the initiator dissociates to other areas in which chain oxidation occurs.

It is noteworthy that dibenzoyl peroxide present in a relatively high amount in a PEO melt depresses the reaction; as its concentration increases from 0.12 to 0.38 mol kg^{-1}, the rate v_3 diminishes 1.4 fold at 90 °C,[19] which is inconsistent with the homogeneous model.

The 'bottle-neck' effect is clearly manifested in the experiments on oxidation of solid-like IPP in the presence of dibenzoyl peroxide.[21] Figure 5 shows how the total concentrations of BP being consumed and POOH being accumulated vary during the

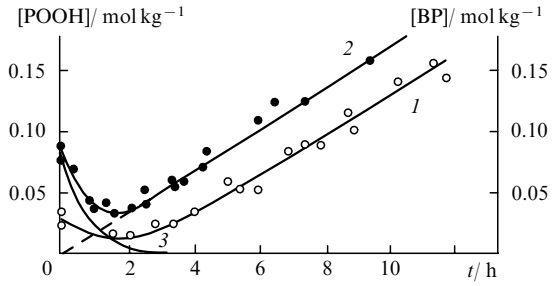


Figure 5. Variation of the total concentration of hydroperoxide and dibenzoyl peroxide (*1*, *2*) and the concentration of only dibenzoyl peroxide (*3*) during oxidation of IPP films in air at 100 °C.[21]
$[BP]_0$/ mol litre^{-1}: (*1*) 0.025, (*2*, *3*) ~0.8.

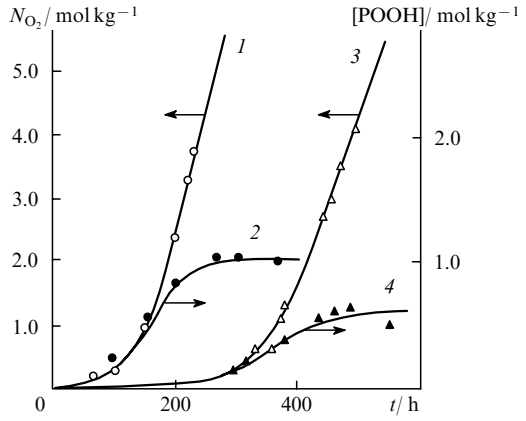


Figure 6. Amount of the absorbed oxygen (*1*, *3*) and accumulated hydroperoxide (*2*, *4*) *vs.* time of oxidation of low-molecular-mass APP with M_n = 4500 (*1*, *2*) and 5-fold orientationally drawn IPP films (*3*, *4*) at T = 120 °C and P_{O_2} = 10^3 kPa.[26]

oxidation of IPP films in air at 100 °C. In this particular case, the presence of a structural filter for the radicals arising is quite obvious: the higher the content of BP in the polymer, the greater fraction of BP decomposes unproductively with respect to the accumulation of POOH. In addition, the steady-state rate of the process does not depend on the initial concentration of BP or on the current concentration of POOH.

Yet another result obtained in a study of oxidation of a low-viscosity melt of atactic polypropylene (APP) with the molecular mass M_n = 4500 and orientationally drawn IPP films (Fig. 6) is worth noting.[26] The rate of oxidation at 120 °C increases for a long period in direct proportion to the concentration of the accumulating POOH; simultaneously, the amount of absorbed oxygen increases with time according to an exponential law and $\upsilon \sim \exp(\Phi t)$. The same pattern is followed at 110 and 130 °C. Meanwhile, oxidation of solutions of these polymers in inert trichlorobenzene (concentration 0.56 mol kg^{-1} per monomer unit) obeys kinetic laws of homogeneous reactions, *i.e.* the dependences $\upsilon \sim t$ and $\upsilon \sim$ [POOH]$^{0.5}$ hold. Thus, the kinetics of oxidation of polymer samples in which the molecular sponge exists in the state of enhanced thermal fluctuation mobility differ from the kinetics of oxidation of liquid hydrocarbons or high-molecular-mass polyolefins in the structural steady state.

To summarise, it can be noted that oxidation of the same (from the chemical viewpoint) polymer is described, depending on its thermomechanical state, by a whole range of kinetic laws different in kind, which is inconsistent with the model of homogeneous reactions. Thus a new model taking into account the nanosize heterogeneity of the non-crystalline polymeric phase needs to be developed.

III. The microreactor model and kinetic regimes of oxidation

In several studies,[15, 16, 18–22, 28, 29, 33, 34, 38, 39] non-crystalline polymers are considered as systems of molecular-chain spongy micelles which fill the cells of an infinite three-dimensional framework (Fig. 7 *a*). This framework is an open-work lattice of paracrystalline domains, each of them containing up to a dozen parallel segments. The size of spongy micelles is of the order of tens of nanometers. The three-dimensional framework in the matrix of partially crystalline polymers incorporates a more or less shaped carcass of lamellar crystallites (Fig. 7 *b*).

The molecular spongy micelle, which acts as a chemical microreactor, is a heterophase aggregate, the chains of which enter the paracrystalline domains at one end and enter the spongy grains at the other end. The chains within the grain are tightened by cohesion forces but are not completely collapsed, being

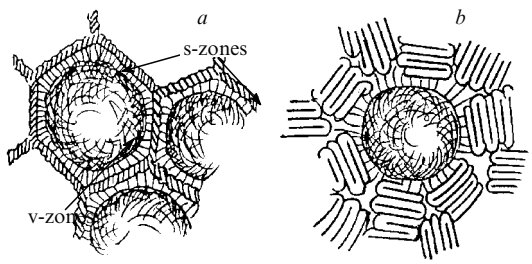


Figure 7. Scheme of the molecular spongy-micellar nanosized reactor for non-crystalline (*a*) and partially crystalline (*b*) polymers.

stabilised as a sponge filled with fairly narrow micropores (more precisely, nanopores). The sizes of the micropores range from a chemical bond length to a polymer chain thickness (0.1–0.5 nm).

Under conditions of balanced elastic forces between the spongy grain and the domains of the continuous framework, a layer is formed consisting of radially arranged chain segments, which constitute the walls of relatively wide nanopores (supernanopores). As a consequence, two types of nanosized zones arise in the micelle, namely, s-zones consisting of radial chain segments (the size of a thermodynamic segment is 2–3 nm), which form supernanopores, and v-zones consisting of grains with narrow nanopores.

The chain segments of these two zones are characterised by different motion dynamics. The segments in the s-zones play a role of mechanical strings fixing the micellar grain; the s-zones themselves can be compared to a porous adsorbent with a rigid framework. A v-grain is close in thermomechanical properties to a mobile drop of a liquid. Such a drop hanging from a domain of the continuous three-dimensional framework can execute, to a certain extent, its own vibrational or rotational motions and volume beats, thus transferring the kinetic momentum to more or less flexible polymer chains composing the drop.

Due to their spongy structure, the micelles can rapidly rearrange and capture even those admixtures where the molecules are larger than the diameter of empty nanopores. In addition, since the molecular sponge is, in essence, a set of coupled pendula, it is subject to interference, *i.e.*, damping or synchronisation of oscillations; this creates conditions for a fluctuation increase in the size of v-nanopores or, correspondingly, for more or less fast migration of admixtures over the sponge bulk.

The nanosized heterogeneity of the molecular spongy micelles influences the chemistry of chain reactions. Firstly, foreign compounds (oxygen, initiators, inhibitors) are distributed non-uniformly between the zones, being mainly accumulated in the v-grains. Secondly, due to different sizes of the s- and v-nanopores, the reactivities of macromolecules and admixtures absorbed in them are appreciably dissimilar. Indeed, a reacting species in a narrow v-micropore resides most of the time under constrained conditions — either on a nanopore wall (if it belongs to the macromolecule) or in the pore bulk (if it is a foreign species). A foreign molecule is expelled to the pore bulk under the influence of dispersion electromagnetic forces.[28, 29] The situation in an s-nanopore is different: most of the time, a foreign molecule is adsorbed on the walls of a pore.

The difference between the chemical reactivities of a species caused by the steric and energetic nonequivalence of s- and v-nanopores affects all the intermediates of a chain reaction. The quantitative changes in the reactivity of the same reactant can be very pronounced; the pathways of transformations in the two zones can differ even qualitatively.

Chain reactions in spongy micelles can proceed in different modes; kinetic modelling can be performed most easily for the steady-state heterophase and homophase modes, which are realised in the pure form when the rate of structural evolution is negligibly low, *i.e.* when the volumes and the properties of the zones are virtually invariant.

By definition, the scheme of a heterophase process should include separate charts for the reactions in each zone and the chart for the transfer of the reacting species from one zone to another. The primary reactions occur usually in s-zones because these zones provide more favourable conditions for the dissociative generation of free radicals, which subsequently migrate to v-zones.

If a chemical reaction is localised in one zone, it can formally be referred to as a homophase reaction. This situation is observed, for example, when free radicals are generated in v-zones when v-nanopores undergo high-frequency fluctuations and thus reach the size of s-nanopores. In this case, the initiating activity of the POOH groups captured by v-nanopores increases and the fluctuation initiation of a chain reaction starts to prevail.

The heterophase mode, involving coupling of non-uniform reaction chains, is more frequently encountered in the absence of clear-cut structural evolution of high-molecular-mass polyolefins. Oxidation of a polymer without an admixed initiator starts upon direct reaction of oxygen adsorbed on s-nanopore walls with the CH groups of the polymer s-segments. The greater part of the generated free radicals enter into subsequent reactions and decay without leaving the s-nanopore. When a small portion of radicals has passed from s-zones to the bulk of v-grains and has induced there reaction v-chains, the process acquires a heterophase character.

The sequence of s,v-transitions (s,v-translations) of free radicals described by the corresponding chart means physically the passage of free valences through the structural 'bottle-neck'. The 'bottle-neck' capacity depends on the thermomechanical state of the polymer sample and on the presence of impurities able to promote or, conversely, suppress the s,v-translation of free valences.

The secondary reaction chains induced by this transfer (in v-zones) differ fundamentally from the primary chains (in s-zones) in the character of transformations. In particular, oxygen is mainly accumulated in v-zones. In addition, the rate of rupture of polymer chains with participation of alkyl macroradicals and the rate of termination of oxidation chains in v-zones are lower than those in s-zones. Consequently, the reaction v-chains are longer. Thus, the amount and composition of the oxidation products are mainly determined by the transformations of polymer units of v-zones, which constitute the main bulk of the molecular spongy micelles.

The steady-state oxidation mode includes the steps of transfer of hydroperoxide groups from v-zones to s-zones. The hydroperoxide formed in narrow v-nanopores dissociates into radicals very slowly due to unfavourable steric and energetic conditions. However, as hydroperoxide is accumulated, it starts to occupy the stationary s-zones, which have supernanopores favourable for dissociation. Thus the process passes from the induction period to the self-accelerated stage.

IV. Kinetic model of oxidation of polyolefins

1. Induction period

In accordance with the foregoing, the overall scheme of an initial period of autooxidation of polyolefins includes two charts for reactions in s- and v-zones and a chart for the inter-zone chemical induction, responsible for coupling of inhomogeneous reaction chains.

In the absence of a foreign initiator, free radicals are generated in s-nanopores upon the reaction of oxygen with the CH groups of the polymer.

The scheme of the primary reaction chain (in the s-zone) can be written in the following general form:

$$PH_s + O_{2,s} \xrightarrow{k'_{0s}} \delta_1 P_s^{\bullet} \text{ (generation of radicals)},$$

$$P_s^{\bullet} \xrightarrow{k_d} R_s^{\bullet} + R^{=} \text{ (rupture of polymer chain)},$$

$$R_s^{\bullet} \xrightarrow{k_{1s}} R_{1s}^{\bullet} \text{ (isomerisation)},$$

$$R_s^{\bullet} + R_{1s}^{\bullet} \longrightarrow \text{recombination and disproportionation products},$$

where PH_s is a polymer unit in zone s, which includes reactive hydrogen atoms, $P_s^{\bullet}$ is the macroradical with a free valence on an internal unit of the macromolecule [for polyethylene (PE), this is $\sim CH_2\dot{C}H\sim$ and for polypropylene (PP), these are $\sim CH_2\dot{C}(CH_3)\sim$ and $\sim\dot{C}HCH(CH_3)\sim$], δ_1 is a factor characterising the yield of free radicals, $R_s^{\bullet}$ and $R^{=}$ are a terminal radical and a terminal unsaturated group, respectively, and $R_{1s}^{\bullet}$ is the product of isomerisation of the terminal radical $R_s^{\bullet}$ (the structures of $R_s^{\bullet}$ and $R_{1s}^{\bullet}$ for PP have been considered previously [21]).

The pattern of the inter-zone transfer of free valence includes migration of the radical $R_s^{\bullet}$ from the supermolecular framework structure to the s-nanopore bulk (with transition to the $R_m^{\bullet}$ state) and subsequent oxidation of $R_m^{\bullet}$:

$$R_s^{\bullet} \underset{k_{-m}}{\overset{k_m}{\rightleftharpoons}} R_m^{\bullet},$$

$$R_m^{\bullet} + O_{2,s} \xrightarrow{k_{tr}} R_mOO^{\bullet} \longrightarrow R_{1m}^{\bullet}OOH \longrightarrow R_{1m}O + HO_m^{\bullet}.$$

The subscript 'm' implies belonging to the nanopore bulk and 'tr' stands for belonging to the inter-zone chain transfer process.

As noted above, the rate of the s,v-transfer is negligibly low compared to the rate of radical transformations in the s-zone. It is determined by the thermomechanical ability of the radicals $R_s^{\bullet}$ to oscillate with some frequency between the rigid framework of s-segments and the s-nanopore bulk and to pass to the state $R_m^{\bullet}$, more convenient for the reaction with oxygen. The terminal radical $R_mOO^{\bullet}$ thus formed undergoes α-isomerisation [40] to a hydroperoxyalkyl radical, which decomposes with elimination of free hydroxyl $HO_m^{\bullet}$.

The free hydroxyl migrates to the v-zone and induces there a chain reaction

$$HO_m^{\bullet} \longrightarrow HO_v^{\bullet},$$

$$HO_v^{\bullet} + PH_v \xrightarrow{k'_1} H_2O + P_v^{\bullet},$$

$$P_v^{\bullet} + O_2 \xrightarrow{k_1} POO_v^{\bullet}$$

$$POO^{\bullet} = \sim\underset{\displaystyle X}{\overset{\displaystyle OO^{\bullet}}{\overset{|}{\underset{|}{C}}}}-CH_2\sim .$$

The $POO^{\bullet}$ radical thus formed can be converted according to three pathways to give hydroperoxides, epoxides, or chain termination products.

$$\sim\underset{\displaystyle X}{\overset{\displaystyle OO^{\bullet}}{\overset{|}{\underset{|}{C}}}}-CH_2\sim \xrightarrow{k'_2,\ PH} \sim\underset{\displaystyle X}{\overset{\displaystyle OOH}{\overset{|}{\underset{|}{C}}}}-CH_2\sim + \sim\underset{\displaystyle X}{\overset{}{\overset{|}{\underset{|}{\dot{C}}}}}-CH_2\sim$$

$$\sim\underset{\displaystyle X}{\overset{\displaystyle OO^{\bullet}}{\overset{|}{\underset{|}{C}}}}-CH_2\sim \xrightarrow[\text{isomerisation}]{k_3,\ \beta\text{-isomer-}} \sim\underset{\displaystyle X}{\overset{\displaystyle OOH}{\overset{|}{\underset{|}{C}}}}-\dot{C}H\sim \longrightarrow \sim\underset{\displaystyle X}{\overset{\displaystyle O}{\overset{/\backslash}{\underset{|}{C}}}}-CH\sim + HO^{\bullet}$$

$$\mathbf{E}$$

$$\xrightarrow{k_t,\ POO^{\bullet}} \text{chain termination products}$$

Epoxides **E**, which are highly reactive towards free radicals, undergo subsequent transformations giving rise to carbonyl compounds (the corresponding reactions are considered below).

When calculating the s-scheme, we employed the condition of steady-state concentration of free radicals and did not take into account the loss of s-radicals by the inter-zone transfer; however, this transfer needs to be taken into account (as an initiation step) in the calculation of the v-scheme. The concentration of macroradicals responsible for the inter-zone chemical induction can be described by the expression

$$[R^{\bullet}_s]_1 = \frac{k''_{0s}[O_{2,s}]}{2k_{1s}}$$

($k''_{0s} = \delta_1 k'_{0s}[PH_s]$, the subscript 1 at the values of radical concentrations and reaction rates implies the first stage of oxidation), the rate of the s,v-transfer is given by the expression

$$\upsilon_{tr,1} = \frac{k_{tr}k_m k''_{0s}[O_{2,s}]^2}{2k_{1s}(k_{-m} + k_{tr}[O_{2,s}])},$$

and the concentration of the peroxyl radicals in the v-zones at the first stage of oxidation is determined by the equation

$$[POO^{\bullet}]_1 = \frac{(k_{tr}k_m k''_{0s})^{0.5}[O_{2,s}]}{[4k_t k_{1s}(k_{-m} + k_{tr}[O_{2,s}])]^{0.5}}. \quad (2)$$

Now we use Eqn (2) to express the rates of the absorption of oxygen (υ_1), accumulation of hydroperoxide ($\upsilon_{[POOH],1}$), and evolution of water ($\upsilon_{aq,1}$)

$$\upsilon_1 = -\left(\frac{d[O_2]}{dt}\right)_1 = k_1[P^{\bullet}][O_2] = (k'_2[PH] + k_3)[POO^{\bullet}]_1 = \quad (3)$$

$$= \frac{(k_2 + k_3)aP_{O_2}}{(b + P_{O_2})^{0.5}},$$

$$\upsilon_{[POOH],1} = \left(\frac{d[POOH]}{dt}\right)_1 = k'_2[PH][POO^{\bullet}]_1 = \frac{k_2 aP_{O_2}}{(b + P_{O_2})^{0.5}},$$

$$\upsilon_{aq,1} = k'_1[HO^{\bullet}][PH] = k_3[POO^{\bullet}]_1 = \frac{k_3 aP_{O_2}}{(b + P_{O_2})^{0.5}},$$

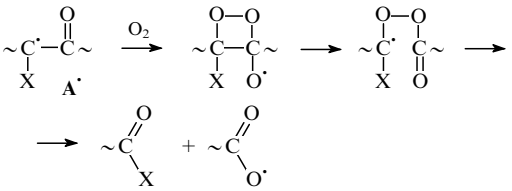
where $k_2 = k'_2[PH]$, $a = (k_m k''_{0s}\gamma_s/4k_t k_{1s})^{0.5}$, $b = k_{-m}(k_{tr}\gamma_s)^{-1}$ ($\gamma_s = [O_{2,s}]\,P_{O_2}^{-1}$). The υ values found from these expressions are in good agreement with experimental data.[15,20–22]

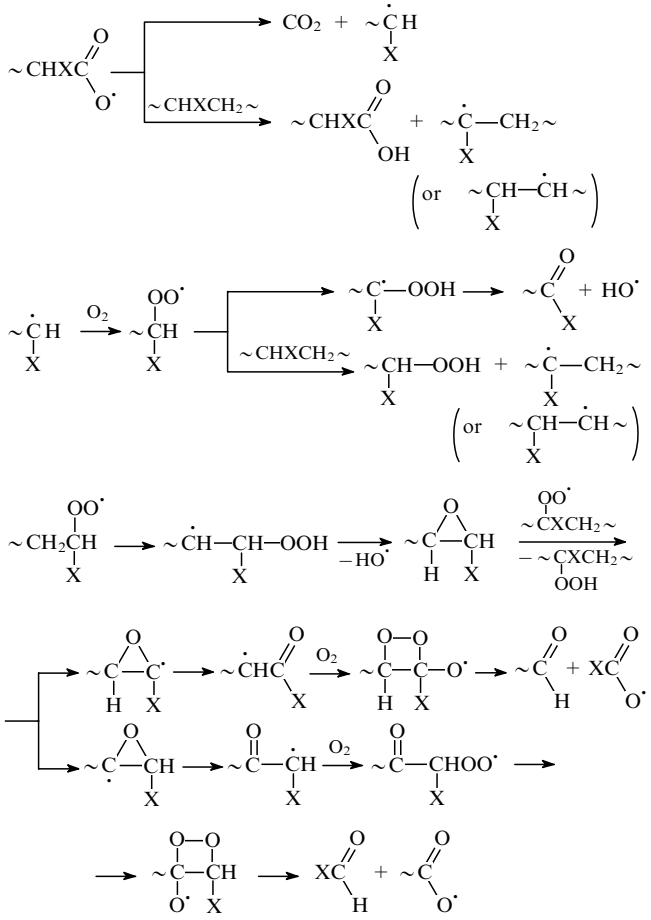
According to the heterophase oxidation model (unlike the homogeneous model), water is mostly formed *via* a chain reaction involving free hydroxyls rather than upon decomposition of POOH.

Oxidation of the intermediate epoxides is accompanied by additional absorption of oxygen and the formation of POOH and water but these transformations do not influence the form of Eqn (2). The products of epoxide oxidation appear somewhat later than POOH;[15,21] however, they are formed at a noticeable rate even in the induction period; after that, the rate rapidly increases and becomes stabilised for a long period.[41–43]

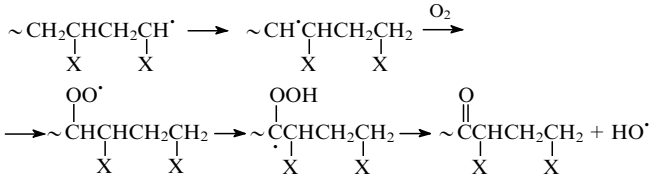
The steady-state concentration of the epoxides is relatively low because they efficiently react with free radicals (Scheme 1).

The carbonyl compounds formed are fairly diverse (they include polymeric and volatile aldehydes, ketones, acids); their formation can be described by the following reactions:

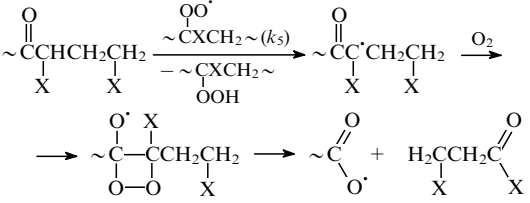




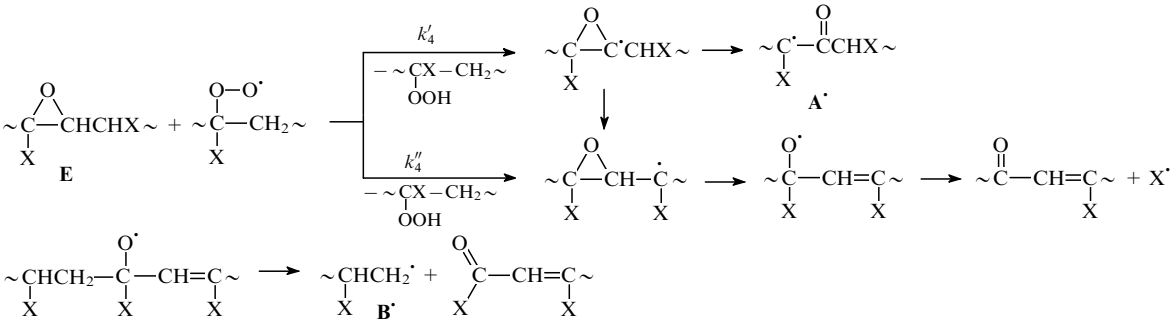
Isomerisation of the terminal $\sim C^{\bullet}HX$ radical ensures migration of the free valence along the macromolecule and the formation of ketone groups at some distance from the chain end.



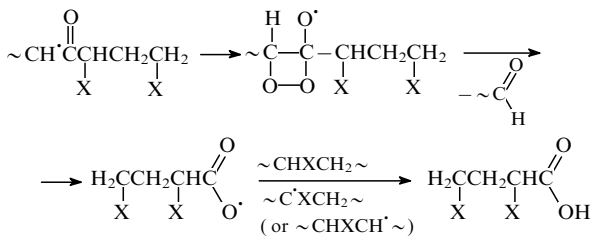
Further oxidation of these ketones results in the formation of larger fragments with aldehyde, ketone and acid groups



Scheme 1



Here and later X = H, Me.



The presence of some compounds such as methyl ethyl ketone, methyl propyl ketone, butyraldehyde, pentanone, hexanone, *etc.* among the products of oxidation of polyolefins proves the occurrence of the above reactions.[41–43]

The transformations of the terminal radical $\mathbf{B}^{\bullet}$ are shown in Scheme 2.

This set of reactions, which is far from being complete, is still sufficient to demonstrate the pathways to the final products of polyolefin oxidation and to state the fact that transformations of radicals $\mathbf{A}^{\bullet}$ and $\mathbf{B}^{\bullet}$ and carbonyl compounds have no influence on the steady-state concentration of peroxyl radicals [Eqn (2)]. The concentration of carbonyl compounds, which are oxidised and formed again in the chain process, continuously increases.

In view of the foregoing, one can write the following condition for the steady-state concentration of epoxide

$$\frac{d[E]}{dt} = k_3[POO^{\bullet}]_1 - k_4[E][POO^{\bullet}]_1 = 0, \qquad (4)$$

where $k_4 = (k'_4 + k''_4)$. It follows from Eqn (4) that $[E] = k_3 / k_4 =$ const. The total rate of accumulation of carbonyl compounds (CO) in the epoxide branch of the reaction is equal to

$$\upsilon_{CO,1} = \left(\frac{d[CO]}{dt}\right)_1 = (\alpha_1 + \alpha_2)k_4[E][POO^{\bullet}]_1 = \alpha k_3[POO^{\bullet}]_1 ,$$

where α_1 and α_2 are the yields of polymeric and volatile compounds, respectively, and α is their sum. Thus, after condition (4) has been reached, the rate $\upsilon_{CO,1}$ depends on the pressure of oxygen in the same way as the rates υ_1 and $\upsilon_{[POOH],1}$ and the content of CO groups increases with time in accordance with the equation

$$[CO]_1 = \upsilon_{CO,1}\, t. \qquad (5)$$

The same is true for the growth of the concentration of broken polymer chains (n) in the v-zones of spongy micelles detected by viscometry. The total rate of chain rupture is composed of two fractions proportional to the constants k'_4 and k''_4:

$$\upsilon_{n,1} = \left(\frac{dn}{dt}\right)_1 = (\nu_1 k'_4 + \nu_2 k''_4)[E][POO^{\bullet}]_1 = \text{const}[POO^{\bullet}]_1, \quad (6)$$

where ν_1 and ν_2 are coefficients.

The direct proportionality between the amount of oxidation products and the amount of oxygen absorbed in the induction period, which follows from the scheme in question, is also retained for some time after the induction period has been completed, this time being much longer for the processes of accumulation of carbonyl compounds and destruction of macromolecules than for accumulation of POOH.[41–43]

It should be emphasised that Eqn (5) refers to the overall process of formation of carbonyl compounds accompanied by abstraction of monomeric fragments. These destruction steps change the viscosity of the polymer solution only slightly compared to the primary scission steps in the epoxide branches, the rates of which are described by Eqn (6).

2. Hydroperoxide-initiated process

The induction period in the autooxidation of polyolefins usually ends when 10^{-2} mol kg^{-1} of oxygen has been absorbed due to the occupation of the s-zones of the spongy matrix by the hydroperoxide from v-zones. This occupation is provided by the transfer of free valence and migration of OOH groups along the polymer chain and by the fluctuation steps of rearrangement of the molecular sponge units.[15, 20, 21, 33]

By expressing the total frequency of the v,s-transfer of the OOH groups in terms of the effective constant k_{vs}, taking into account the fact that activation of these processes requires a fluctuation of the sponge with opening of narrow v-micropores, we can express the scheme of the hydroperoxide v,s-transfer as

$$POOH_v \underset{k_{-f}}{\overset{k_f}{\rightleftharpoons}} POOH_f \xrightarrow{k_{vs}} POOH_s ,$$

where the subscript 'f' refers to a fluctuationally excited v-nanopore with a trapped OOH group.

Having got into the s-nanopores, the OOH groups become able to dissociate to give free radicals

$$POOH_s \xrightarrow{k_{0s}} (HO^{\bullet} + PO^{\bullet})_s \xrightarrow{PH_s} \delta P^{\bullet}_s$$

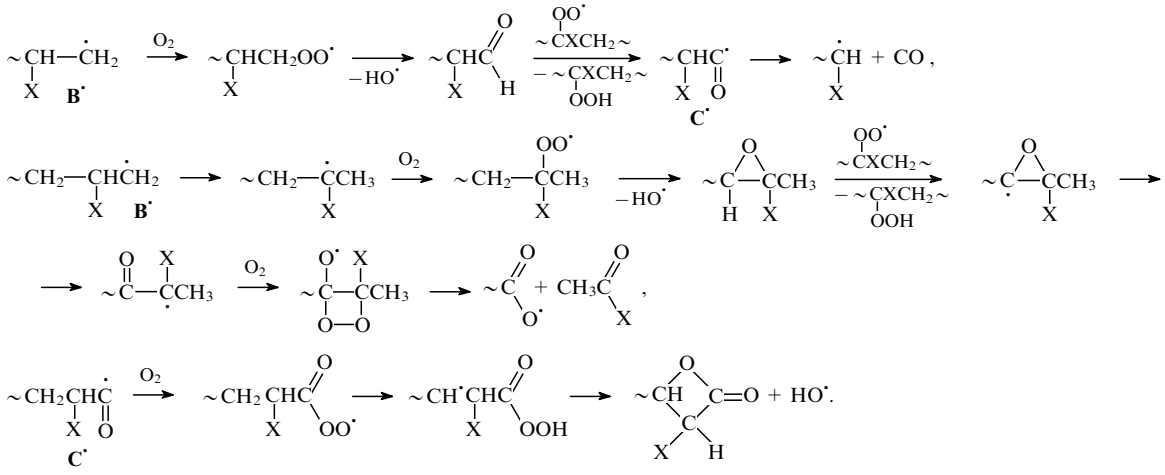
and, as their concentration increases, to enter into the bimolecular reaction

$$POOH_s + POOH_f \xrightarrow{k^f} 2\,POH + O_2$$

giving no free radicals. This scheme of the chemical inter-zone feedback permits us to express the steady-state concentrations of the OOH groups in the fluctuationally active and s-states by the equation

$$\frac{d[POOH]_f}{dt} = k_f[POOH]_v - k_{-f}[POOH]_f - k_{vs}[POOH]_f - k^f[POOH]_s[POOH]_f = 0 .$$

Scheme 2



In view of the high rate of deactivation of fluctuations, the last two terms can be neglected and the resulting expression

$$[\mathrm{POOH}]_\mathrm{f} = \frac{k_\mathrm{f}[\mathrm{POOH}]_\mathrm{v}}{k_{-\mathrm{f}}}$$

can be used in the equation for the rate of the reaction involving s-hydroperoxide

$$\frac{\mathrm{d}[\mathrm{POOH}]_\mathrm{s}}{\mathrm{d}t} = k_\mathrm{vs}[\mathrm{POOH}]_\mathrm{f} - k^\mathrm{f}[\mathrm{POOH}]_\mathrm{s}[\mathrm{POOH}]_\mathrm{f} - - k_{0\mathrm{s}}[\mathrm{POOH}]_\mathrm{s} = 0.$$

The concentration $[\mathrm{POOH}]_\mathrm{s}$ found in this way,

$$[\mathrm{POOH}]_\mathrm{s} = \frac{k_\mathrm{vs}k_\mathrm{f}[\mathrm{POOH}]_\mathrm{v}}{k_{-\mathrm{f}}k_{0\mathrm{s}} + k^\mathrm{f}k_\mathrm{f}[\mathrm{POOH}]_\mathrm{v}}, \quad (7)$$

can be used to express the overall rate of radical generation in s-zones by the equation

$$\upsilon_\mathrm{is} = k_0''[\mathrm{O}_{2,\mathrm{s}}] + \delta k_{0\mathrm{s}}[\mathrm{POOH}]_\mathrm{s} \approx \delta k_{0\mathrm{s}}[\mathrm{POOH}]_\mathrm{s}.$$

The contribution of the direct reaction between CH bonds and oxygen soon becomes negligibly small and the expression for $\upsilon_{\mathrm{tr},1}$ derived previously is replaced by the equation

$$\upsilon_{\mathrm{tr},2} = \frac{k_\mathrm{tr}k_\mathrm{m}\delta k_{0\mathrm{s}}[\mathrm{POOH}]_\mathrm{s}[\mathrm{O}_{2,\mathrm{s}}]}{2k_{1\mathrm{s}}(k_{-\mathrm{m}} + k_\mathrm{tr}[\mathrm{O}_{2,\mathrm{s}}])}$$

(the subscript 2 denotes the second stage of the oxidation process).

The equation describing the concentration of peroxyl radicals also changes

$$[\mathrm{POO}^\bullet]_2 = \frac{(k_\mathrm{tr}k_\mathrm{m}\delta k_{0\mathrm{s}}[\mathrm{POOH}]_\mathrm{s}[\mathrm{O}_{2,\mathrm{s}}])^{0.5}}{[4k_\mathrm{t}k_{1\mathrm{s}}(k_{-\mathrm{m}} + k_\mathrm{tr}[\mathrm{O}_{2,\mathrm{s}}])]^{0.5}}. \quad (8)$$

During an initial period of the accelerated stage of autooxidation, the final reaction products are accumulated synchronously with the hydroperoxide. Being unable to dissociate in the v-zones of the spongy matrix, hydroperoxide is accumulated for some period almost without reacting with other oxidation products because their concentrations are too low. The rate of hydroperoxide accumulation during this period is described by the equation

$$\upsilon_{[\mathrm{POOH}],2} = k_2[\mathrm{POO}^\bullet] = A(\delta k_{0\mathrm{s}}[\mathrm{POOH}]_\mathrm{s})^{0.5},$$

where

$$A = k_2\left\{\frac{k_\mathrm{tr}k_\mathrm{m}[\mathrm{O}_{2,\mathrm{s}}]}{4k_\mathrm{t}k_{1\mathrm{s}}(k_{-\mathrm{m}} + k_\mathrm{tr}[\mathrm{O}_{2,\mathrm{s}}])}\right\}^{0.5},$$

or, with allowance for Eqn (7) and the relation $[\mathrm{POOH}]_\mathrm{v} \approx [\mathrm{POOH}]$, which means that the major portion of OOH groups of the non-crystalline polymer phase is concentrated in the v-zones, by the equation

$$\upsilon_{[\mathrm{POOH}],2} = A\left\{\frac{\delta k_0 k_\mathrm{vs}}{k^\mathrm{f}[1 + k_{0\mathrm{s}}k_{-\mathrm{f}}/(k^\mathrm{f}k_\mathrm{f}[\mathrm{POOH}]_\mathrm{v})]}\right\}^{0.5} = \frac{\upsilon_{[\mathrm{POOH}],3}}{(1 + C/[\mathrm{POOH}])^{0.5}}, \quad (9)$$

where $\upsilon_{[\mathrm{POOH}],3} = A(\delta k_{0\mathrm{s}}k_\mathrm{vs}/k^\mathrm{f})^{0.5}$, $C = k_{0\mathrm{s}}k_{-\mathrm{f}}(k^\mathrm{f}k_\mathrm{f})^{-1}$.

The expressions for the rates of the other macroscopic processes have the following form:

$$\upsilon_\mathrm{CO} = \alpha k_4[\mathrm{E}][\mathrm{POO}^\bullet] = \frac{\upsilon_{\mathrm{CO},3}}{(1 + C/[\mathrm{POOH}])^{0.5}} = \frac{\gamma\upsilon_{[\mathrm{POOH}],3}}{(1 + C/[\mathrm{POOH}])^{0.5}}, \quad (10)$$

$$\upsilon_\mathrm{aq} = k_1'[\mathrm{HO}^\bullet][\mathrm{PH}] = \beta k_3[\mathrm{POO}^\bullet] = \frac{\upsilon_{\mathrm{aq},3}}{(1 + C/[\mathrm{POOH}])^{0.5}},$$

$$\upsilon = \upsilon_\mathrm{CO} + \upsilon_{[\mathrm{POOH}],2} = \frac{\upsilon_3}{(1 + C/[\mathrm{POOH}])^{0.5}} = \frac{\upsilon_{[\mathrm{POOH}],3}}{\varphi(1 + C/[\mathrm{POOH}])^{0.5}}, \quad (11)$$

$$\upsilon_n = (\nu_1k_4' + \nu_2k_4'')[\mathrm{E}][\mathrm{POO}^\bullet] = \frac{\upsilon_{n,3}}{(1 + C/[\mathrm{POOH}])^{0.5}}, \quad (12)$$

where $\gamma = \alpha k_3 k_2^{-1}$, β is the yield of water, φ is the yield of the hydroperoxide, $\upsilon_{[\mathrm{POOH}],3}$, $\upsilon_{\mathrm{CO},3}$, $\upsilon_{\mathrm{aq},3}$, υ_3 and $\upsilon_{n,3}$ are the maximum rates at the third macroscopic stage of autooxidation, attained when $C/[\mathrm{POOH}] < 1$. This inequality transforms Eqn (7) to the form

$$[\mathrm{POOH}]_\mathrm{s} = \frac{k_\mathrm{vs}}{k^\mathrm{f}} = \mathrm{const}. \quad (13)$$

It follows from Eqn (13) that the self-accelerated stage of oxidation should sooner or later come to an end because the s-zone is the structural boundary of the micellar reactor, which terminates the chemical relay of the OOH groups and thus favours the bimolecular reaction giving no free radicals.

Since a hydroperoxide-involving reaction takes place in the s-zone, oxidation takes place again in a regime which obeys a zero order with respect to hydroperoxide. In this case, hydroperoxide still acts as an initiator and simultaneously plays the role of a specific buffer because it maintains a constant rate of initiation of the reaction v-chains and a certain time-independent concentration of free peroxyl radicals [Eqn (8)].

Equations (9)–(11) and (13) derived theoretically have been confirmed experimentally in a number of studies [15, 18, 20–22] in which the third macrokinetic stage of autooxidation with the zero order with respect to hydroperoxide was defined for the first time.

When oxidation follows the zero order with respect to POOH, the maximum rate of oxygen absorption in the third steady-state stage (υ_3) depends on the oxygen pressure and tends to a limit at high P_{O_2}:

$$\upsilon_3 \sim \left(\frac{P_{\mathrm{O}_2}}{b + P_{\mathrm{O}_2}}\right)^{0.5}.$$

Unlike υ_3, the rate υ_1 (in the induction period) does not reach a constant value as P_{O_2} increases; according to Eqn (3), $\upsilon_1 \to P_{\mathrm{O}_2}^{0.5}$. These differences, which have not been interpreted in terms of the homogeneous model, are explained in the heterophase model by assuming that oxygen acts twice as an initiator of oxidation chains during the induction period — first, in the generation of s-radicals and, second, in the s,v-transfer of the free valence. In the steady-state stage of the process, oxygen no longer acts as the main initiator but still promotes the passage of radicals through the structural 'bottle-neck'.

3. The mechanism of decomposition of POOH by oxidation products

As has already been noted, the synchronism of the absorption of oxygen and accumulation of the hydroperoxide is violated starting from some point due to the reaction of POOH with reaction products (note that decomposition of POOH in oxidised polyolefin in the absence of oxygen follows a chain mechanism,[16, 34] as opposed to the non-chain decomposition of POOH during polymer oxidation).

Carboxylic acids are known to accelerate hydroperoxide decomposition.[3, 44, 45] Study of reactions in mixtures of cumene hydroperoxide with acetophenone, dimethylphenylcarbinol, and benzoic acid showed that only the acid can markedly accelerate hydroperoxide decomposition (giving free radicals).[45] Acids are among the major products of oxidation of polyolefins; they are characterised by a broad molecular-mass distribution. It should be expected that acids with long molecular tails incorporated in the micellar sponge would not affect much the decomposition of POOH because they cannot freely migrate over the matrix. The decomposition is catalysed, most probably, by the mobile frag-

ment acids formed upon oxidative abstraction of terminal ketone groups.

The equation for the rate of formation of terminal ketones

$$\upsilon_{CO,t} = \alpha_t k_4[E][POO^\bullet] = \alpha_t k_3[POO^\bullet] = \frac{\gamma_t \upsilon_{[POOH],3}}{(1 + C/[POOH])^{0.5}}$$

[α_t is the yield of $(CO)_t$ and $\gamma_t = \alpha_t k_3 k_2^{-1}$] can be simplified taking into account the fact that the accelerated stage on the curves of absorption of O_2 (and accumulation of CO groups) is substantially shorter than the steady-state stage (see Fig. 2) [15, 21, 41–43, 46, 47]

$$\upsilon_{CO,t} = \gamma_t \upsilon_{[POOH],3} = \text{const},$$

$$[CO]_t = \gamma_t \upsilon_{[POOH],3}\, t\,.$$

Then the rate of the formation of mobile acids (AH) can be written as

$$\frac{d[AH]}{dt} = k_5[CO]_t[POO^\bullet] = k_5\,\gamma_t\,\upsilon_{[POOH],3} t$$

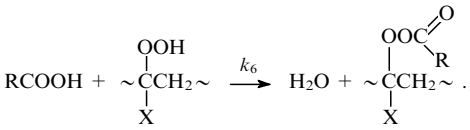
and their amount is equal to

$$[AH] = Bt^2\,, \qquad (14)$$

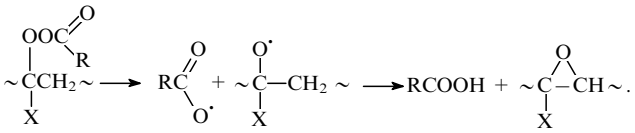
where $B = 0.5 k_5 \gamma t \upsilon_{[POOH],3} = \text{const}$. Equation (14) is quadratic with respect to time. This accounts for the accelerated accumulation of acids observed at high levels of polyolefin oxidation, despite the substantial decrease in the concentration of POOH after the $[POOH]_{max}$ has been attained.[48, 49]

It should be noted that the consumption of POOH, which accelerates with time, does not influence the invariant rate υ_3 of the third macrokinetic stage of autooxidation; this indicates that the yield of radicals in the catalysed reaction is negligibly low.

An adequate scheme of the catalysed process should include condensation of POOH with the acid migrating in the sponge



The peroxy ester thus formed dissociates when the v-nanopore containing it undergoes fluctuation expansion to the volume of an s-nanopore; dissociation gives radicals, which disproportionate with regeneration of the acid without having time to depart from the expanded 'rigid cage'



This scheme is equivalent to the scheme of an intra-cage reaction in which radicals do not migrate to the bulk of the reacting material.[16]

Taking account of these considerations, we obtain a fuller kinetic equation for the rate of accumulation of hydroperoxide

$$\frac{d[POOH]}{dt} = \frac{\upsilon_{[POOH],3}}{(1 + C/[POOH])^{0.5}} - k_6[AH][POOH];$$

with allowance for Eqn (14), it acquires the form

$$\frac{d[POOH]}{dt} = \frac{\upsilon_{[POOH],3}}{(1 + C/[POOH])^{0.5}} - K[POOH]t^2, \qquad (15)$$

where $K = 0.5 k_6 k_5 \gamma_t \upsilon_{[POOH],3}$, and the rate $\upsilon_{[POOH],3}$ at a saturating pressure of oxygen is

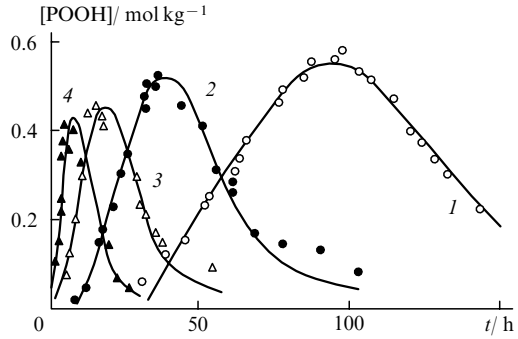


Figure 8. Calculated curves for accumulation of hydroperoxide during the oxidation of APP in air at temperatures of 90 (*1*), 100 (*2*), 110 (*3*) and 120 °C (*4*) (dots correspond to experimental results from Ref. 50).

$$\upsilon_{[POOH],3} = k_2\left(\frac{\delta k_{0s} k_{vs} k_m}{4k^f k_t k_{1s}}\right)^{0.5}. \qquad (16)$$

The equation describing the rate of oxygen absorption remains the same in the steady-state period [see Eqn (11)]

$$\upsilon = k_1[P^\bullet][O_2] = (k_2 + \eta k_3)[POO^\bullet] = \upsilon_{CO} + \upsilon_{[POOH],2} = \frac{\upsilon_3}{(1 + C/[POOH])^{0.5}} = \frac{\upsilon_{[POOH],3}}{\varphi(1 + C/[POOH])^{0.5}},$$

where η is the multiplicity of oxygen absorption steps in the epoxide branches of oxidation and φ is the yield of POOH after absorption of 1 mol kg^{-1} of oxygen.

The data obtained using differential kinetic equations (11) and (15) were compared with experimental data on the oxidation of molten APP (Fig. 8),[50] LDPE (Fig. 9),[9] ethylene–propylene copolymers (EPC) (Fig. 10),[51] solid-like IPP-1 and IPP-2 films differing in the size of spherulites (Fig. 2),[24, 31] and home-manufactured polypropylene (IPP-3) (Fig. 11).† The theoretical curves presented in Figs 2 and 8–11, were calculated by the Runge–

† Data on the oxidation of polypropylene were provided by L N Guseva.

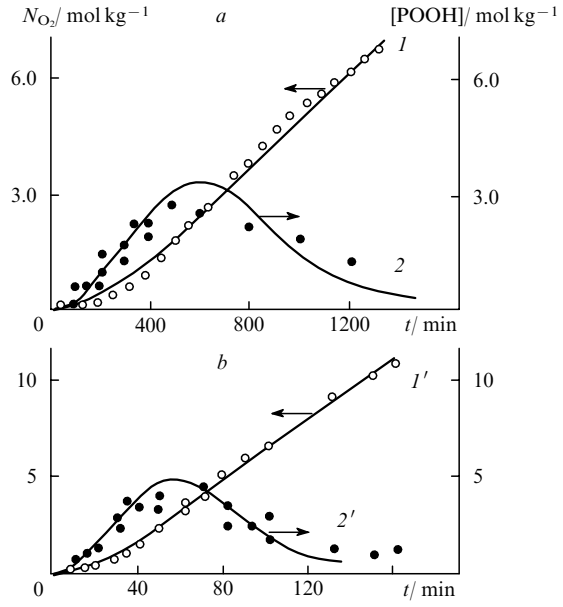


Figure 9. Calculated curves for the absorption of oxygen (*1*, *1′*) and accumulation of hydroperoxide (*2*, *2′*) during oxidation of a LDPE melt at temperatures of 130 (*a*) and 160 °C (*b*) and $P_{O_2} = 100$ kPa (dots correspond to the experimental data from Ref. 9).

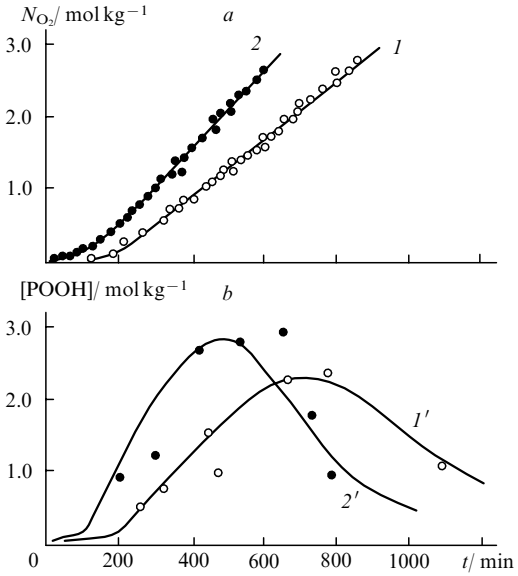


Figure 10. Calculated curves for the absorption of oxygen (*a*) and accumulation of hydroperoxide (*b*) in EPC-1 (*1*, *1′*) and EPC-2 (*2*, *2′*) melts at 130 °C and P_{O_2} = 40 kPa (dots correspond to the experimental data from Ref. 51).

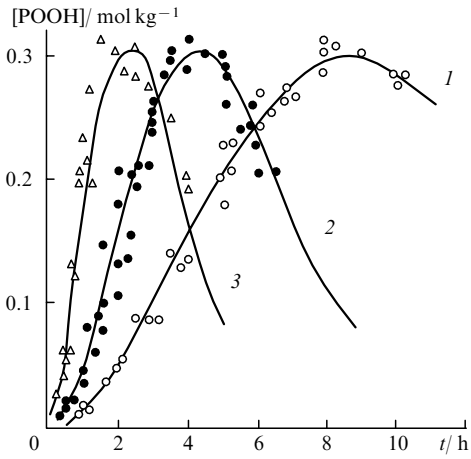


Figure 11. Experimental points and calculated curves for the accumulation of hydroperoxide during oxidation of IPP-3 in air at temperatures of 120 (*1*), 130 (*2*) and 140 °C (*3*).

Kutta method using a simplified version in which Eqns (11) and (15) were integrated separately.[52] This simplification, used instead of solving the set of two equations, restricts the scope of calculations at high degrees of oxidation by the condition $C/[POOH] < 1$, which is still quite sufficient to perform the given task.

The υ_3 and $\upsilon_{[POOH],3}$ values were found by drawing tangents to the ascending branches of the curves shown in Figs 2 and 8–11. The coefficients C and K were determined using Eqns (11) and (15). Due to the scatter of experimental points and the values for the induction periods (τ) and the accumulated hydroperoxide concentrations $[POOH]_1$ corresponding to these periods, all the above-listed parameters had to be refined by performing series of calculations in order to attain the best agreement between the calculated curves and experimental points.

The curves for the variation of the concentration of POOH in APP being oxidised in air at temperatures of 90, 100, 110 and 120 °C are presented in Fig. 8.[50] These curves are matched by the following kinetic characteristics:

T/ °C	τ/ h	$\upsilon_{[POOH],3}$ /mol kg^{-1} h^{-1}	K/ h^{-3}
90	33	0.0129	6.3×10^{-6}
100	10	0.0255	5.6×10^{-5}
110	2	0.0400	3.0×10^{-4}
120	0–1	0.0700	2.0×10^{-3}

In all cases, the equality $C = [POOH]_1 = 0.02$ mol litre^{-1} holds. The relevant general equations have the following form on the minute time scale

$$\tau = 5.25 \times 10^{-19} \exp(E_\tau/RT) \text{ min},$$

$$\upsilon_{[POOH],3} = 2.1 \times 10^{6} \exp(-E_{[POOH]}/RT) \text{ mol litre}^{-1} \text{min}^{-1},$$

$$K = 3.9 \times 10^{22} \exp(-E_K/RT) \text{ min}^{-3},$$

where $E_\tau = 150$, $E_{[POOH]} = 69.5$, $E_K = 230$ kJ mol^{-1}.

Figure 9 presents the calculated curves for the absorption of oxygen and for the accumulation of POOH in a melt of LDPE subjected to oxidation at an oxygen pressure of 100 kPa and temperatures of 130 and 160 °C. These curves are matched by the following kinetic characteristics:

T/ °C	τ/min	υ_3 /mol kg^{-1} min^{-1}	$\upsilon_{[POOH],3}$ /mol kg^{-1} min^{-1}	K/ min^{-3}
130	160	0.006	1.05×10^{-3}	1.7×10^{-8}
160	12	0.076	1.45×10^{-2}	1.6×10^{-5}

The curves for LDPE obtained in another publication[9] at 150 °C (P_{O_2} = 100 kPa), which are not given in Fig. 9, are in good agreement with experimental data for $\tau = 35$ min, $\upsilon_3 = 0.036$, $\upsilon_{[POOH],3} = 0.005$ mol kg^{-1} min^{-1} and $K = 1.0 \times 10^{-6}$ min^{-3}. In the case of LDPE, the equality $C = [POOH]_1 = 0.02$ mol kg^{-1} also holds. The corresponding general equations have the following form:

$$\tau = 4.34 \times 10^{-15} \exp(E_\tau/RT) \text{ min},$$

$$\upsilon_3 = 8.86 \times 10^{13} \exp(-E/RT) \text{ mol kg}^{-1} \text{ min}^{-1},$$

$$\upsilon_{[POOH],3} = 1.48 \times 10^{13} \exp(-E_{[POOH]}/RT) \text{ mol kg}^{-1} \text{ min}^{-1},$$

$$K = 1.86 \times 10^{31} \exp(-E_K/RT) \text{ min}^{-3},$$

where $E_\tau = 128.4$, $E = 124.4$, $E_{[POOH]} = 124.4$, $E_K = 300$ kJ mol^{-1}. The average yield of hydroperoxide is $\varphi = 0.167$.

Figure 10 shows the calculated curves for the absorption of oxygen and accumulation of POOH in the EPC-1 and EPC-2 samples, the macromolecules of which contain 1.5 mass % and 24 mass % of propylene units, respectively.[51] In this case, the results of calculations are in good agreement with experimental data for the following kinetic parameters:

for EPC-1 — $C = [POOH]_1 = 0.01$ mol kg^{-1}, $\tau = 180$ min, $\upsilon_3 = 0.004$, $\upsilon_{[POOH],3} = 6.2 \times 10^{-4}$ mol kg^{-1} min^{-1}, $K = 1.0 \times 10^{-8}$ min^{-3}, $\varphi = 0.15$;

for EPC-2 — $C = [POOH]_1 = 0.02$ mol kg^{-1}, $\tau = 100$ min, $\upsilon_3 = 0.005$, $\upsilon_{[POOH],3} = 1.1 \times 10^{-3}$ mol kg^{-1} min^{-1}, $K = 2.8 \times 10^{-8}$ min^{-3}, $\varphi = 0.22$.

Similar calculated curves for samples of IPP-1 (with small spherulites) and IPP-2 (with large spherulites) subjected to oxidation at 130 °C and P_{O_2} = 40 kPa are presented in Fig. 2. Satisfactory agreement between theoretical and experimental results is attained with the following parameters:

for IPP-1 — $C = 0.025$ mol kg^{-1}, $[POOH]_1 = 0.01$ mol kg^{-1}, $\tau = 10$ min, $\upsilon_3 = 0.0365$, $\upsilon_{[POOH],3} = 0.005$ mol kg^{-1} min^{-1}, $K = 3.0 \times 10^{-6}$ min^{-3}, $\varphi = 0.14$;

for IPP-2 — $C = 0.025$ mol kg^{-1}, $[POOH]_1 = 0.01$ mol kg^{-1}, $\tau = 40$ min, $\upsilon_3 = 0.022$, $\upsilon_{[POOH],3} = 0.004$ mol kg^{-1} min^{-1}, $K = 1.7 \times 10^{-6}$ min^{-3}, $\varphi = 0.18$.

The theoretical curves for the accumulation of POOH in IPP-3 samples being oxidised in air (Fig. 11) were constructed for $C = [POOH]_1 = 0.01$ mol kg^{-1}. These curves are matched by the parameters presented below

T /°C	τ /h	$\upsilon_{[POOH],3}$ /mol kg^{-1} h^{-1}	K /h^{-3}
120	1	0.056	0.003
130	0.4	0.115	0.026
140	0	0.190	0.110

The general equations for the parameters τ, $\upsilon_{[POOH],3}$ and K on the minute time scale have the form

$$\tau = 6.66 \times 10^{-15} \exp(E_\tau/RT) \text{ min},$$

$$\upsilon_{[POOH],3} = 7.72 \times 10^{8} \exp(-E_{[POOH]}/RT) \text{ mol kg}^{-1} \text{ min}^{-1},$$

$$K = 1.94 \times 10^{23} \exp(-E_K/RT) \text{ min}^{-3},$$

where $E_\tau = 120$, $E_{[POOH]} = 90$, $E_K = 234$ kJ mol^{-1}.

Calculations show that the theoretical equations (11) and (15) for a heterophase process describe correctly the relationship between the curves for the absorption of oxygen and accumulation of POOH and account for their non-synchronism over a long time interval and for the succession of induction and self-acceleration periods and a steady-state period characterised by a constant rate of oxygen absorption. During these periods, the yield of POOH per mole of absorbed oxygen does not change, although the concentration of POOH passes through a maximum. This indicates that the process is mainly due to the reaction of POOH with the accumulating reaction products and that the contribution of the chain reaction of POOH is negligibly small.

Catalytic decomposition of polymeric hydroperoxides is characterised by a high effective activation energy E_K. In accordance with the heterogeneous scheme, the rate of catalytic reaction is determined by the rate of interaction of peroxyl radicals with the terminal ketone groups and of the condensation of POOH with acids (the activation energies of these reactions are E_5 and E_6, respectively). The occurrence of these reactions might require strong thermomechanical fluctuations able to extend a v-nanopore of the micellar sponge to the appropriate size. Thus for a LDPE melt, $E_K = 300$ kJ mol^{-1}, *i.e.* it is greater than the corresponding values for APP and IPP melts in which the activation energies are 230 and 234 kJ mol^{-1}, respectively; this can be due to the more ordered arrangement of the chain segments in LDPE [32, 53] (or to a smaller size of steady-state v-nanopores and greater relative increase in the volume during fluctuation beats).

When the degree of oxidation is high, the theoretical curves for the variation of the concentration of POOH presented in Figs 8–11 can markedly deflect downwards from the experimental points. This can be explained by assuming that the acids (catalysing decomposition of POOH) are lost due to evaporation and to side reactions which are not taken into account in the scheme. Evaporation of monomeric fragments from a polymer being oxidised is limited, unlike the transfer of oxygen,[54] by physical diffusion at any sample thickness admissible from the experimental standpoint; therefore, the average concentration of volatile acids depends on the thickness of polymer films, which substantially influences $[POOH]_{max}$.

It is also noteworthy that experimental curves *3*, *4* in Fig. 2 deviate at high degrees of oxidation from the theoretical curves *5*, *6* (when the concentration of POOH markedly decreases having passed through a maximum). Among other reasons, this may be due to the distortion of the amount of absorbed oxygen measured by a pressure gauge, caused by the accumulation of gaseous oxidation products, namely, CH_4, CO and H_2, which are not absorbed by sorbents meant for H_2O and CO_2 and do not freeze out at the liquid nitrogen temperature. These gases are not only evolved during polymer oxidation but are also formed in the gas-phase oxidation of the volatile oxidation products.

4. Phenomenological consequences

The sequential replacement of macroscopic stages of the reaction is a general feature of the oxidation of high-molecular-mass hydrocarbons (Fig. 12).

The whole set of experimental data presented in Fig. 12 can be described by only one curve, characterised by a rather long self-acceleration period.[4, 27] However, this masks the real patterns of individual curves for each particular polymer. Meanwhile, by distinguishing a series of points for each polymer (see Fig. 12), one can easily make sure that the self-accelerated stage, which follows the induction period, is actually much shorter and is soon replaced by a prolonged steady-state period, which obeys zero-order kinetics with respect to hydroperoxide, *i.e.* the pattern described above is represented in this case.

The above relation giving the induction period of the oxidation of LDPE [$\tau = 4.34 \times 10^{-15} \exp(128\,000/RT)$ min] can be supplemented by two other relations, which were derived from the plots taken from two publications:[27, 55] $\tau = 3.93 \times 10^{-12} \exp(107\,000/RT)$ min (see Ref. 27) and $\tau = 2.5 \times 10^{-9} \exp(85\,700/RT)$ min (Ref. 55). The presence of three different expressions for one polymer (LDPE) implies, on the one hand, that the activation energies E_τ vary over wide limits and, on the other hand, that the pre-exponential factor (τ_0) varies simultaneously with E_τ, *i.e.* the so-called compensation effect (CEF) is observed.[6]

For each of the above-mentioned polymers, the following relation holds:

$$\ln \frac{1}{\tau_0} = -12.0 + 3.6 \times 10^{-4} E_\tau.$$

The compensation effect is also displayed in the description of the steady-state rates of the accumulation of hydroperoxide in APP, IPP-3 and LDPE (in mol kg^{-1} min^{-1}):

for APP — $\upsilon_{[POOH],3} = 2.1 \times 10^{6} \exp(-69\,500/RT)$,

for IPP-3 — $\upsilon_{[POOH],3} = 1.93 \times 10^{9} \exp(-90\,000/RT)$ (recalculated in relation to the non-crystalline phase of the polymer),

for LDPE — $\upsilon_{[POOH],3} = 1.48 \times 10^{13} \exp(-124\,700/RT)$.

These formulae can be supplemented by the results of calculations performed using the plots given in the study by Iring *et*

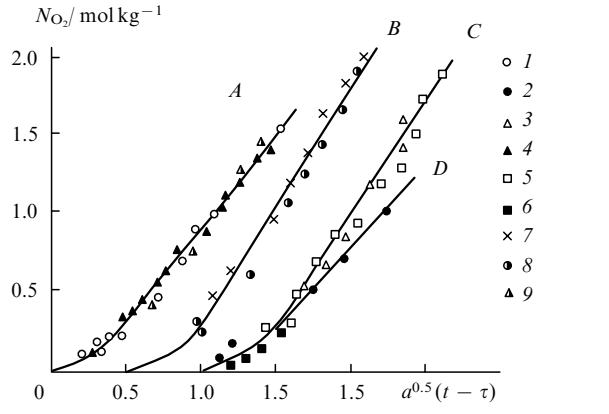


Figure 12. Amount of absorbed oxygen *vs.* the $a^{0.5}(t - \tau)$ value in the oxidation of several polymers:
(*1*) polyethylene (90 °C); (*2*) polypropylene (130 °C); (*3*) ethylene copolymer with 13.5% of propylene (130 °C); (*4*) poly-4-methylpent-1-ene (130 °C); (*5*) a vulcanised synthetic rubber (110 °C); (*6*) polystyrene (160 °C); (*7*) polyhept-1-ene (100 °C); (*8*) polynon-1-ene (100 °C); (*9*) epoxy rubber (200 °C).[4, 27]
Curves *B*, *C* and *D* are shifted relative to curve *A* along the abscissa axis by one (*B*) or two (*C*, *D*) scale units (one scale unit is equal to 0.5). The $a^{0.5}$ values, induction periods and oxygen pressures are given in a monograph [4].

al.[55] for the oxidation of LDPE (the value $\varphi = 0.17$ found for LDPE was employed in the calculations):

in the region of $T < T_m$,

$$\upsilon_{[POOH],3} = 1.87 \times 10^6 \exp(-76\,000/RT) \text{ mol kg}^{-1} \text{ min}^{-1},$$

in the region of $T > T_m$

$$\upsilon_{[POOH],3} = 4.25 \times 10^{15} \exp(-145\,000/RT) \text{ mol kg}^{-1} \text{ min}^{-1},$$

where T_m is the melting point of crystallites.

In this case, the relationship between the $E_{[POOH]}$ values and the pre-exponential factors ($\upsilon^0_{[POOH],3}$) is described by a common equation

$$\ln(\upsilon^0_{[POOH],3}) = -7.0 + 3 \times 10^{-4} E_{[POOH]},$$

which does not depend on the presence of substituents in macromolecules or on the change in $E_{[POOH]}$ following the transition of LDPE from the solid-like state to the molten state.

Attention is drawn to a peculiar inversion of the position of APP on the CEF plots; the point corresponding to this polymer is located right at the top of the straight section in the dependence of $\ln(1/\tau_0)$ on E_τ but it moves to the very bottom of the straight section in the dependence of $\ln(\upsilon^0_{[POOH],3})$ on $E_{[POOH]}$. Isotactic polypropylene behaves in a similar way.

The heterophase model of oxidation of polymers is at an early stage of development when structural-kinetic reaction models are tested; it still cannot provide a theoretical interpretation of the presence of CEF. However, even now, it is clear that the widely held opinion that the reaction rate should necessarily increase upon an increase in the molecular-segment mobility of macromolecules is unfounded.

Indeed, the rates of accumulation of the hydroperoxide groups at the third macroscopic stage of oxidation of molten APP and LDPE at 130 °C are 2.0×10^{-3} and 1.0×10^{-3} mol kg^{-1} min^{-1}, respectively; however, in solid IPP-3, this rate is 4.0×10^{-3} mol kg^{-1} min^{-1}.

It is noteworthy that, although IPP is oxidised faster than LDPE at 130 and 150 °C, the rate of the rupture of the IPP macromolecules determined by viscometry is 6 times as low.[42] According to our heterophase scheme, this fact, which had not been interpreted previously,[42] is associated with the existence of a competing pathway for the decomposition of the polymeric alkoxyl arising in the epoxide oxidation of IPP, accompanied by liberation of a methyl radical. No route of this type exists for LDPE; thus, the internal alkoxyl radicals formed in LDPE are mainly converted with the rupture of macromolecules.

We are reminded that statistical rupture of macromolecules (not related to the elimination of terminal fragments) can also take place in the s-zones of spongy micelles. The contribution of these events to the overall oxidative degradation is rather low due to the low mass fraction of polymeric s-segments. Meanwhile, in some cases, they can determine the physical essence of the process, for example, by ensuring the observance of the first kinetic order with respect to the initiator under conditions of chemically initiated relaxation of stress applied to cross-linked polymers.[56] The first order with respect to the initiator means that the mechanical strength of polymer samples under the experimental conditions is determined, first of all, by the degree of damage of the continuous three-dimensional paracrystalline framework, *i.e.* by the degree of development of the process that occurs directly in the s-zones of the spongy micelles.[21]

Yet another important remark concerns the coefficient C [see Eqns (9)–(12)], found for the IPP-1 and IPP-2 films ($C = 0.025$ mol kg^{-1}).[24, 31] This coefficient is exactly equal to the constant C determined previously in the experiments on anaerobic decomposition of hydroperoxide in films of previously oxidised IPP-1.[34] The point is that decomposition of POOH in this polymer in the absence of oxygen is due to a chain heterophase reaction, whose rate depends not only on the POOH concentration in the v-zones of spongy micelles but also on the POOH concentration in s-zones and is proportional to $[POOH]_s^{0.5}$. The initial concentration $[POOH]_s$ in an anaerobic reaction is determined using Eqn (7); therefore, the constant C characterises both the oxidation and the anaerobic process. Thus, the value $C = 0.025$ mol kg^{-1} reflects the real relationship between the rates of two heterophase processes which occur in the IPP-1 samples under conditions different in kind, namely, in the absence of oxygen and with active participation of oxygen.

It should be emphasised that the third macroscopic stage of the oxidation of a hydrocarbon polymer is not the last stage because the content of CH and OOH groups in the s-zones should sooner or later substantially decrease. This fact, together with the simultaneous change in the structure of molecular spongy micelles would inevitably produce a situation where Eqn (7) no longer holds and the reaction kinetics have changed. Nevertheless, the heterogeneous-heterophase model appreciably extends the capacities of the kinetic description of the oxidative transformation of hydrocarbon polymers.

V. Oxidation of molten polystyrene

The kinetic curves for the absorption of oxygen and accumulation of POOH in the oxidation of molten polystyrene (PS) (Figs. 13, 14), presented in a publication,[57] are qualitatively similar to those characterising oxidation of polyolefins. This is quite natural for a carbochain polymer with reactive CH bonds like PS, which is characterised by the same micellar spongy organisation of polymer chains as any non-crystalline polymer.[38] Meanwhile, the concentration of the POOH groups formed in PS is 100 times lower (Fig. 14).

Our calculations showed that the experimental data found in the study cited[57] are adequately described by theoretical equations (11) and (15). Using these equations, the following values were found for the parameters τ, K, and φ

T /°C	τ /h	υ_3 /mol kg^{-1} h^{-1}	$10^3\,\upsilon_{[POOH],3}$ /mol kg^{-1} h^{-1}	K /h^{-3}	$10^2\,\varphi$
180	0.4	0.06	1.35	0.07	2.25
190	0.05	0.14	2.35	0.44	1.68
200	~0.00	0.30	3.8	2.8	1.27
210	~0.00	0.61	–	–	–

The coefficient C (2.0×10^{-4} mol kg^{-1}) and the concentration of $[POOH]_1$ (1.5×10^{-4} mol kg^{-1}) are constant in the temperature range of 180–210 °C.

The relevant generalised expressions used to calculate υ_3, $\upsilon_{[POOH],3}$, and K have the form (on the minute time scale)

$$\upsilon_3 = 9.7 \times 10^{12} \exp(-138\,500/RT) \text{ mol kg}^{-1} \text{ min}^{-1},$$

$$\upsilon_{[POOH],3} = 3.6 \times 10^5 \exp(-88\,300/RT) \text{ mol kg}^{-1} \text{ min}^{-1},$$

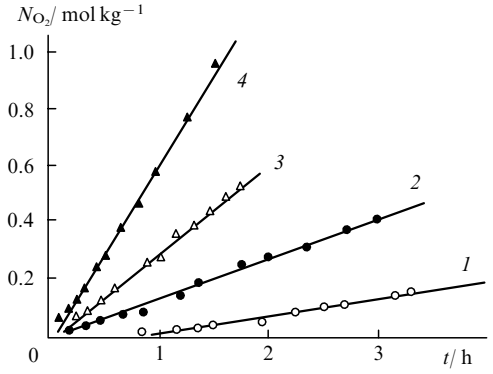


Figure 13. Oxygen absorption during oxidation of a PS melt at 180 (*1*), 190 (*2*), 200 (*3*) and 210 °C (*4*) and $P_{O_2} = 26.7$ kPa.[57]

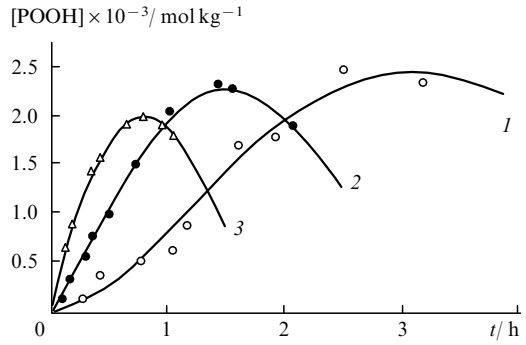


Figure 14. Calculated curves for hydroperoxide accumulation during oxidation of a PS melt at 180 (*1*), 190 (*2*) and 200 °C (*3*) (the dots correspond to experimental data from Ref. 57).

$$K = 7.6 \times 10^{10} \exp(-151\,000/RT)\ \text{min}^{-3}.$$

Polystyrene is much less reactive in oxidation than polyolefins. When comparing characteristics of oxidation of PS with the corresponding characteristics of polyolefin oxidation, one can note lower C and $[POOH]_1$ values.

The low C and hydroperoxide concentrations $[POOH]_1$ at the end of the induction period are due to high fluctuation mobility of the molecular sponge in a PS melt. This is indicated by the expression $C = k_{0s}k_{-f}(k^f k_f)^{-1}$, the denominator of which is the product of the fluctuation rate constants. In this particular case, it is 100 times as great as that for an LDPE melt. Presumably, the much higher frequency of beats of the nanopores in the PS sponge ensures a higher rate of migration of the OOH groups from the v-zones of spongy micelles to s-zones

$$POOH_v \longrightarrow POOH_f \longrightarrow POOH_s,$$

and a higher rate of the radical-free bimolecular reaction,

$$POOH_f + POOH_s \xrightarrow{k^f} 2POH + O_2,$$

which manifests itself as the fulfillment of Eqns (7), (8), (11) and (13).

In view of the high flickering activity of nanopores in the molecular sponge of PS, a simultaneous increase in the rate of the quadratic termination of reaction v-chains should be expected. However, the notation chosen previously for this step of the oxidation of polyolefins,

$$2POO^{\bullet} \xrightarrow{k_t} \text{termination}$$

does not reflect in an explicit form the influence of the structural factor and formally corresponds to a homogeneous reaction. This simplified approach does not change much the kinetic description of the oxidation of high-molecular-mass polyolefins; however, when considering a wider range of objects, it is necessary to define the chain termination mechanism in more detail.

A more precise scheme of reactions of polymeric peroxyl radicals in the molecular sponge should include the steps of fluctuation excitation and deactivation of the nanopores in which the peroxyl radicals are located and the step of peroxyl migration into a common nanopore and should also reflect the competition between the reaction steps and the departure of the peroxyls from the common nanopore

$$POO^{\bullet} \underset{k_{-t,1}}{\overset{k_{t,1}}{\rightleftharpoons}} POO^{\bullet}_f,$$

$$POO^{\bullet}_f + POO^{\bullet} \xrightarrow{k_{t,2}} (POO^{\bullet} + POO^{\bullet})_f,$$

$$(POO^{\bullet} + POO^{\bullet})_f \xrightarrow{k_{t,3}} \text{termination},$$

$$(POO^{\bullet} + POO^{\bullet})_f \xrightarrow{k_{t,4}} POO^{\bullet}.$$

By applying the steady-state concentration condition to fluctuationally excited peroxyls and radical pairs, one can easily derive an expression for the chain termination rate

$$\upsilon_t = -\frac{d[POO^{\bullet}]}{dt} = \frac{2k_{t,1}k_{t,2}k_{t,3}[POO^{\bullet}]^2}{(k_{-t,1} + k_{t,2}[POO^{\bullet}])(k_{t,3} + k_{t,4})}.$$

When the probability of deactivation of the fluctuationally excited peroxyls is high, *i.e.* $k_{-t,1} > k_{t,2}[POO^{\bullet}]$, this expression acquires the form

$$\upsilon''_t = \frac{2k_{t,1}k_{t,2}k_{t,3}}{k_{-t,1}(k_{t,3} + k_{t,4})}[POO^{\bullet}]^2 = k''_t[POO^{\bullet}]^2, \qquad (17)$$

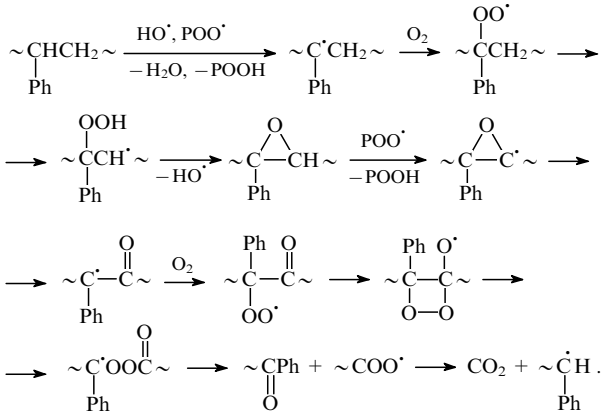
and when the frequency of encounter of two peroxyls in one nanopore is high, *i.e.* $k_{-t,1} < k_{t,2}[POO^{\bullet}]$, it has the form

$$\upsilon'_t = \frac{2k_{t,1}k_{t,3}}{k_{t,3} + k_{t,4}}[POO^{\bullet}] = k'_t[POO^{\bullet}]. \qquad (18)$$

Although Eqn (17) implies a quadratic dependence of the termination rate on the peroxyl concentration, it actually refers to a heterogeneous process. Equation (18) describes heterogeneous linear termination of reaction chains, which would be impossible if equivalent peroxyl radicals reacted in a homogeneous medium.

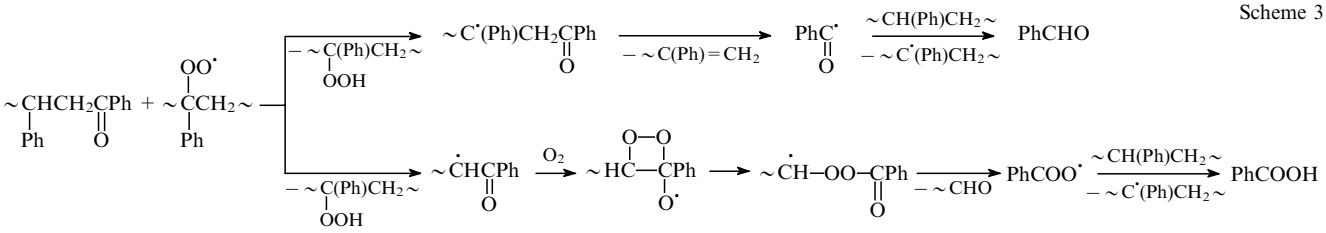
The fact that the kinetics of oxidation of PS are described by Eqns (11) and (15) implies the quadratic chain termination in accordance with Eqn (17). Thus, the low rate of oxidation of PS (compared to polyolefins) can be attributed to the great value of the termination rate constant $k''_t = 2k_{t,1}k_{t,2}k_{t,3}/k_{-t,1}(k_{t,3} + k_{t,4})$; this is due to the fact that the rate constant for the fluctuations ($k_{t,1}$) is high and the rate constant for the 'collapse' of the v-nanopores with an increased size to the initial size ($k_{-t,1}$) is low. The benzene rings present in PS occupy room in nanopores and thus decrease the probability of their 'collapse'. As a consequence, the fluctuation oscillations of the surrounding sponge units become cooperative. The constant $k_{t,2}$ for the capture of the OOH groups by flickering nanopores can increase for the same reason.

The mechanisms of heterophase initiation and termination of reaction chains in the zones of the PS matrix do not change due to the presence of the benzene rings; therefore, expressions (7) and (13) for the steady-sate concentrations of peroxyl radicals remain valid. The qualitative similarity of the oxidation kinetics of PS and polyolefins implies that the chemical reactions involved in these two processes are the same. In particular, in PS, the terminal ketone groups are formed *via* the following route



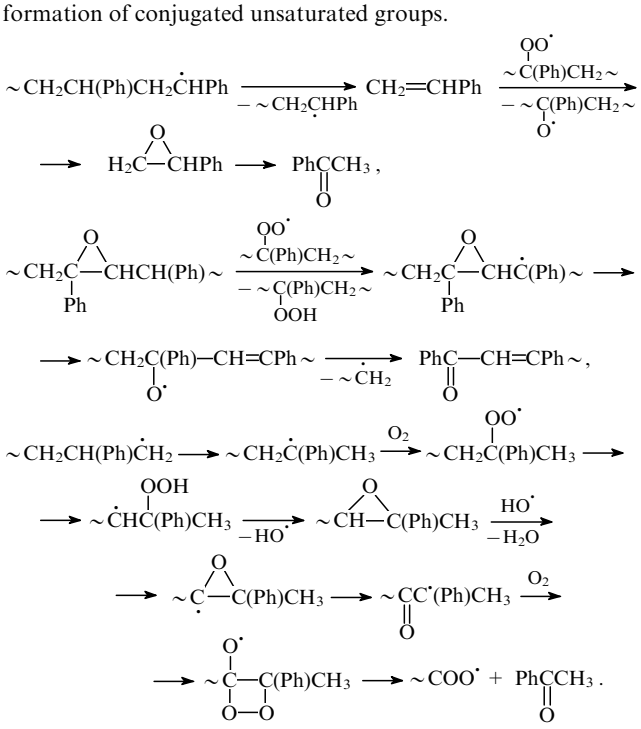
In turn, the terminal ketone groups serve as the source of formation of bnzaldehyde and benzoic acid (Scheme 3).

Scheme 3



The benzoic acid accumulated in the PS melt catalyses decomposition of POOH according to Eqn (15). Benzoic acid is stronger than aliphatic carboxylic acids; therefore, it condenses more efficiently with the POOH groups to give the intermediate alkylaromatic peroxo ester, which dissociates at the peroxide bond more readily than aliphatic peroxo esters.

The formation of acetophenone can be interpreted as being due to the oxidation of the styrene formed or to transformations of the epoxide derivatives accompanied by the simultaneous formation of conjugated unsaturated groups.



In the oxidation of LDPE, the rates of formation of POOH and epoxide rings are determined by the rates of abstraction of hydrogen atoms by peroxyls, which are characterised by constants k_2 and k_3, respectively, and have nearly equal activation energies E_2 and E_3. As a consequence, the equality $E_{[POOH]} = E$ holds and the yield of hydroperoxide, found from the formula

$$\varphi = \frac{k_2[POO^{\bullet}]}{(k_2 + \eta k_3)[POO^{\bullet}]},$$

does not depend on the temperature ($\varphi = 0.167$).

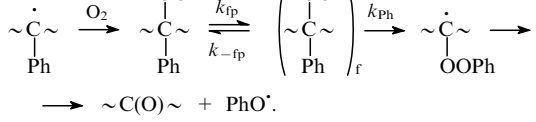
Meanwhile, oxidation of PS is subject to the inequality $E > E_{[POOH]}$, which accounts for the decrease in the yield of hydroperoxide following an increase in the temperature.

T/°C	130	180	190	200
$10^2\,\varphi$	11.8	2.25	1.68	1.27

This indicates the existence of yet another route of peroxyl conversions, which competes with the formation of POOH and epoxide rings. The existence of this route does not alter the mechanism of reaction chain termination; however, since it has a higher activation energy than E_2 or E_3, the rate of oxygen consumption increases with temperature. This route is taken into account in the equation for the hydroperoxide yield as an additional term in the denominator

$$\varphi = \frac{k_2[POO^{\bullet}]}{(k_2 + \eta k_3 + k_{Ph})[POO^{\bullet}]},$$

where k_{Ph} is the rate constant for this new process. The most probable reaction of this sort is attack by the peroxyl oxygen on the neighbouring benzene ring followed by elimination of free phenoxyl



The free space needed for this process can arise due to the volume beats of nanopores.

The free phenoxyl radical thus formed continues the reaction chain, being converted into phenol, owing to its relatively high reactivity and to the high temperature of PS oxidation. The formation of phenol in the oxidation of PS has been confirmed experimentally.[58, 59]

VI. Oxidation of molten poly(ethylene oxide)

Poly(ethylene oxide) (PEO) — a polyether with the molecular mass M_n = 20 000 ($T_m \sim 60$ °C) — was the first polymer the oxidation of which was considered in terms of the heterophase chain reaction model. During the oxidation of a PEO melt, as in the case of hydrocarbon polymers, the concentration of POOH groups first increases to reach a definite maximum value and then gradually decreases. Meanwhile, the rates of oxygen absorption, consumption of the CH bonds, and accumulation of aldehyde groups reach a constant value and then remain invariant.[15, 18, 19]

At temperatures below 100 °C, the rates υ_3 and $\upsilon_{[POOH],3}$ depend substantially on the way used to apply the initial polymer powder (weighing several milligrams) onto the surface of the ampoules in which the oxidation is performed.[18] This is due to the fact that during melting, PEO particles experience the influence of two opposing mechanical forces — adhesion, which keeps the material on the surface, and cohesion, which induces sintering of the particles into a lump. The balance of forces depends on the bulk weight of the powder, particle size and the shape of the conglomerate formed. These characteristics can vary over wide limits, which results in elastoplastic deformations of polymer chains and influences the reaction rate.

In the oxidation of films of molten PEO, closest to the thermomechanical equilibrium, the rate of oxygen absorption υ_3 reaches a constant level much earlier than the maximum concentration of POOH is attained; the yield of hydroperoxide

$$\varphi = \frac{\upsilon_{[POOH],3}}{\upsilon_3} = 0.6$$

remains invariant despite the extremum pattern of the variation of the POOH concentration during the reaction (Figs 4, 15).

According to experimental data,[19] oxidation of PEO at 99 °C is characterised by $\upsilon_3 = 1.5$ mol kg^{-1} h^{-1} and $\upsilon_{[POOH],3} = 0.9$ mol kg^{-1} h^{-1}. The difference $\upsilon_3 - \upsilon_{[POOH],3} = 0.6$ mol kg^{-1} h^{-1} is nearly equal to the total consumption of oxygen for the formation of a volatile carboxylic acid

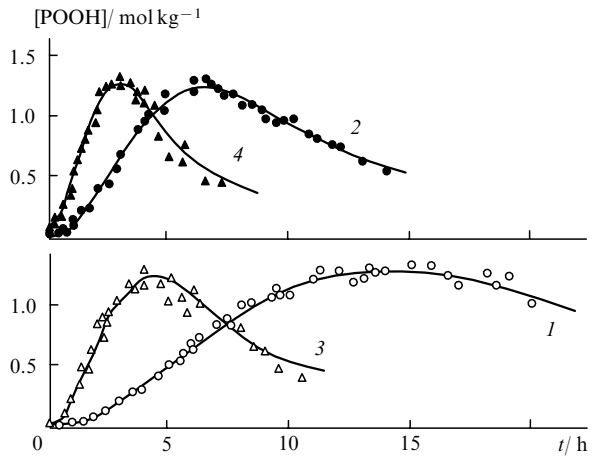


Figure 15. Calculated curves for hydroperoxide accumulation during oxidation of molten PEO in air at 80 (*1*), 90 (*2*), 95 (*3*) and 99 °C (*4*) (the dots correspond to experimental data from Ref. 18).

(0.2 mol kg^{-1} h^{-1}) and ester groups in the polymer (0.35 mol kg^{-1} h^{-1}). Accumulation of polymeric aldehydes proceeds at a high rate (5 mol kg^{-1} h^{-1}) without the addition of gas-phase oxygen to macromolecules.

It is worth noting that oxidation of PEO in chlorobenzene and dichlorobenzene (75–95 °C) follows a mechanism of homogeneous chain reaction with the quadratic termination of reaction chains;[60] this was demonstrated using an initiator — azobisisobutyronitrile. For low degrees of the initiated reaction, the amount of POOH formed coincides almost entirely with the amount of absorbed oxygen. This indicates that the contribution of reactions of alkyl and peroxyl macroradicals resulting in the rupture of polymer chains is insignificant.

The initiated oxidation of PEO in solution gives rise to ester groups. The initial rate of formation of these groups is close to zero but it increases to reach a constant value as POOH groups are accumulated.[61] This finding points to the occurrence of induced decomposition of hydroperoxide

$$\sim CH_2CH(OOH)O\sim \xrightarrow[-ROOH]{ROO^{\bullet}} \sim CH_2\dot{C}(OOH)O\sim \longrightarrow$$

$$\longrightarrow \sim CH_2C(O)O\sim + HO^{\bullet},$$

$$HO^{\bullet} + \sim CH_2CH_2O\sim \longrightarrow H_2O + \sim CH_2\dot{C}HO\sim$$

($ROO^{\bullet}$ is a peroxyl radical of the initiator). In addition, this means that the probability of α- and β-isomerisation is relatively low. The β-isomerisation steps still do occur, although at a low rate, and thus ensure rupture of internal bonds in macromolecules

$$\sim CH(OO^{\bullet})CH_2O\sim \longrightarrow \sim CH(OOH)\dot{C}HO\sim \xrightarrow[-HO^{\bullet}]{}$$

$$\longrightarrow \sim \underset{\diagdown\,O\,\diagup}{CH{-}CHO}\sim \xrightarrow[-H_2O]{HO^{\bullet}} \sim \underset{\diagdown\,O\,\diagup}{CH{-}C^{\bullet}O}\sim \longrightarrow \sim \dot{C}HCOO\sim \xrightarrow{O_2}$$

$$\longrightarrow \sim CH(OO^{\bullet})COO\sim \longrightarrow \sim \underset{O{-}O}{\overset{O^{\bullet}}{\overset{|}{HC{-}CO}}}\sim \longrightarrow$$

$$\longrightarrow \sim H\dot{C}OOCO\sim \longrightarrow \sim CHO + {}^{\bullet}OCO\sim,$$

$$\overset{\bullet}{O}COCH_2CH_2\sim \xrightarrow[-CO_2]{} \sim CH_2CH_2O^{\bullet} \xrightarrow[-\sim CH_2\dot{C}HO\sim]{\sim CH_2CH_2O\sim} \sim CH_2CH_2OH\,.$$

We would like to emphasise that the rate of scission of PEO macromolecules in solutions is relatively low and decreases during the reaction.[61]

Oxidation of low-molecular-mass molten PEO (M_n = 6000), unlike oxidation of PEO in solution, is accompanied, even at high temperature (145 °C), by vigorous formation of water and ester groups (at low concentrations of POOH). Apparently, under these conditions, the macromolecules are not split at the internal bonds.[62] The same is true for oxidation of molten low-molecular-mass tetraethylene glycol, which is a homologue of PEO.[63] The difference between the oxidation processes in solutions and in melts is apparently due to the high concentration of CH_2 groups in the melts and to the predominant role of intermolecular propagation of oxidation chains. The frequency of contacts between macromolecules in solutions of PEO is much lower than in the melts; therefore, the role of intramolecular oxidation increases.

High-molecular-mass molten PEO, unlike the low-molecular-mass homologue, tends to undergo rather vigorous rupture of polymer chains under oxidation conditions. What is significant is that this process does not involve chemical binding of molecular oxygen. This specific feature can be interpreted by assuming that in the melt, long PEO molecules form heterophase spongy micelles, which contain zones with relatively large supernanopores. In these zones, oxygen molecules reside most of the time in the adsorbed state on the pore walls; hence, the alkyl macroradicals formed in the polymer s-segments can react without being oxidised. In view of the foregoing, by analogy with the mechanism of oxidation of polyolefins, the following scheme of reactions in the s-zone can be proposed:

$$\underset{PH_s}{(\sim CH_2CH_2O\sim)_s} + O_{2,s} \xrightarrow{k'_{0s}} \delta_1(\sim CH_2\dot{C}HO\sim)_s,$$

$$\underset{P^{\bullet}_s}{(\sim CH_2CH_2OCH_2\dot{C}HO\sim)_s} \xrightarrow{k_d} \sim CH_2\underset{A}{\overset{O}{\overset{\|}{C}}}\overset{H}{\diagdown} + \underset{R^{\bullet}_s}{(\sim OCH_2\dot{C}H_2)_s},$$

$$\underset{R^{\bullet}_s}{(\sim OCH_2\dot{C}H_2)_s} \xrightarrow[\text{isomerisation}]{k_{1s}} \underset{R^{\bullet}_{1s}}{(\sim O\dot{C}HCH_3)_s}$$

$$\xrightarrow{k_{2s},\ R^{\bullet}_{1s}} \text{products}$$

$$\xrightarrow{k_{3s},\ PH_s} \sim OCH_2CH_3 + (\sim CH_2\dot{C}HO\sim)_s$$

This scheme, unlike that considered above, takes into account the participation of the terminal $R^{\bullet}_s$ radicals in the chain propagation steps giving rise to the $\sim CH_2C^{\bullet}HO\sim$ radicals, which then dissociate to yield aldehydes.

Full scheme of the oxidation process covers also the inter-zone chemical induction

$$\underset{R^{\bullet}_s}{(\sim OCH_2\dot{C}H_2)_s} \rightleftharpoons \underset{R^{\bullet}_m}{(\sim OCH_2\dot{C}H_2)_m},$$

$$(\sim OCH_2\dot{C}H_2)_m \xrightarrow{O_2} \left(\sim OCH_2CH_2\overset{|}{OO^{\bullet}}\right)_m \longrightarrow \left(\sim OCH_2CH^{\bullet}\overset{|}{OOH}\right)_m \longrightarrow$$

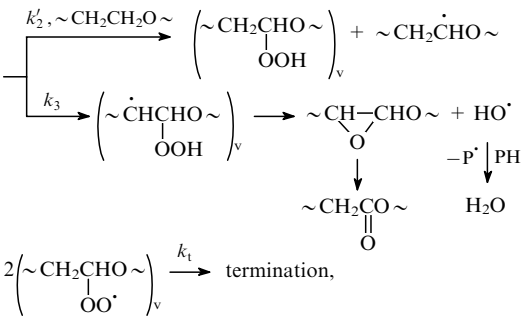
$$\longrightarrow \sim OCH_2\underset{A}{\overset{O}{\overset{\|}{C}}}\overset{H}{\diagdown} + HO^{\bullet}_m,$$

$$HO^{\bullet}_m \longrightarrow HO^{\bullet}_v,$$

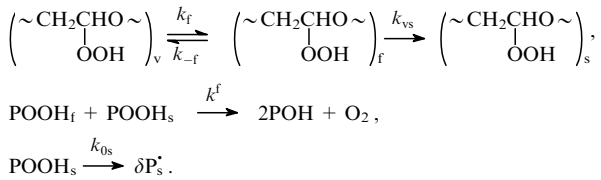
the oxidation chains in v-zones

$$\underset{PH}{HO^{\bullet}_v + \sim CH_2CH_2O\sim} \xrightarrow{k'_1} H_2O + (\sim CH_2\dot{C}HO\sim)_v,$$

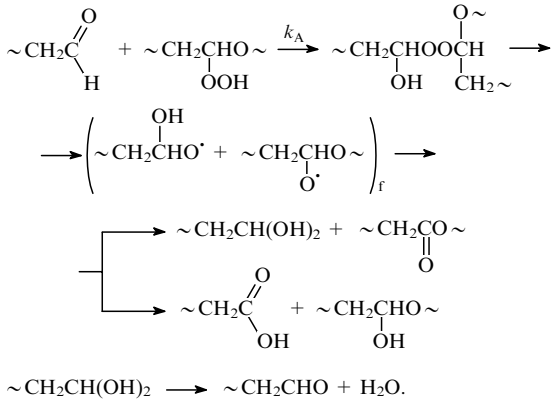
$$(\sim CH_2\dot{C}HO\sim)_v \xrightarrow{O_2} \left(\sim CH_2\underset{|}{\overset{OO^{\bullet}}{\overset{|}{C}}}HO\sim\right)_v \longrightarrow$$



and the steps of occupation of s-zones by hydroperoxide



The main differences between the oxidation mechanisms of PEO and polyolefins are associated with the formation of aldehydes *via* a chain reaction in s-zones and with the decomposition of hydroperoxide *via* the intermediate condensation of aldehydes with POOH considered below



According to this scheme, simultaneously with regeneration of aldehydes, carboxylic acids, which also catalyse decomposition of POOH, can be accumulated in a PEO melt. However, the amount of carboxylic acids is much smaller than that of aldehydes and their role as catalysts must be insignificant.

This heterophase scheme accounts for the existence in the oxidation of PEO of macroscopic induction and self-accelerated periods and a period of steady-state oxidation with a zero order with respect to hydroperoxide. However, the differential kinetic equation describing the variation of the concentration of POOH differs somewhat from the corresponding equation for polyolefins.

By applying the condition of steady-state concentrations to the free radicals appearing in the s-scheme, one can easily derive an expression for the rate of accumulation of aldehydes (A):

$$\upsilon_A = \frac{d[A]}{dt} = k_d[P_s^{\cdot}] = \frac{k_{3s}[PH_s]\upsilon_i}{2k_{1s}},$$

where υ_i is the rate of generation of free radicals in s-zones.

Since the CH bonds are highly reactive, oxidation of PEO soon passes from the induction period to the self-accelerated stage in which the relation

$$\upsilon_i = \delta\, k_{0s}[POOH]_s = \frac{\delta k_{0s}k_{vs}k_f[POOH]_v}{k_{-f}k_{0s} + k^f k_f[POOH]_v}.$$

starts to be obeyed.

Substitution of this relation to the expression for υ_A and taking into account that $k_{-f}k_{0s} < k^f k_f[POOH]_v$ (the self-accelerated stage is much shorter than the subsequent stages of the process) gives a simplified equation for the rate of accumulation of aldehydes

$$\upsilon_A = k_{3s}[PH_s]\frac{\delta k_{0s}k_{vs}}{2k_{1s}k^f} = \upsilon_{A,3},$$

where $\upsilon_{A,3}$ is the maximum constant rate of accumulation of aldehydes in the third stage of oxidation.

The equation for the overall rate of variation of the POOH concentration in the oxidation of PEO has the form

$$\frac{d[POOH]}{dt} = \frac{\upsilon_{[POOH],3}}{(1 + C/[POOH])^{0.5}} - k_A[POOH][A], \qquad (19)$$

where k_A is the effective rate constant for the condensation. Substitution into relation (19) of the concentration of aldehyde

$$[A] = \upsilon_{A,3}t = k_{3s}[PH_s]\frac{\delta k_{0s}k_{vs}}{2k_{1s}k^f}t,$$

gives the final equation for the rate of accumulation of POOH

$$\frac{d[POOH]}{dt} = \frac{\upsilon_{[POOH],3}}{(1 + C/[POOH])^{0.5}} - K[POOH]t,$$

where

$$K = k_A k_{3s}[PH_s]\frac{\delta k_{0s}k_{vs}}{2k_{1s}k^f}. \qquad (20)$$

The points determined from the experimental data obtained in Ref. 18 fit well in the integral curves calculated from Eqn (20) using the Runge–Kutta method (Fig. 15). The curves shown in Fig. 15 were constructed using the values $C = 0.08$ mol kg^{-1} and $[POOH]_1 = 0.02$ mol kg^{-1} (the concentration of POOH at the end of the induction period) and the following kinetic parameters:

T /°C	τ /h	$\upsilon_{[POOH],3}$ /mol kg^{-1} h^{-1}	K /h^{-2}
80	1.5	0.184	0.0105
90	0.7	0.40	0.0504
95	0.4	0.60	0.122
99	0.25	0.90	0.263

These parameters match the general formulae of the form

$$\tau = 3.7 \times 10^{-13}\exp(-97\,400/RT)\ \text{min},$$

$$\upsilon_{[POOH],3} = 1.0 \times 10^{11}\exp(-91\,400/RT)\ \text{mol kg}^{-1}\ \text{min}^{-1},$$

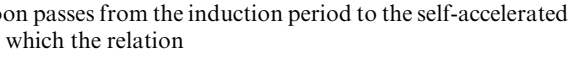
$$K = 1.42 \times 10^{21}\exp(-180\,600/RT)\ \text{min}^{-2}.$$

The experimental dependence of the rate of oxygen absorption υ_3 on the pressure of oxygen P_{O_2} at 95 °C found by Mikheev *et al.*[19] is described by the theoretical equation for the heterophase process (see Section IV)

$$\upsilon_3 = -\frac{aP_{O_2}^{0.5}}{(b + P_{O_2})^{0.5}},$$

where $a = 0.79$ mol kg^{-1} h^{-1}, $b = 1.0 \times 10^{-4}$ Pa.

As regards the mechanism of the catalytic decomposition of POOH, it can be assumed that the terminal aldehyde groups, which differ from internal units by a higher fluctuation mobility, are more efficient in approaching the OOH groups, which are mainly localised in the internal units of macromolecules. In this case, the effective rate constant for the condensation



has the form

$$k_A = \frac{k'_A k_{fA}}{k_{-fA}}, \qquad (21)$$

where k_{fA} and k_{-fA} are the frequencies of the fluctuation excitation and deactivation, respectively, of v-nanopores containing aldehyde groups and k'_A is a quasi-elementary constant, which corresponds to the activation energy E'_A.

The activation energy E'_A can be estimated by using the above expression for the constant k_A, appearing in the relation for K. For this purpose, we multiply the numerator and denominator of this expression by k_f and replace k_A by the value from Eqn (21)

$$K = \frac{k'_A k_{fA} k_{3s} [PH_s] \delta k_{0s} k_{vs} k_f}{2 k_{-fA} k_{1s} k^f k_f}.$$

Let us assume that the reactions with the abstraction of hydrogen atoms (they are characterised by the constants k_{1s} and k_{3s} in the scheme) have virtually equal activation energies ($E_{1s} \approx E_{3s}$). Keeping in mind that the constant C does not depend on the temperature and assuming that the activation energy of the 'collapse' of the excited nanopores is equal to zero ($E_{-f} = E_{-fA} \approx 0$), we obtain the equality $E_{0s} = E^f + E_f$. By examining the expression for the constant K, we can find that the effective activation energy related to K ($E_K = 180.6$ kJ mol^{-1}) is the sum

$$E_K = E'_A + E_{fA} + E_{vs} + E_f.$$

Hence,

$$E'_A = 180.6 - E_{fA} - E_{vs} - E_f.$$

Since the fluctuation excitation of nanopores and the migration of OOH groups (with the constants k_f, k_{fA} and k_{vs}) are limited [33] by kinetic jumps of the PEO chain segments and the activation energy of this process is ~ 40 kJ mol^{-1}, the E'_A value is found to be equal to ~ 60 kJ mol^{-1}; this fits in the series of values for the effective activation energy of the corresponding liquid-phase transformation.[64]

The results of calculations lead to the following conclusions.

1. The fact that the kinetics of accumulation of POOH in a PEO melt at 80–100 °C are described by the single kinetic equation (20) of the heterophase process indicates that the structure of the micellar framework of s-zones is rapidly restored during oxidation, despite the destruction of s-units of macromolecules to give aldehydes.

2. Poly(ethylene oxide) is oxidised much faster than polypropylene, although the effective activation energies ($E_{[POOH]}$) in these two cases are close (90 and 91.4 kJ mol^{-1} for IPP-3 and PEO, respectively). This is due to the large difference between the pre-exponential factors in the expressions for the oxidation rate $v_{[POOH],3}$ (the corresponding factors are 1.93×10^9 and 1.0×10^{11} mol kg^{-1} min^{-1}); in all probability, this is a consequence of the specific features of the heterogeneous mechanism of the oxidation chain termination.

According to Eqn (17), the rate constant for the heterogeneous chain termination k_t comprises several partial structure-mechanical constants, which are directly related to the fluctuation activity of the sponge units in the micellar grains of the polymeric matrix. In the case of PEO, which differs from IPP-3 by the absence of substituents and the presence of a large number of polar ether bonds and, hence, by a high density of intermolecular contacts, restructuring of the sponge during the volume beats of nanopores is apparently hampered. This should either decrease the probability of formation of a pair of peroxyl radicals in one nanopore or increase the probability of the escape of peroxyl radicals from the intermediate radical pairs.

It should also be emphasised that the activation energy of oxidation of molten PEO is lower than the activation energy of oxidation of a solution of PEO in trichlorobenzene,[62] which is equal to 147 kJ mol^{-1}. This attests that the molecular-sponge structure, typical of a block polymer, is not formed in solution.

VII. Characteristic features of initiated oxidation of polymers

Initiators are finding extensive practical application in the studies of the kinetics of polymer oxidation. It is believed that they can stabilise for some period the rate of initiation of the transformations (v_{i0}) and thus ensure the non-branching-chain reaction mode. The researchers relying on the theory of homogeneous liquid-phase oxidation often restrict the measurements to the oxygen absorption rate.[8] By calculations carried out in terms of homogeneous schemes, researchers find the apparent length of the oxidation chains and other kinetic parameters, which allow theoretical construction of the initial sections of kinetic curves for the absorption of oxygen; the results obtained by different authors can be compared more or less successfully.

When oxidation of polymers is treated as a homogeneous process, the scope of the use of the initiation method in kinetic investigations is restricted by several conditions.[8] In particular, it is required that the initiator be the main source of radicals throughout the experiment (t) {*i.e.* the condition $v_{i0} > k_i$[POOH] should hold}; the admissible working time interval estimated from the inequality $k_i t < 1$ should be ~ 1000 s. The restrictions imposed on the parameters of initiated processes actually result in a purely formal mathematical description of the short stage of the process. This description is in fact adjusted to the known schemes of homogeneous reactions.

Meanwhile, as shown above, the kinetic features of the polymer process do not fit into the framework of the homogeneous reaction model. In the preceding Sections, we disclosed the mechanism of successive macroscopic stages of oxidation, caused by functioning in polymers of a 'structural-kinetic filter,' restricting the migration of free radicals and hydroperoxide between the structural zones of the matrix. This structural filter is also effective in the case of initiated oxidation of PEO and polyolefins.[15, 19, 20] This is why the introduction of initiators, which reduce the time it takes to reach the maximum rate of the chain reaction, does not increase the maximum rate; excess initiator is either wasted (Fig. 4, 5) or even decreases the oxidation rate.[19]

It should be noted that kinetic features of the initiated oxidation of polymers can be elucidated much more comprehensively by analysing them in terms of heterophase models.

1. Structural filter effects

The presence of a structural filter, restricting transfer of the radicals formed upon decomposition of the initiator, is indicated, for example, by the kinetic curves for the variation of the total concentration of peroxides in IPP samples being oxidised in air at 100 °C in the presence of dibenzoyl peroxide [21] (see Fig. 5). In the absence of BP, oxidation of IPP at 100 °C has an extended induction period (~ 35 h). In the presence of BP, the induction period vanishes; however, dibenzoyl peroxide, which readily dissociates and ensures an appreciably higher rate of initiation in homogeneous solutions than POOH, does not realise in full measure its potential as a source of free radicals. Curves *1* and *2* in Fig. 5 indicate that BP substantially accelerates oxidation of IPP; however, when its content is fairly high, the role of the leading initiator rapidly passes to hydroperoxide, while the BP itself becomes an inefficient ballast.

The unproductive loss of the initiator seems to be due to the 'cage effect,' which is considered in the literature as an analogue of the Franck–Rabinovich homogeneous liquid-phase effect.[8] However, this approach does not provide interpretation of the curves in Fig. 5. In particular, curve *2* shows that accumulation of POOH proceeds at a constant rate from the very first moment when decomposition of BP has just begun (curve *3*).

On the one hand, it can be suggested that only the first, minor portion of the initiator is active in the oxidation of IPP; after this portion has decomposed, the process is initiated only by hydroperoxide. In this case, the main bulk of BP should be located as if inside exceptionally rigid 'cages,' which do not let free radicals

migrate to the bulk of the polymeric matrix. In this case, BP is consumed for no result.

On the other hand, one can suggest with equal success that the free radicals formed from BP migrate to the matrix bulk throughout the whole period of BP decomposition, *i.e.* BP does not lose the initiating activity at the beginning. In this case, the invariance of the rate of POOH accumulation observed from the beginning (curve *2*) under conditions of continuous decomposition of BP (curve *3*) can be interpreted as pointing to the migration of the free radicals derived from BP from the 'homogeneous liquid-phase cages' to the matrix bulk, which is first insignificant and then permanently increases during the process. It can be easily seen that these two 'cage' models are mutually exclusive.

In addition, the homogeneous model of oxidation does not answer the following questions: why does the rate of accumulation of POOH at a relatively high initial concentration of BP (curve *2*) remain constant even when BP has completely decomposed? and why do the rates of accumulation of POOH corresponding to the straight sections of curves *1*, *2* remain equal and not increase as its concentration grows?

Such 'abnormal features' of the kinetic curves shown in Fig. 5 can be interpreted within the framework of the model of coupled heterophase s- and v-reaction chains. It should be borne in mind that the initiator molecules decompose mainly in the s-zones of the molecular spongy micelles,[16, 38, 65] into which they get *via* inter-zone exchange. The BP concentration in the s-zones is

$$c_s = \frac{K_e c}{\beta},$$

where K_e is the equilibrium constant for the migration of BP molecules between the zones, c is the overall BP concentration calculated for the whole sample, and β is the fraction of non-crystalline polymeric phase.

When the polymer contains no POOH in the beginning of the process, the following reactions proceed in the s-zone:

$$\left(\mathrm{PhC(O)-OO-C(O)Ph}\right)_s \xrightarrow{k_{BP,s}} 2\mathrm{PhC(O)O^{\bullet}_s},$$

$$\mathrm{PhC(O)O^{\bullet}_s + PH_s \xrightarrow{k_{1,BP}} P^{\bullet}_s + PhC(O)OH_s},$$

$$\mathrm{P^{\bullet}_s \xrightarrow{k_d} R^{\bullet}_s},$$

$$\mathrm{R^{\bullet}_s \xrightarrow{k_{1s}} R^{\bullet}_{1s}},$$

$$\mathrm{PhC(O)O^{\bullet}_s + R^{\bullet}_s \xrightarrow{k_{2s}} PhC(O)OR},$$

$$\mathrm{PhC(O)O^{\bullet}_s + R^{\bullet}_{1s} \xrightarrow{k_{3s}} PhC(O)OR_1}.$$

According to this scheme, half the BP radicals add to polypropylene macromolecules to give the compounds PhC(O)OR and $\mathrm{PhC(O)OR_1}$.[65]

Thus, the concentration of the $R^{\bullet}_s$ radicals

$$[R^{\bullet}_s] = \frac{k_{BP,s} c_s}{(k_{1s} + k_{2s} k_{BP,s} c_s / k_{1,BP})},$$

responsible for the induction of the oxidation chains in v-zones, increases as the BP concentration in the polymer grows and at high concentration c, it reaches a limiting value,

$$[R^{\bullet}_s]_{lim} = \frac{k_{1,BP}}{k_{2s}}.$$

For this reason, the rate of initiation of the oxidation chains in v-zones also reaches a limiting value for a high concentration of BP; therefore, the 'bottle-neck' effect manifests itself quite clearly in the inter-zone transfer of free valence as the unproductive loss of a great amount of the initiator.

The radical s,v-translation steps are known to be related to the oscillations of the terminal $R^{\bullet}_s$ radicals between the framework s-domains and the nanopore cavities. In the absence of BP, the s,v-transfer is due to the interaction of the $R^{\bullet}_m$ radicals with oxygen (see Section IV). However, the $R^{\bullet}_m$ radicals are highly reactive towards the benzene rings of BP.[16, 38, 65] The σ-complexes formed in this reaction are readily oxidised with oxygen with the evolution of free hydroperoxyl radicals $HOO^{\bullet}$, which participate in the decay of s-radicals

$$\mathrm{R^{\bullet}_m + PhC(O)OOC(O)Ph_s \xrightarrow{k_{mt}} \left(\text{R, H, O}^{\bullet}\text{, COOC(O)Ph}\right)_s \xrightarrow{O_{2,s}}}$$

$$\longrightarrow \mathrm{HOO^{\bullet}_s + RC_6H_4C(O)OOC(O)Ph},$$

$$\mathrm{HOO^{\bullet}_s + PhC(O)O^{\bullet}_s \longrightarrow PhCOOH + O_2}.$$

Thus, when no POOH is initially present and the content of BP in the polymer is high, one should expect that not only the limiting rate of the inter-zone chemical induction would be attained but also that the oxidation rate would diminish due to the competing trapping of free valences by dibenzoyl peroxide during the s,v-transfer (in the 'bottle-neck').

In view of the above consideration and with allowance for the scheme of oxidation v-chains, considered in Section IV, we obtain the following expressions for the initial rates of the initiated hydroperoxide accumulation ($\upsilon_{[POOH],BP}$) and oxygen absorption (υ_{BP}):

$$\upsilon_{[POOH],BP} = k_2[POO^{\bullet}] = k_2 \left(\frac{\upsilon_{tr,BP}}{k''_t}\right)^{0.5},$$

$$\upsilon_{BP} = (k_2 + \eta k_3)[POO^{\bullet}] = \frac{k_2 \upsilon 0.5_{tr,BP}}{\varphi k''^{0.5}_t},$$

where

$$\upsilon_{tr,BP} = k_{tr}[R^{\bullet}_m][O_{2,s}] = \frac{k_m k_{BP,s} c_s P_{O_2}}{(b + b_1 c_s + P_{O_2})(k_{1s} + b_2 c_s)} \qquad (22)$$

$[b_1 = k_{mt}(\gamma_s k_{tr})^{-1}, b_2 = k_{2s} k_{BP,s} k^{-1}_{1,BP}]$. Equation (22) implies that the relation

$$\upsilon_{BP} \sim \frac{\upsilon^{0.5}_{tr,BP}}{k''^{0.5}_t} \sim (k_i c)^{0.5},$$

where $k_i = k_{BP,s} K_e \beta^{-1}$, should hold at a relatively low BP concentration in the polymer. It actually does hold, as has been confirmed experimentally. The relation $\upsilon_{BP} \sim (k_i c)^{0.5}$ is usually discussed in terms of homogeneous reaction schemes,[8] although it basically refers to a special case of a heterophase process.

It follows from Eqn (22) that, at low concentrations of the initiator (c_s), the initial rate of oxygen absorption υ_{BP} should increase with an increase in pressure P_{O_2} as long as the condition $(b + b_1 c_s) \leqslant P_{O_2}$ is fulfilled and until the limiting value $\upsilon_{BP,lim}$ is attained. As the BP concentration increases, the pattern of the curve $\upsilon_{BP} = f(P_{O_2})$ should change in a fairly complex manner. Over some range of the initiator concentration c, the limiting rate $\upsilon_{BP,lim}$ would increase but, simultaneously, the range of variation of υ_{BP} in the pressure range from 0 to $P_{O_2,lim}$ would become wider. The oxidation of polypropylene at relatively low concentrations of BP has displayed exactly this type of behaviour.[8, 66] In addition, when the BP concentration is very high, even a decrease in $\upsilon_{BP,lim}$ can be expected in conformity with Eqn (22).

Note that the logic of reasoning accepted in the studies by Denisov[8, 66] was based on the homogeneous reaction model; the observed transformation of the curves for the variation of the oxidation rate *vs.* pressure of O_2 was explained by the existence of diffusion restrictions on the absorption of oxygen. Meanwhile, the heterophase model treats this fact as being due to the 'bottle-neck' effect, which exists even in the absence of diffusion restrictions.

A method for determining kinetic parameters of the processes discussed here borrowed from the homogeneous oxidation practice has been described in a monograph;[8] this is the method of mixed initiation, which assumes the additivity of the rates of reactions initiated by the hydroperoxide and by an admixed initiator. Within the framework of the heterogeneous scheme, the overall rate of the process can be represented as the sum of the

rates of transfer of free valences through the structural 'bottleneck', $\upsilon_\Sigma \sim (\upsilon_{tr,BP} + \upsilon_{tr,2})^{0.5}$. The kinetics of the oxygen absorption would formally comply with the laws of a homogeneous reaction. However, this additivity is often disturbed because POOH groups react with the initiator in the s-zones of the spongy micelles. The mechanisms of these reactions and the specific features of the kinetics of the initiated oxidation of polymers brought about by these reactions are considered below.

2. Suppression of the initiator by the hydroperoxide

We have considered above the decrease in the initiation efficiency according to the 'self-locking' mechanism at relatively high initiator (BP) concentrations. This mechanism implies capture of the $R_s^{\bullet}$ radicals, responsible for the inter-zone chemical induction, by the primary $PhC(O)O_s^{\bullet}$ radicals and by the dibenzoyl peroxide itself. However, this does not exhaust the specific features of the initiated process. Indeed, it can be seen from Fig. 5 (curve *2*) that the oxidation rate in the presence of a high concentration of BP not only reaches the maximum possible value at the very beginning but also does not change subsequently during decomposition of BP and accumulation of POOH. In other words, POOH soon becomes the main initiator (note that the role of the hydroperoxide in restricting the initiator efficiency can also be clearly followed in experiments with initiators that dissociate with difficulty [15, 19, 21]).

After POOH groups have appeared in the s-zones, in addition to the reactions described above (see Section VII.1), trapping of the initiator free radicals by hydroperoxide occurs followed by recombination and disproportionation steps

$$PhC(O)O_s^{\bullet} + POOH_s \xrightarrow{k_s} PhC(O)OH + POO_s^{\bullet},$$

$$PhC(O)O_s^{\bullet} + POO_s^{\bullet} \longrightarrow (PhC(O)OOOP)_s \longrightarrow$$

$$\longrightarrow (PhC(O)OO^{\bullet} + {}^{\bullet}OP)_s \longrightarrow PhC(O)OOH_s + P{=}O.$$

Peroxobenzoic acid reacts with hydroperoxide giving no free radicals

$$PhC(O)OOH_s + POOH_s \longrightarrow PhC(O)OH + POH + O_2.$$

Taking into account the schemes for the s,v-transfer of radicals and for the oxidation chains in the v-zones and the steps of hydroperoxide migration and transformations, the rate of oxygen absorption can be expressed as follows:

$$\upsilon_\Sigma = (k_2 + \eta k_3)[POO^{\bullet}] = \frac{k_2}{\varphi}\left(\frac{\upsilon_{tr,\Sigma}}{k_t''}\right)^{0.5},$$

where the value

$$\upsilon_{tr,\Sigma} = \frac{k_m P_{O_2}}{k_{1s}(b + P_{O_2})}\left(\frac{k_{1,BP}k_{BP,s}c_s}{k_{1,BP} + k_s[POOH]_s} + \delta k_{0s}[POOH]_s\right) =$$

$$= k_t''[POO^{\bullet}]^2 \qquad (23)$$

corresponds to the condition of a low concentration of BP ($b_1c_s < b$, $b_2c_s < k_{1s}$).

At the very beginning of oxidation when $[POOH]_s$ is close to zero and the relations $k_{1,BP} > k_s[POOH]_s$ and $k_{BP,s}c_s > \delta k_{0s}[POOH]_s$ are obeyed, Eqn (23) becomes simpler and assumes the form

$$\upsilon_{tr,BP} = \frac{k_m P_{O_2} k_{BP,s} c_s}{(b + P_{O_2})k_{1s}} = k_t''[POO^{\bullet}]^2,$$

and the rate of oxygen absorption is determined by the equation

$$\upsilon_{BP} = A(k_{BP,s}\, c_s)^{0.5} \sim (k_i\, c)^{0.5},$$

where

$$A = \frac{k_2}{\varphi}\left[\frac{k_m P_{O_2}}{(b + P_{O_2})k_{1s}k_t''}\right]^{0.5}.$$

This equation is consistent with the experimental data obtained with relatively low rates of decomposition of the initiator.[8, 19]

Having occupied s-zones, the hydroperoxide becomes the main initiator. Since benzoyloxyl radicals detach hydrogen from the OOH groups hundreds times as fast as from the CH groups,[16] which ensures the fulfillment of the inequality $k_{1,BP}(k_s[POOH]_s)^{-1} \ll 1$, Eqn (23) can be transformed to the form

$$\upsilon_{tr,\Sigma} = \frac{k_m P_{O_2} \delta k_{0s}[POOH]_s}{k_{1s}(b + P_{O_2})}.$$

Thus, the oxidation rate is described by the relation

$$\upsilon_\Sigma = A(\delta k_{0s}[POOH]_s)^{0.5}. \qquad (24)$$

To determine the concentration $[POOH]_s$, which appears in Eqn (24), the above reactions involving POOH need to be supplemented by the reactions of the proper transformations of the hydroperoxide (see Section IV.2). This gives the expression

$$[POOH]_s = \frac{k_{vf}[POOH]}{k_{0s} + k^{ff}[POOH] + 2k_s k_{BP,s}c_s/(k_{1,BP} + k_s[POOH]_s)},$$

which can be simplified. An identical transformation with the assumption that $k_{1,BP} \ll k_s[POOH]_s$ (this means that the hydroperoxide located in s-zones traps almost all radicals of the admixed initiator) gives

$$[POOH]_s = \frac{k_{vf}[POOH] - 2k_{BP,s}c_s}{k_{0s} + k^{ff}[POOH]}.$$

Here k_{vf} and k^{ff} are constants corresponding to the $POOH_v \longrightarrow POOH_s$ transfer and the $POOH_v + POOH_s$ reaction, respectively (accomplished through an excited v-nanopore; the detailed mechanism is described in Section IV.2), $[POOH] \approx \beta[POOH]_v$.

By substituting the concentration $[POOH]_s$ into Eqn (24), one can determine the rate of the oxygen absorption in the stage in which two sources of free radicals are effective

$$\upsilon_\Sigma = A\left(\delta k_{0s}\frac{k_{vf}[POOH] - 2k_{BP,s}c_s}{k_{0s} + k^{ff}[POOH]}\right)^{0.5}.$$

It follows from the above relation that, during the accumulation of the hydroperoxide, the oxidation rate increases to a certain limit, which is attained when $k_{0s} < k^{ff}[POOH]$

$$\upsilon_{max} = A\left(\delta k_{0s}\frac{k_{vf}[POOH] - 2k_{BP,s}c_s}{k^{ff}[POOH]}\right)^{0.5}. \qquad (25)$$

If the subtrahend in Eqn (25) is sufficiently small, the reaction acquires the zero order with respect to both the initiator and hydroperoxide. Then

$$\upsilon_{max} = A\left(\frac{\delta k_{0s}k_{vf}}{k^{ff}}\right)^{0.5}.$$

This conclusion has been confirmed experimentally.[15, 19, 21]

If the subtrahend in Eqn (25) is great, which is the case for a relatively high rate of dissociation of the initiator ($k_{BP,s}c_s \sim k_i c$), this term makes a contribution to the decrease in the steady-state oxidation rate. This has been observed in experiments with samples of readily oxidisable PEO; an increase in the BP concentration from 0.12 to 0.38 mol kg^{-1} decreases the oxygen absorption rate by a factor of 1.4.[19] This outcome appears as a paradox but it has a clear physical meaning in terms of the heterophase scheme, pointing to the interaction between two sources of free radicals, which is unproductive for oxidation.

In the scheme that we propose, the formation of peroxobenzoic acid in disproportionation steps and the radical-free reaction of peroxobenzoic acid with POOH can be classified as unproductive consumption of radicals. The possibility of radical-free bimolecular decomposition of peroxobenzoic acid can also be

assumed, by analogy with the heterogeneous reaction $POOH_f$ + $POOH_s$ or, for example, with the known decomposition of *tert*-butyl hydroperoxide [67] and aromatic dihydroperoxide [68] in liquid solutions.

In this connection, the known fact of retardation of the initiated oxidation of polypropylene and polyethylene by the addition of cumene hydroperoxide [8] (with BP as the initiator) can be considered from a new standpoint. In all probability, this fact is due to the decrease in the rate of initiation ($\upsilon_{tr,\Sigma}$) of oxidation v-chains caused by the unproductive loss of the radicals generated in s-zones. Anyway, the idea of acceleration of the oxidation chain termination upon the involvement of mobile cumene peroxyl radicals [8] does not seem quite convincing because the rate of injection of free valences into v-zones is extremely low. In our opinion, the conditions in s-zones are much more favourable for trapping of the BP free radicals by the admixed cumene hydroperoxide molecules and for unproductive (with respect to the oxidation chains) interaction between these components.

3. Synergism of the action of hydroperoxide and an initiator

In some cases, the hydroperoxide accumulated in the polymer enhances the efficiency of an admixed initiator. This is indicated by the fact that hydroperoxide has a promotory influence on azobisisobutyronitrile (AIBN),[69] although the researchers themselves did not interpret this effect. It was found that the rate of oxygen absorption by solid IPP at 82 °C in the presence of 7.5×10^{-2} mol kg^{-1} of AIBN increases from the very beginning until it reaches a constant level, 4 to 7 times as high as the initial level. This increase is at variance with the view [8] that the oxidation rate always remains constant as long as the initiation rate is constant. Meanwhile, the rate of oxidation of pre-oxidised IPP samples containing 5×10^{-3} mol kg^{-1} of POOH and 7.5×10^{-2} mol kg^{-1} of AIBN is equal from the beginning to the steady-state rate of oxidation of non-oxidised IPP.

The rates of radical generation upon dissociation of POOH and AIBN, found by the inhibitor method (based on the consumption of stable nitroxides) are 7.5×10^{-9} and 7.5×10^{-7} mol kg^{-1} s^{-1}, respectively. Proceeding from these values and relying on the homogeneous reaction model, the researchers [69] concluded that AIBN is responsible for the initiation virtually alone, whereas the hydroperoxide ensures branching of the oxidation chains and efficiently decreases the rate constant for the termination of these chains by increasing their length. The last-mentioned conclusion was criticised in a monograph by Popov *et al.*,[5] who proved that the rate constant for the termination of oxidation chains in IPP does not depend on the content of POOH. This result is confirmed, in particular, by the fact that the radiation-induced oxidation of IPP proceeds at a constant rate. When other initiators are employed (for example, BP and dicumene peroxide), no noticeable change in the rate constant for chain termination upon accumulation of POOH has been identified either.[8]

The discussion around the 'AIBN effect' [5,8] precluded elucidation of its mechanism because the effect was discussed within the framework of the homogeneous model, which is not valid for this particular case. However, if the mechanism of AIBN initiation is considered in terms of the heterophase model, two initiation rates should be distinguished: (1) the rate of generation of free radicals found by the inhibitor method and corresponding to the process localised in the s-zones of the micellar sponge and (2) the much lower rate of initiation (and termination) of the proper oxidation chains which are continued in v-zones. In this case, the essence of the AIBN effect in question can be explained as follows. Azobisisobutyronitrile decomposes in the s-zones of spongy micelles and generates alkyl cyanoisopropyl radicals, $R_j^{\bullet}$, which readily react with nitroxides but virtually do not react with macromolecules. The primary $R_j^{\bullet}$ radicals partially decay without leaving a radical pair, while some of the radicals are oxidised to give reactive peroxyl radicals, which do react with macroradicals.

$$\left(\begin{array}{ccc} Me_2C & -N=N- & CMe_2 \\ | & & | \\ CN & & CN \end{array}\right)_s \xrightarrow{k_{sj}} (Me_2\dot{C}CN,\ Me_2\dot{C}CN)_s + N_2,$$

$$(Me_2\dot{C}CN,\ Me_2\dot{C}CN)_s \xrightarrow{k_{0j}} \text{products},$$

$$(Me_2\dot{C}CN,\ Me_2\dot{C}CN)_s \xrightarrow{k_{1j}} 2\underset{R_j^{\bullet}}{Me_2\dot{C}CN}.$$

In accordance with the experimental data, the ratio of the rate of formation of the $R_j^{\bullet}$ radicals to the rate of AIBN decomposition in the IPP matrix at 82 °C amounts to $2k_{1j}/(k_{0j}+k_{1j}) = 0.054$.[8] Thus, a substantial portion of AIBN radicals decay at the beginning of the process and do not participate in the oxidation.

The situation changes as POOH groups are accumulated in s-zones. Since alkyl radicals are highly reactive towards the abstraction of hydrogen from the OOH groups,[70,71] they provide an additional opportunity for the formation of the terminal $R_s^{\bullet}$ macroradicals, which are responsible for the transfer of free valences to the v-zones. In this case, all the generated $R_j^{\bullet}$ radicals are consumed for the oxidation reaction and thus ensure a hundred percent initiating efficiency of AIBN.

The above considerations can be summarised by the following simplified scheme of transformations (Scheme 4):

Scheme 4

$$Me_2\dot{C}CN_s + O_{2,s} \xrightarrow{k_{2j}} \underset{\dot{O}O}{Me_2CCN_s},$$

$$\underset{\dot{O}O}{Me_2CCN_s} + PH_s \xrightarrow{k_{3j}} Me_2C(CN)OOH + P_s^{\bullet},$$

$$P_s^{\bullet} \longrightarrow R_s^{\bullet} \begin{cases} \xrightarrow{} R_{1s}^{\bullet} \\ \xrightarrow{R_{1s}^{\bullet}} \text{products}, \end{cases}$$

$$(Me_2\dot{C}CN,\ Me_2\dot{C}CN)_s + POOH \xrightarrow{k_{4j}} Me_2CHCN + Me_2\dot{C}CN_s + POO_s^{\bullet},$$

$$POO_s^{\bullet} \xrightarrow{PH_s} P_s^{\bullet} + POOH.$$

Here we neglect the contribution of POOH to the generation of free radicals, in compliance with the results obtained by the inhibitor method.[69]

According to Scheme 4, the quasi-steady-state concentration of the $[R_s^{\bullet}]$ radicals, responsible for the chemical s,v-induction,

$$[R_s^{\bullet}] = \frac{2k_{sj}c_j(k_{1j}+k_{4j}[POOH]_s)}{k_{1s}(k_{0j}+k_{1j}+k_{4j}[POOH]_s)}$$

(c_j is the concentration of AIBN in s-zones) increases during the accumulation of POOH from the initial value

$$[R_s^{\bullet}]_0 = \frac{2k_{1j}k_{sj}c_j}{k_{1s}(k_{0j}+k_{1j})} \text{ for } k_{4j}[POOH]_s \ll k_{1j}$$

to the limiting value

$$[R_s^{\bullet}]_{lim} = \frac{2k_{sj}c_j}{k_{1s}} \text{ for } k_{4j}[POOH]_s \gg (k_{0j}+k_{1j}).$$

Under these conditions, the rate of oxygen absorption

$$\upsilon = \frac{k_2[POO^{\bullet}]}{\varphi} = \frac{k_2}{\varphi}\left(\frac{\upsilon_{tr}}{k_t''}\right)^{0.5}$$

increases from the initial value υ_0 to the limiting value υ_{lim} in conformity with the equation

$$\frac{\upsilon_{lim}}{\upsilon_0} = \left(\frac{\upsilon_{tr,lim}}{\upsilon_{tr,0}}\right)^{0.5} = \left(\frac{[R_s^{\bullet}]_{lim}}{[R_s^{\bullet}]_0}\right)^{0.5} = \left(\frac{k_{0j}+k_{1j}}{k_{1j}}\right)^{0.5}.$$

Substitution into this equation of the $k_{1j}(k_{0j}+k_{1j})^{-1} \approx 0.027$ determined experimentally [8] gives the equality $\upsilon_{lim} = 6\upsilon_0$, which is consistent with the value found in another study.[69]

Thus, within the framework of the heterophase reaction model, the specific kinetic feature observed in the initial stage of oxidation of polymers in the presence of AIBN is interpreted as being due to the increase in the initiating efficiency of AIBN,

caused by the hydroperoxide suppression of the unproductive loss of primary radicals. This conclusion is in agreement with the finding that the rate constant for the termination of oxidation chains does not depend on the POOH concentration.

4. Initiated discontinuous increase in the rate of oxygen absorption in the oxidation of polycyclohexadiene

The heterophase model provides explanation for an interesting kinetic feature observed in the initiated oxidation of polycyclohexadiene (PCH), which is vitreous at room temperature.[72–74] The initial PCH always contains hydroperoxide in a concentration of 0.02–0.1 mol kg^{-1}. Its oxidation ($T = 60–90$ °C, $P_{O_2} =$ 100 kPa) has no induction period, rapidly passes through self-accelerated stage and occurs subsequently at a constant rate of oxygen absorption, $\upsilon_3 = 1 \times 10^{-4}$ mol kg^{-1} s^{-1} (at 80 °C). This rate does not change even after a tenfold increase in the POOH concentration. The yield of hydroperoxide per mole of absorbed oxygen is close to unity ($\varphi = 0.8–0.9$).

The introduction of initiators — AIBN or dilauroyl peroxide (LP) — into PCH induces a discontinuous increase in the oxygen absorption rate (υ_I).

The following relation for the oxygen absorption rate has been proposed on the basis of a modified homogeneous reaction model:

$$\upsilon_I = B\left(1 + \frac{\upsilon_{i,[POOH]}}{\upsilon_{ij}}\right),$$

where $\upsilon_{i,[POOH]}$ and υ_{ij} are the rates of initiation by hydroperoxide and initiator, respectively, B is a complex constant.

The rates υ_I attained upon the introduction of initiators are constant over a broad range of concentrations of the initiators (0.005–0.1 mol kg^{-1}) and amount to 5×10^{-4} and 9×10^{-4} mol kg^{-1} s^{-1} in the PCH + POOH + AIBN and PCH + POOH + LP samples, respectively. This is substantially higher than the υ_3 values for the PCH samples containing only POOH.

These kinetic 'jumps' were attributed [72–74] to the participation of low-molecular-mass radicals formed from the initiator (cyanoisopropyl radicals in the case of AIBN and undecyl radicals in the case of LP) not only in the induction of oxidation chains but also in the cross termination of these chains. In the opinion of the researchers cited, the rate of cross termination is limited by the diffusion of the primary radicals; therefore, the difference between the υ_I values upon the addition of AIBN and LP was explained by the difference between the diffusion constants of the primary radicals.

However, it has been found experimentally that the rate of consumption of an inhibitor, 2,2′-methylenebis(4-methyl-*tert*-butylphenol), is directly proportional to the concentration of the initiator.

The rates of initiation by hydroperoxide and by the initiator ($\upsilon_{i,[POOH]}$ and υ_{ij}) for [POOH] = 4.6×10^{-2} mol kg^{-1} and [AIBN] = 0.1 mol kg^{-1}, found from the consumption of the bisphenol, were as follows.

T/ °C	$10^7 \upsilon_{i,[POOH]}$ /mol kg^{-1} s^{-1}	$10^7 \upsilon_{ij}$ /mol kg^{-1} s^{-1}
80	5.7	2.5
85	9.9	3.9
90	15.0	5.0

A 20-fold decrease in the AIBN concentration (from 0.1 to 0.005 mol kg^{-1}) should increase the $\upsilon_{i,[POOH]}/\upsilon_{ij}$ ratio by the same factor (because the υ_{ij} value is directly proportional to the concentration of the initiator and $\upsilon_{i,[POOH]}$ does not change when the initial concentration of POOH is constant); the υ_I value presented above should also increase, which obviously contradicts the experimental fact that this rate remains constant over the whole range of AIBN concentrations studied.

Let us turn to the heterophase model, resorting to the experimental results obtained in Ref. 69 and assuming that the real rate of initiation due to POOH in the PCH matrix is much lower than the rate of initiation due to AIBN or LP ($\upsilon_{i,[POOH]} \ll \upsilon_{ij}$). The high rate of consumption of bisphenol observed in the oxidation of PCH containing POOH is accounted for by the participation of bisphenol in the kinetic chains of POOH decomposition.[16]

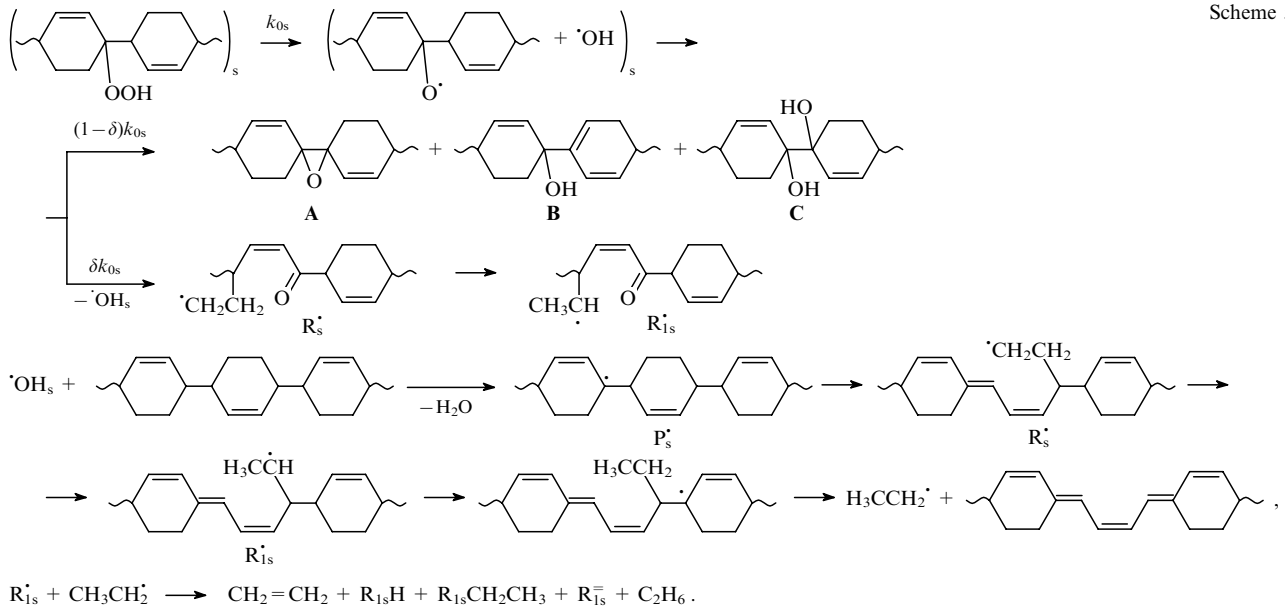
The structure of the monomer unit in PCH suggests that the hydroperoxide which decomposes in s-zones without an initiator is converted in a high yield into molecular compounds (**A**–**C**) and only a minor portion of the primary radical pairs induces the subsequent transformations of macroradicals (Scheme 5).

Scheme 5 includes stages involving opening of six-membered carbon rings and elimination of ethyl radicals; this is confirmed by detection of ethylene upon the oxidation of PCH.[74] This scheme can be supplemented by the forward and backward inter-zone chemical induction steps considered above for polyolefins.

The assumption that oxidation of PCH in the absence of AIBN (LP) actually follows the same heterophase mechanism as oxidation of polyolefins is confirmed by the fact that, after a self-accelerated period, a non-initiated process switches to a regime characterised by a zero order with respect to hydroperoxide.

When discussing specific features of the initiated oxidation of PCH, one should take into account the high efficiency of the formation of POOH ($\varphi = 0.8–0.9$) characteristic of this process.

Scheme 5



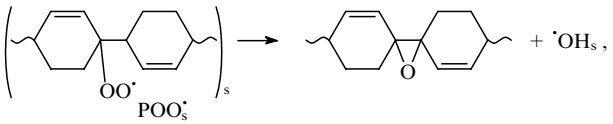
This means that the main reaction involving free radicals in the oxidation of non-crystalline PCH is abstraction of hydrogen atoms giving rise to allyl type radicals. The subsequent transformations of these radicals in the s- and v-zones of the PCH matrix differ in kind. Indeed, due to the substantial steric restrictions hampering opening of the six-membered carbon rings and epoxidation in narrow v-zones, an intermolecular mechanism of the propagation of oxidation chains comes to the fore.

$$P^{\bullet} + O_2 \longrightarrow POO^{\bullet} \xrightarrow{PH} POOH + P^{\bullet}.$$

Now we return to the s-scheme of reactions involving AIBN (see Scheme 4), eliminate the reaction of radical pairs with the hydroperoxide POOH (k_{4j}) (which is unlikely in a vitreous polymer), add reactions involving the $Me_2C(CN)OO^{\bullet}$, $POO_s^{\bullet}$ and $^{\bullet}OH_s$ radicals

$$Me_2C(CN)OO^{\bullet} + R_s^{\bullet} \xrightarrow{k_{5j}} \text{products},$$

$$Me_2C(CN)OO^{\bullet} + POOH_s \xrightarrow{k_{6j}} Me_2C(CN)OOH + POO_s^{\bullet},$$



$$+ {}^{\bullet}OH_s,$$

$$^{\bullet}OH_s + PH \longrightarrow P_s^{\bullet} + H_2O,$$

and write the algebraic condition for the steady-state concentrations of radicals participating in the inter-zone s,v-chemical induction,

$$\frac{d[R_s^{\bullet}]}{dt} = k_{3j}[Me_2C(CN)OO^{\bullet}][PH_s] + k_{6j}[Me_2C(CN)OO^{\bullet}][POOH]_s - k_{5j}[Me_2C(CN)OO^{\bullet}][R_s^{\bullet}] = 0.$$

By solving this equation, we make sure that the concentration

$$[R_s^{\bullet}] = \frac{k_{3j}[PH_s] + k_{6j}[POOH]_s}{k_{5j}}$$

does not depend on the concentration of the initiator.

The s-scheme for the reactions involving LP is qualitatively the same.

Now we employ the scheme of the s,v-translation of free valences, which is similar in kind to the corresponding scheme for polyolefins, and express the balance of the rates of initiation and termination of oxidation v-chains by the equation

$$\upsilon_{tr} = \frac{k_m P_{O_2}[R_s^{\bullet}]}{b + P_{O_2}} = k_t''[POO^{\bullet}]^2,$$

and the rate of oxygen absorption by the equation

$$\upsilon_I = \frac{k_2[POO^{\bullet}]}{\varphi} = \frac{k_2}{\varphi}\left(\frac{P_{O_2}}{b + P_{O_2}}\right)^{0.5}\left(\frac{k_m k_{3j}[PH_s] + k_m k_{6j}[POOH]_s}{k_{5j}k_t''}\right)^{0.5}.$$

It can be seen from the latter equation that υ_I does not depend on the concentration of an admixed initiator.

In the absence of an admixed initiator, the steady-state rate of the absorption of oxygen by PCH does not depend on the content of POOH either [Eqn (9)]

$$\upsilon_3 = \frac{k_2}{\varphi}\left(\frac{P_{O_2}}{b + P_{O_2}}\right)^{0.5}\left(\frac{\delta k_{0s} k_m k_{vs}}{2k^{ff}k_{1s}k_t''}\right)^{0.5},$$

and the relatively low value of this rate is stipulated by the small value of the product $\delta k_{0s}k_{vs}$.

It is worth noting that, in accordance with the mechanism in question, the constant values of $[R_s^{\bullet}]$ and υ_I correspond to a relatively high content of the initiator, which provides the 'self-locking' effect in the passage of free valences through the 'bottle-neck'. It is evident that at low concentrations of the initiator, the 'self-locking' condition is not met; however it is met in the range of AIBN and PL concentrations studied by Chaplanova *et al.*[72–74] In terms of this mechanism, the dissimilarity between the υ_I values observed in the AIBN- and LP-involving processes is due to the different values of the complex constant

$$\frac{k_{3j}[PH_s] + k_{6j}[POOH]_s}{k_{5j}},$$

characterising the reactions of peroxyl radicals derived from AIBN and LP with the CH bonds of the oxidised PCH (POOH) and the macroradicals $R_s^{\bullet}$. According to experimental data, this complex constant is greater for the LP radicals.

Thus, the heterophase reaction model interprets the initiated 'jumps' in the oxygen absorption rate, observed in the oxidation of PCH samples, without violating the logical link between this partial model and those describing oxidation of other polymers.

VIII. The model of oxidation of thermofluctuationally active objects

In the preceding Sections, we considered oxidation processes that occur in the mode of heterophase injection of free valences from the zones in which they are generated to the zones in which chain reaction of macroradicals with oxygen takes place. This mode is typical of specimens with relatively low molecular-segment mobility.

Meanwhile, the mobility of units of the molecular sponge can increase appreciably under certain conditions. This is accompanied by an increase in the frequency of formation of fluctuationally excited nanopores (f-nanopores) directly in the grains of spongy micelles. These conditions are fulfilled, for example, in polymers with relatively low molecular masses and, correspondingly, with low macroscopic viscosity (for example, for low-molecular-mass APP) and in a polymer matrix in the state of thixotropic excitation, caused by structural and mechanical relaxation (for example, in oriented IPP).[26]

Due to excitation in a dynamically active molecular sponge, f-nanopores reach the size of s-nanopores and their lifetime increases because relaxation requires spatial redistribution of numerous units of the sponge in the vicinity of the f-nanopore formed. Since the frequency of formation of f-nanopores is relatively high, they increase the rate of dissociation of the POOH groups in the v-zones of spongy micelles [16] and also trigger off the mechanism of quasi-linear termination of reaction chains according to Eqn (18).

The new steps of initiation and termination of oxidation chains, which are added to the heterogeneous initiation and quadratic termination steps or even prevail in the oxidation, should necessarily change qualitatively the reaction kinetics.

The kinetics of oxidation of low-molecular-mass APP and oriented IPP provide an example of such a change (see Fig. 6). This process displays a fairly prolonged exponential increase in the amounts of oxygen absorbed (curves *1*, *3*) and the POOH formed (curves *2*, *4*).[26] The amount of oxygen absorbed in the exponential stage reaches 1.5–2.0 mol kg^{-1}, which markedly differentiates this process from the oxidation of high-molecular-mass polyolefins, which includes a short-term 'parabolic' self-accelerated stage and, after 0.1–0.2 mol kg^{-1} of oxygen has been absorbed, switches to the mode characterised by zero-order kinetics with respect to hydroperoxide.

The long-term exponential acceleration of the reaction has also been found in experiments with a model analogue of polyolefins, cetane (oxidation was carried out with the removal of the resulting aqueous phase containing acidic products),[44] and in experiments with low-molecular-mass APP (M_n = 2250) in the temperature range of 120–160 °C [75] (Fig. 16).

The change in the kinetics of the absorption of oxygen upon orientational drawing has been observed in experiments with IPP (Fig. 6), polyethylene and polymethylpentene films (Fig. 17).[5,76]

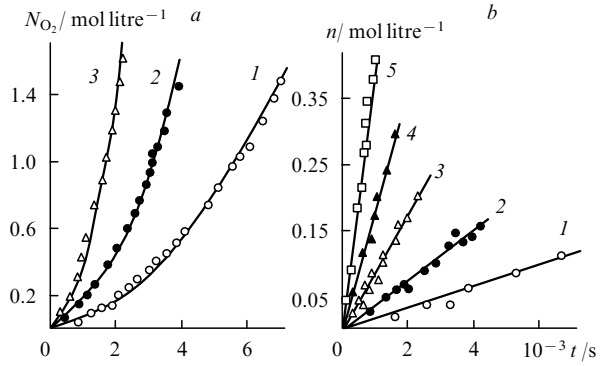


Figure 16. Variation of the amount of oxygen absorbed (*a*) and the number of breaks in macromolecules (*b*)[75] during oxidation of molten APP (M_n = 2250) at an oxygen pressure of 97.3 kPa and temperatures of 120 (*1*), 130 (*2*), 140 (*3*), 150 (*4*) and 160 °C (*5*) (the dots correspond to experimental data from Ref. 75).

It can be clearly seen in Fig. 17 how curve *1* for isotropic films (with short self-acceleration and then zero-order kinetics with respect to POOH) is replaced upon film drawing by curves *2*–*5*, characterised by continuous variation of the oxygen absorption rate.

The presence of a long period in which the kinetic law $\exp(\Phi t)$ is fulfilled does not exhaust the specific features of the oxidation of polymers with enhanced thermofluctuation mobility of the molecular sponge. Yet another feature is the substantial dependence of the reaction rate on the pressure of oxygen in the 26–100 kPa range[75] (the rate of oxidation of liquid hydrocarbons in this range is close to the limiting value).

In addition, it can be seen from Fig. 6 (curves *2*, *4*) that this oxidation mode is characterised by a high limiting concentration of POOH, which barely changes for a long period of time. Unlike this situation, in the oxidation of high-molecular-mass polyolefins (and quite often, of low-molecular-mass liquid hydrocarbons), the

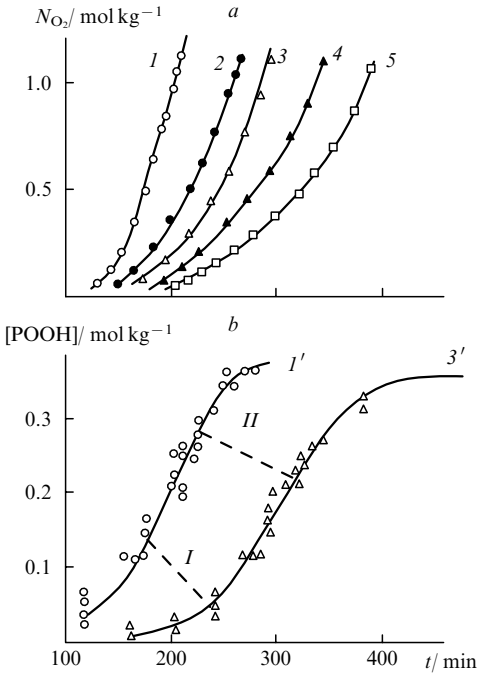


Figure 17. Variation of the amount of oxygen absorbed (*a*) and hydroperxide accumulated (*b*) in the initial (non-oriented) polymethylpentene film (*1*, *1′*) and in films stretched to a ratio of 4 (*2*), 6 (*3*, *3′*), 9 (*4*) and 12 (*5*) during oxidation at 130 °C and an oxygen pressure of 80 kPa.[76]

POOH concentration passes through a relatively sharp maximum, which appears due to the decomposition of hydroperoxide induced by organic acids, which accelerates with time. The carboxylic acids formed in large amounts in the oxidation of liquid cyclohexane, *n*-decane[77] and nonene[78] destroy another oxidation product, hydroperoxide, its maximum concentration being thus limited to ~0.3, 0.2 and 0.4–0.5 mol kg^{-1}, respectively.

However, oxidation of a melt of low-molecular-mass APP and orientationally drawn IPP films gives POOH and polymeric ketones as the major products, whereas the yield of acids is insignificant.[26] It is the low concentration of acids that accounts, in all probability, for the absence of sharp maxima in curves *2*, *4* in Fig. 6. The presence of a concentration limit in these curves can be regarded as evidence for the occurrence of chain decomposition of POOH under the action of free radicals. The rate of chain decomposition of POOH corresponding to this limiting concentration should be equal to the rate of its chain formation, the quasi-steady-state concentration of radicals that induce the decomposition remaining virtually constant for a long period.

Yet another important feature of the oxidation of low-molecular-mass APP is the fact that the kinetic laws of the cleavage of the macromolecules established by Iring *et al.*[26] using the gel-chromatographic method for the determination of the molecular mass distribution do not coincide with the kinetic laws established by Ivanov *et al.*,[75] who used a variant of osmometry.

For example, in the former study,[26] in which the oxidation of APP was carried out at a high pressure of oxygen (10^3 kPa), the number of breaks in the polymer chains increased according to the same law as the amount of absorbed oxygen and was equal to 0.01 mol litre^{-1} at 120 °C over a period of 50 min, while in the latter study,[75] in which APP was oxidised at $P_{O_2} \leqslant 100$ kPa, the number of breaks was 0.033 mol litre^{-1} over the same period of time. The rate of polymer chain scission remained constant during the whole process (Fig. 16*b*), although it was directly proportional to the pressure of oxygen. In this particular case (when the pressure of oxygen is low) more intense degradation takes place due to the cleavage of those macroradicals the concentrations of which do not depend on the oxidation time or on the concentration of POOH formed.

The factors listed above give grounds for claiming that neither the model of homogeneous oxidation of hydrocarbons nor the models of heterophase oxidation of high-molecular-mass polymers, considered in the preceding Sections, are suitable for describing the oxidation of molten low-molecular-mass APP. The law $\exp(\Phi t)$ characterising the self-accelerated stage coincides only formally with the regularity established for gas-phase reactions with avalanche-like branching of reaction chains. In the condensed phase, the avalanche-like chain branching is impossible for several reasons reported in the literature.[79]

Thus, a kinetic model for the oxidation of polymers distinguished by high thermofluctuation mobility of the molecular sponge should take into account the structural and physical changes of the chemical quasi-elementary steps, specific for the given state, which are actually heterogeneous.

The high frequency of excitation of f-nanopores in a spongy matrix makes it possible to propose the following scheme of the frequency-modulated oxidation process

$$\mathrm{POOH} \xrightarrow{k_f} \mathrm{POOH_f} \longrightarrow (\mathrm{PO^{\bullet}} + {}^{\bullet}\mathrm{OH})_f \xrightarrow{\mathrm{PH}} \delta\mathrm{P^{\bullet}},$$

$$\mathrm{P^{\bullet}} \xrightarrow{\mathrm{O_2},\, k_1} \mathrm{POO^{\bullet}},$$

$$\mathrm{POO^{\bullet}} + \mathrm{PH} \underset{k_{-2}}{\overset{k_2'}{\rightleftharpoons}} \mathrm{POOH} + \mathrm{P^{\bullet}},$$

$$\mathrm{POO^{\bullet}} \xrightarrow{k_3} (\mathrm{E} + \mathrm{HO^{\bullet}}) \longrightarrow \mathrm{P^{\bullet}} + \text{products},$$

$$\mathrm{POO^{\bullet}} \xrightarrow{k_{t,1}} \mathrm{POO^{\bullet}_f},$$

$$POO^{\bullet} + POO^{\bullet}_{f} \xrightarrow{k_{t,2}} \text{termination.}$$

By applying the condition of steady-state concentrations of free radicals, one can easily find the concentration of peroxyl radicals $POO^{\bullet}$, involved in the oxidation chains, which will be referred to as linear chains

$$[POO^{\bullet}] = \frac{\delta k_f [POOH]}{2k_{t,1}}$$

(δ is the yield of macroradicals in the decomposition of $POOH_f$), the concentration of alkyl macroradicals

$$[P^{\bullet}] = \frac{0.5\delta k_f [POOH](k_2 + k_3)}{k_{t,1}(k_1[O_2] + k_{-2}[POOH])},$$

the rate of accumulation of POOH, which is made up of the rates of chain formation, chain decomposition and spontaneous decomposition

$$\frac{d[POOH]}{dt} = \frac{0.5k_2\delta k_f[POOH]}{k_{t,1}} - \frac{0.5k_{-2}(k_2 + k_3)\delta k_f[POOH]^2}{k_{t,1}(k_1[O_2] + k_{-2}[POOH])}$$

$$- k_f[POOH] = \Phi[POOH] - \frac{\Phi[POOH]^2}{\varphi(\chi + [POOH])}, \qquad (26)$$

and the rate of oxygen absorption (the contribution of the spontaneous decomposition of POOH can be neglected)

$$-\frac{d[O_2]}{dt} = \frac{d\Delta[O_2]}{dt} = k_1[P^{\bullet}][O_2] = \frac{\Phi\chi[POOH]}{\varphi(\chi + [POOH])}, \qquad (27)$$

where $\Phi = k_f(0.5k_2\delta k_{t,1}^{-1} - 1) \approx 0.5k_2\delta k_f k_{t,1}^{-1}$, $\varphi = k_2(k_2 + k_3)^{-1}$, $\chi = k_1[O_2]k_{-2}^{-1}$.

It follows from Eqn (26) that at the beginning of the self-accelerated oxidation stage, when $d[POOH]/dt = \Phi[POOH]$, the content of POOH increases with time by an exponential law

$$[POOH] = [POOH]_\tau \exp(\Phi t),$$

where $[POOH]_\tau$ is the concentration of POOH at the end of the induction period.

During this period, the rate of oxygen absorption also increases according to an exponential law in view of the relation $[POOH] < \chi$:

$$\frac{d\Delta[O_2]}{dt} = \frac{\Phi[POOH]}{\varphi} = \frac{\Phi[POOH]_0}{\varphi}\exp(\Phi t). \qquad (28)$$

The Φ, φ, and χ values were found by solving the set of differential equations (26) and (27) using the simple Euler method.[52] The results of calculations were compared with experimental data presented in Figs 6, 16 and 17.

The theoretical curves *1* and *2* in Fig. 6, corresponding to low-molecular-mass APP, are in agreement with experimental data obtained by Iring *et al.*[26] The Φ, φ, χ and $[POOH]_\tau$ values corresponding to these curves are

$\Phi = 0.034\ min^{-1}$, $\varphi = 0.5$, $\chi = 1.1$ mol litre^{-1},
$[POOH]_\tau = 0.02$ mol litre^{-1}.

The theoretical curves *3* and *4* in Fig. 6, which refer to IPP films stretched orientationally by a factor of 5, are also in good agreement with experimental points. The corresponding coefficients are

$\Phi = 0.027\ min^{-1}$, $\varphi = 0.4$, $\chi = 1.05$ mol litre^{-1},
$[POOH]_\tau = 0.02$ mol litre^{-1}.

The qualitative difference between curves *3*, *4* and curves *1*, *2* is associated with the appearance of an induction period with $\tau = 200$ min in the oxidation of oriented films (in the case of a melt, $\tau \approx 0$ min).

Figure 16 shows the theoretical curves corresponding to the oxidation of an APP melt at a lower pressure $P_{O_2} = 100$ kPa. They are also in good agreement with experimental data[75] with the following coefficients Φ, φ and χ:

T/ °C	Φ/ s^{-1}	φ	χ/ mol litre^{-1}
120	1.0×10^{-3}	0.5	0.4
130	1.8×10^{-3}	0.5	0.4
140	3.6×10^{-3}	0.5	0.4

The calculations were performed with the assumption that the yield of POOH per mole of oxygen absorbed in linear chains does not depend on temperature and corresponds to the φ value taken from a study by Iring *et al.*,[26] the $[POOH]_\tau$ value remains equal to 0.02 mol litre^{-1}, and the limiting concentration of the hydroperoxide, needed to estimate the coefficient χ, is $[POOH]_{lim} = 0.4$ mol litre^{-1}.

Taking into account the variation of the coefficient Φ *vs.* temperature and using the Arrhenius equation, one can calculate the effective activation energy $E_\Phi = 86.0$ kJ mol^{-1}. This value differs from the effective activation energy of scission found from Fig. 16 *b* ($E_n = 106.0$ kJ mol^{-1}).

The thermomechanical modulation of the chemical events is also manifested in the experiments with oriented polymethylpentene films (Fig. 17). As in the case of oriented IPP films, the modulation is due to the enhancement of the molecular-segment mobility as a result of relaxation of internal stress. The qualitative difference between curves *1*, *1′*, describing the oxidation of isotropic films, and curves *3*, *3′*, which refer to oriented films can be clearly seen in Fig. 17. Curves *3* (Fig. 17 *a*, oxygen absorption) and *3′* (Fig. 17 *b*, POOH accumulation) were constructed by solving the set of equations (26) and (27). For $\Phi = 0.03\ min^{-1}$, $\varphi = 0.13$, $\chi = 2.4$ mol kg^{-1}, $[POOH]_\tau = 0.01$ mol kg^{-1} and $\tau = 160$ min, they are in good agreement with experimental data reported by Rapoport *et al.*[76] (130 °C, $P_{O_2} = 80$ kPa).

It should be noted that the yield of hydroperoxide φ in oriented films permanently varies during oxidation. Indeed, it can be seen in Fig. 17 *b,* which shows the curves for 0.5 (curve *I*) and 1.4 mol kg^{-1} (curve *II*) of absorbed oxygen, that $\varphi = 0.1$ at the point of intersection of curves *I* and *3′* and $\varphi = 0.16$ at the point of intersection of curves *II* and *3′*. The value $\varphi = 0.13$ assumed in our calculations is the average of these two values.

The fact that the parameter φ (and, hence, χ) depends on the draw ratio and on the degree of oxidation suggests that the good agreement between the calculated and experimental data for oriented films results, most likely, from a favourable superposition of the chemical reaction and structural relaxation. In other cases, this agreement may be missing and the process kinetics would undergo substantial changes.[14] Nevertheless, the results indicate that the principle of structure-mechanical modulation of chemical steps is correct at the qualitative level.

The scheme of chemical transformations analysed in this Section differs from the heterophase schemes considered previously not only by the fact that it includes the steps of free radical generation in enlarged f-nanopores but also by the fact that it assumes decomposition of POOH induced by alkyl macroradicals (characterised by the constant k_{-2}) and quasi-linear termination of oxidation chains in f-nanopores [Eqn (18)].

The induced decomposition of POOH can also account for both the presence of the concentration limit in the accumulation of the hydroperoxide and the influence of the pressure of oxygen on the oxidation rate. The latter is due to the competition between oxygen and hydroperoxide for the alkyl macroradicals, which are converted in linear oxidation chains (see above).

According to published data, in liquid-phase systems under conditions of oxygen deficiency, the contribution of the reaction of alkyl radicals with hydroperoxide to the overall scheme is fairly high. This has been explained by the 'abnormally' high rate of the abstraction of hydrogen atoms from hydroperoxide groups by the attacking alkyl radicals.[70, 71] Previously, based on the idea of

hampered microdiffusion of oxygen, it has been believed[8] that competition between oxygen and hydroperoxide for alkyl macroradicals is always involved in polymer oxidation; however, particular reasons for the restriction of diffusion have not been discussed. Meanwhile, the model of a molecular sponge with nanopores interprets the origin of the structural barrier decreasing the rate of the $P^{\bullet} + O_2$ reaction. Owing to the effect of electromagnetic dispersion forces, which are directed at separating a foreign molecule (*e.g.*, oxygen) from the nanopore wall and transferring it to the bulk of a narrow nanopore,[16, 28, 29, 80] the frequency of collisions of a captured particle with the walls and, hence, with the $P^{\bullet}$ radicals on the units of the nanopore walls decreases.

It should be emphasised that the absorption of oxygen by molten low-molecular-mass APP follows, strictly speaking, two parallel pathways rather than one pathway. The major role is played by the chain reaction

$$P^{\bullet} \xrightarrow{O_2,\, k_1} POO^{\bullet} \xrightarrow{PH,\, k_2} POOH + P^{\bullet},$$

in which the steps involving the $P^{\bullet}$ and $POO^{\bullet}$ radicals alternate. The kinetic features of this reaction at any level are described by Eqn (27) and those in the initial self-accelerated stage are described by Eqn (28). According to Eqn (28), in the beginning (when $[POOH] < \chi$), the rate of oxidation should not depend on the pressure of oxygen. This dependence can appear only after the concentration $[POOH] \approx k_1[O_2]/k_{-2}$ has been attained.

This pattern has actually been observed in the oxidation of low-molecular-mass APP at relatively low pressures of oxygen $P_{O_2} < 43$ kPa (Fig. 18, curves *1–3*).[75] It can be seen that the initial sections of curves *1–3* have a common tangent irrespective of P_{O_2}. However, the slope of the initial section of curve *4* in Fig. 18, corresponding to the pressure 97.3 kPa, does not coincide with the slope of the initial sections of curves *1–3*, indicating an increase in the contribution of a different channel of oxygen absorption.

This different reaction route (which is minor as regards the absorption of oxygen) is directly related to a polymer chain scission process, the activation energy of which (E_n = 106 kJ mol^{-1}) differs substantially from the value E_{Φ} = 86 kJ mol^{-1}, corresponding to the major route of oxygen absorption, and the rate of which is constant from the very beginning, although it is directly proportional to P_{O_2} (Fig. 18, straight lines *1′–4′*).

The unusual kinetics of the minor oxidation chains allow them to be identified as 'spot' oxidation inside fluctuationally excited nanopores involving f-peroxyl radicals captured in the pores. In fact, neither hydroperoxide nor those macroradicals, whose quasi-steady-state concentration depends on the POOH concentration varying with time, could participate directly in the reaction proceeding in these spots. This reaction can involve only those macroradicals the concentration of which does not depend on the content of POOH and remains strictly constant with time.

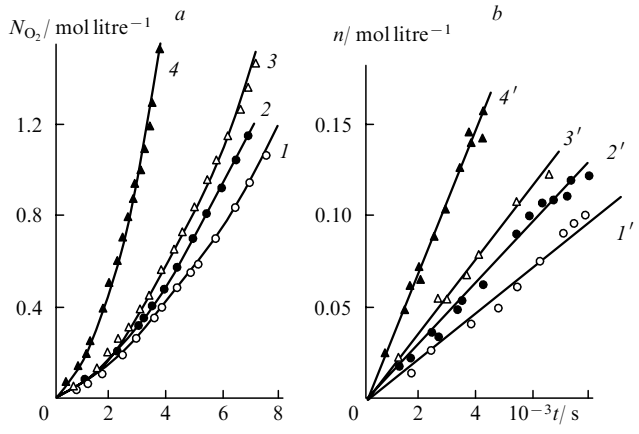
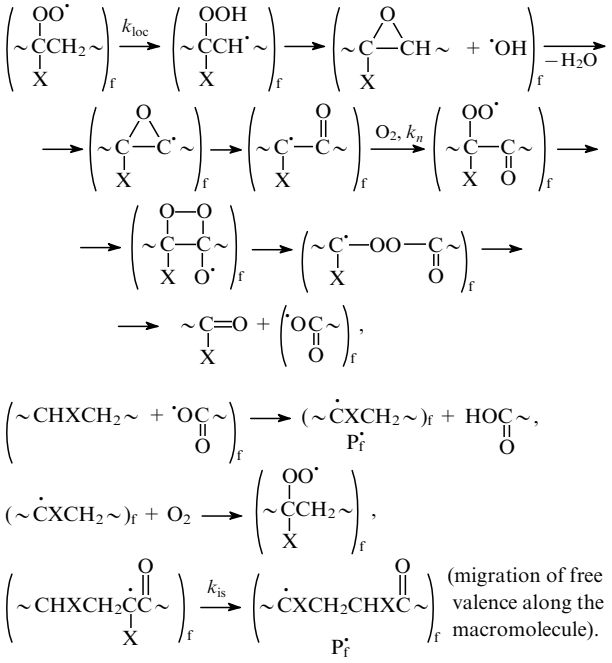


Figure 18. Variation of the amount of oxygen absorbed (*a*) and the number of breaks of macromolecules (*b*) during oxidation of molten APP (M_n = 2250) at 130 °C. Oxygen pressure/ kPa: (*1*, *1′*) 26.6, (*2*, *2′*) 33.3, (*3*, *3′*) 42.7, (*4*, *4′*) 97.3.

The set of participants of the spot process should include f-peroxyl radicals, which, in accordance with the scheme considered above, retain the concentration $[POO^{\bullet}_f] = k_{t,1}/k_{t,2}$, invariant with time, and radicals that are formed inside the f-nanopore upon β-isomerisation of peroxyl radicals and have time to react with oxygen during the f-nanopore lifetime, thus inducing rupture of bonds in macromolecules and regeneration of f-peroxyl radicals



Thus, long-lived f-nanopores actually become self-sustained centres of oxidation and ensure chain scission proceeding at a relatively low pressure of oxygen, P_{O_2} = 100 kPa, at a constant rate (from the beginning of oxidation) ($k_{is} > k_n[O_2]$)

$$\frac{dn}{dt} = k_n[O_2][\sim\dot{C}XC(O)\sim]_f = \frac{k_{loc}k_{t,1}k_n[O_2]}{k_{is}k_{t,2}} = \upsilon_{n,loc}P_{O_2},$$

$$n = \upsilon_{n,loc}P_{O_2}t\,.$$

The rate of oxygen absorption at these spots ($\upsilon_{loc} = k_{loc}k_{t,1}k_{t,2}^{-1}$) is low compared to that in linear chains, which is expressed by Eqn (27).

In experiments with high pressures of oxygen,[26] the spot pathway in the degradation of macromolecules cannot be identified because linear oxidation chains play the predominant role under these conditions. This significant difference between the results is apparently due to the substantial influence of the external mechanical pressure on the chemical transformations in the molecular sponge. The degree of compression of the molecular sponge influences the frequency and amplitude of the beats of nanopores (*i.e.* their size) and thus change to one or another extent the quasi-elementary rate constants. In particular, the decrease in the role of the spot process observed in a study by Iring *et al.*[26] may be due to the decrease in the constants $k_{t,1}$ and k_{loc}.

The view about the existence of chemical response to the mechanical pressure exerted on the polymer by the gas phase is supported by the fact that the coefficient Φ decreases from 0.06 min^{-1} at $P_{O_2} = 10^2$ kPa to 0.034 min^{-1} at $P_{O_2} = 10^3$ kPa.

An influence of the mechanical pressure of the oxidative gas medium on the polymer oxidation has been found previously in the oxidation of polypropylene films.[81] It was definitely shown that the rate of polymer oxidation in the induction period is subject to the

competition between the process acceleration due to the increase in the oxygen concentration and the process retardation due to the increase in the mechanical pressure of the gas phase.

Thus, the mechanical pressure of the gas atmosphere on the chain-segment sponge of the polymers being oxidised should be taken into account as necessarily as is the structural and mechanical previous history of samples and the internal stress relaxation.

IX. Cross-linking of polyolefin macromolecules

Oxidation of polyolefins is accompanied not only by chain scission according to one of the mechanisms considered above but also by the formation of chain cross-links. Cross-linking increases the molecular mass of the polymer and the number of points of branching on individual chains and creates a three-dimensional network, which, under certain conditions, can produce a gel fraction insoluble in liquids. Experimental data available from the literature make it possible to consider the oxidative cross-linking of polyolefins in terms of the micellar-sponge model of the polymeric matrix.

The redistribution of the molecular masses of molecules in an LDPE melt and solid-like IPP films during their oxidation at 130–160 °C has been studied.[5,82,83] Analysis of the molecular-mass distribution (MMD) by gel permeation chromatography showed that even absorption of a slight amount of oxygen changes the molecular masses of IPP and LDPE, the patterns of these changes being different for these two polymers.

During the oxidation of molten LDPE, rupture of macromolecules predominates in the induction period over a broad range of oxygen pressures; a slightly pronounced tendency for the enlargement of macromolecules is detected only for very low pressures ($P_{O_2} \leqslant 2.6$ kPa).[82]

However, in the case of IPP at $P_{O_2} = 10.6, 80.0$ and 101.3 kPa, scission and cross-linking of molecules proceed in the induction period at comparable rates. This gives a bimodal MMD (having two peaks, one at higher and one at lower molecular masses); the yield of the higher-molecular-mass fraction increases as the pressure of oxygen diminishes. As oxidation advances, the high-molecular-mass fraction of IPP becomes involved in the degradation process and an unimodal distribution is established, the MMD maximum being shifted towards lower molecular masses.[5,82,83] In this case, the enlargement of molecules is transient.

No clear view on the mechanism of transient cross-linking can be found in the literature. It has been suggested [5,83] that it is due to the termolecular reaction

$$PH + O_2 + PH \longrightarrow P^{\cdot} + H_2O_2 + P^{\cdot} \longrightarrow P-P,$$

yielding two macroradicals, which recombine in a 'cage'. In the opinion of the researchers cited,[5,83] this assumption is supported by the fact that the yield of cross-linked macromolecules increases upon orientational drawing, which prevents radicals from leaving the cage.

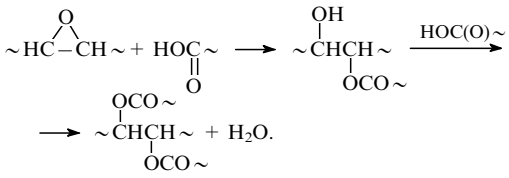
For instance, when isotropic and oriented IPP samples absorb equal amounts of oxygen (0.14 mol kg^{-1}, 130 °C, $P_{O_2} = 78$ kPa), the average molecular mass of isotropic IPP decreases from 3.0×10^5 to 0.6×10^5, while the molecular mass of IPP films stretched 10-fold, conversely, increases from 3.0×10^5 to 6.3×10^5. However, during further oxidation of the stretched films degradation becomes the predominant process. It will be shown below that the transient cross-linking of IPP molecules occurs in s-zones and involves the alkyl macroradicals and the C=C bonds formed in these zones. This is facilitated by the deficiency of free oxygen molecules, typical of s-zones.

The transient cross-linking of molten polyethylene in the beginning of oxidation barely influences the molecular mass of the polymer; however, the formation of the macromolecular network is manifested in full measure in the macroscopic kinetic stage that comes after fairly extensive destruction.[84,85] The process of destruction preceding the formation of the molecular network involves a 200- to 600-μm thick layer of the melt, depending on the temperature (230–150 °C, respectively). This results in a substantial (5–15-fold) decrease in the molecular mass of the polymer; as a consequence, the oxidised polymer becomes waxy.[85] The cross-linking of molecules during further oxidation of the destroyed material proceeds in an autocatalytic mode and yields a 30–160-μm cross-linked shell.

It has been emphasised [85] that cross-linking of the oxidised material starts simultaneously throughout the whole relatively thick near-surface layer (80 μm at 150 °C), although the sources of free radicals, POOH groups, are distributed in this layer non-uniformly, their concentration decreasing on moving away from the surface. The amount of the gel fraction in the oxidised polyethylene increases over some period of time. During this period, a densely cross-linked crust is formed. The process continues until almost all macromolecules are incorporated in the molecular network structure. The density of the gel fraction at the end of the process reaches 1 g cm^{-1}.

No clear views on the mechanism of this process can be found in the literature. A rather obvious reaction is condensation of carboxylic acids with secondary alcohols.[86] However, the mechanisms of formation of the acids and the alcohols are not discussed.

Meanwhile, the fact that cross-linking starts only after accumulation of a particular amount of the oxidised fragments of polyethylene molecules suggests that this process can be associated with the condensation of carboxylic acids with epoxides, formed as intermediate oxidation products (see Section IV), the concentration of which does not depend on the content of POOH:



In accordance with the heterophase structure of the polymeric molecular-sponge microreactors (see Fig. 7), the condensation cross-linking should occur in the v-zones of the micelles, which accumulate the main bulk of oxygen-containing oxidation products, as opposed to the transient cross-linking, which occurs in s-zones.

The condensation, considered in terms of the heterophase model, becomes possible only at a substantial degree of oxidative degradation (after a required amount of acid residues has been accumulated). The condensation can account for the self-accelerated character of cross-linking, which is due to the permanent increase in the acid concentration and for the fact that this process virtually does not depend on the distribution of POOH over the layer depth. This is confirmed by the appearance of ester groups at high degrees of oxidation of molten polyethylene and by their subsequent self-accelerated accumulation (which was demonstrated by NMR [49] and IR spectroscopy [84]). The complete solubility of the gel fraction in strong alkalis and acids proves that the cross-links in the molecular network are actually formed by ester groups.[84]

Let us consider once again the transient cross-linking, which manifests itself most clearly for IPP films stretched 10-fold. It should be noted that the number of cross-links observed in practice under conditions most favourable for the termolecular reaction is 1000 times greater than the value calculated theoretically.[8] Therefore, Denisov [8] proposed that the addition of alkyl and peroxyl macroradicals to the C=C bonds, always present in polyolefins in small amounts, should also be included in the consideration.

However, this assumption does not agree with the kinetics of cross-linking of polymer chains in oriented IPP films. Indeed, in the oxidation of 10-fold stretched films, the cross-linking starts only 75 min after the reaction has begun but before the induction period has been over ($\tau = 100$ min at 130 °C and $P_{O_2} = 78$ kPa). During these 75 min, the mean mass of molecules remains

constant.[5,83] Thus, cross-linking involves only unsaturated C=C bonds, which accumulate during oxidation.

The transient cross-linking of the IPP molecules might occur by a chain mechanism,[87] which has been established previously for the cross-linking of polyethylene molecules initiated by dibenzoyl peroxide. According to this mechanism, cross-links are formed due to the addition of macromolecule fragments having terminal C=C bonds ($R^{=}$) to internal macroradicals ($P^{\bullet}_{s}$):

$$P^{\bullet}_{s} + R^{=} \longrightarrow PR^{\bullet}_{s},$$

$$PR^{\bullet}_{s} + PH_{s} \longrightarrow PRH + P^{\bullet}_{s}.$$

By adding these reactions to the overall scheme of the process occurring in the s-zones of the matrix in the induction period (see Section IV.1) and by using the steady-state concentration conditions for free radicals, one can easily see that these reactions do not change the form of the equation describing the concentration of the $R^{\bullet}_{s}$ radicals, responsible for the s,v-translation of free valence

$$[R^{\bullet}_{s}] = \frac{\delta k'_{0s}[PH_s][O_{2,s}]}{2k_{1s}}.$$

The rate of initiation of the oxidation chains in the v-zones of matrix micelles does not change either.

The validity of the above scheme for the transient chain cross-linking of the IPP molecules is supported by the fact that the rate of this process increases upon orientational drawing of films. Drawing is known to be accompanied by fibrillation of polymer chains, which are reorganised to give bundles (about tens of angstroms in diameter) and acquire enhanced highly elastic tension.[5,88] Despite dense packing, the fibrillar units are separated from one another by clear-cut interfaces, which can be clearly seen in the micrographs taken by an electron microscope.

Judging by the structure of spongy micelles (Fig. 7), one can expect that uniaxial drawing of a polymer film would result in the transformation of spherical grains into ellipsoids filled with fibrils of stretched chains. The mobility of chain units inside the fibrils would decrease and the nanopores in them would become even narrower. However, the interfaces between the fibrils would actually represent newly formed zones of s-nanopores. The increase in the number and the volume of zones filled with s-nanopores should naturally increase the contribution of reactions which occur in these zones including chain cross-linking.

It has been noted that cross-linking lags somewhat behind the rupture of IPP macromolecules. This is due to the fact that the structure-mechanical stabilisation of fibrils in the supermolecular framework depresses for some period the mobility of the fragments of macromolecules with terminal C=C bonds. A definite number of polymer chain scissions is required in order to weaken the rigid mechanical fixing of fragments in the framework structure. During this period, some C=C bonds are accumulated in the interfibrillar layers, and, as the chemically induced relaxation of internal stress goes on, rapid formation of the cross-linked network starts by the radical chain mechanism described above

X. Oxidation of fibrillised polyolefins

The change in the structure of the spongy micellar matrix induced by fibrillation influences the dynamic characteristics of a paramagnetic probe — stable free radical, 2,2,6,6-tetramethylpiperidin-1-oxyl — introduced in a polymer. The behaviour of the nitroxide depends on when it is introduced into the sample.[5,89] If the radical probe is introduced initially and then the sample is drawn, the probe is fixed in a low-mobility state with appreciably hindered rotational and translational motion. However, if the radical probe is introduced into the films after drawing, it populates the accessible areas of the matrix and displays high frequency of rotation and high rate of migration through the matrix.

Owing to the spongy micellar structure of the matrix, the radical probe added before the film drawing is absorbed during drawing in fairly narrow nanopores of the fibrils being formed and is not displaced into the interfibrillar layers. Conversely, the radical probe added after fibrillation is unable to penetrate inside the fibrils and mainly occupies s-nanopores in the interfibrillar layers.

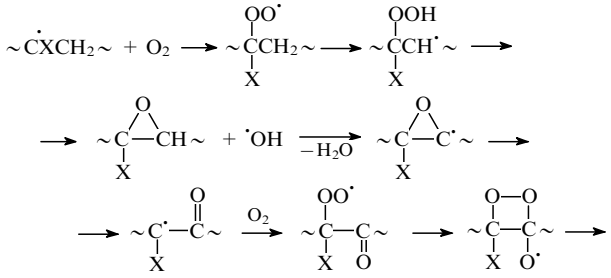
It is obvious that the structural rearrangement induced by drawing should necessarily change the kinetics of oxidation. Indeed, the fairly strong fixing of fibrils due to restructurisation of the crystallite framework can substantially extend the induction period of oxidation by decreasing the frequency of the steps of s,v-transfer of free valence and migration of hydroperoxide groups from the inner space of fibrils to interfibrillar s-nanopores. This situation is observed in the oxidation of highly crystalline IPP, HDPE and polymethylpentene.[5,35,76]

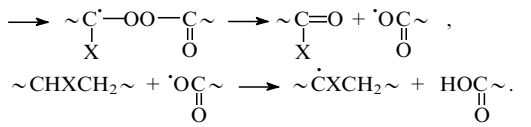
It is typical that the induction period disappears if IPP films have been subjected to non-extensive oxidation (up to the accumulation of ~ 0.02 mol kg^{-1} of POOH) prior to drawing.[5] This fact contradicts the assumption, made in the same study,[5] that drawing enhances the cage effect (*i.e.* decreases the yield of radicals in the dissociation of POOH) but it is in line with the 'bottle-neck' effect in both the forward and backward phase transfer chemical induction processes.

In fact, orientational drawing of non-oxidised films increases the induction period for the structural and mechanical reasons indicated above, whereas drawing of pre-oxidised films, without changing the content of POOH in the previously oxidised s-zones, increases the number of new interfibrillar s-zones, to which hydroperoxide is displaced from the inner bulk of fibrils during their formation. With this type of sample processing, oxidation is effected from the very beginning by vigorous scission of macromolecules and by chemically induced relaxation of internal stresses; this accounts for the absence of a noticeable induction period.

Study of IPP and HDPE films by local IR spectroscopy (by scanning samples by a beam with a 1-mm^2 cross-section) showed that oxidation of oriented films with mechanically fixed ends occurs non-uniformly over the area of the sample and has different rates in different local zones. The ratio of the carbonyl products of oxidation changes.[5] Note that in conventional IR spectra of oxidised fibrillised samples, the intensities of the absorption bands at about 1740–1745 and 1770–1780 cm^{-1}, which correspond to ester and lactone groups,[86,90] are greater[35] than the intensities of the absorption bands at 1710–1720 cm^{-1}, due to acids and ketones.

Qualitatively, the process can be represented as follows. The primary reaction chains are originated in the interfibrillar s-zones. They include the steps of scission and cross-linking of s-units, which ensure restructurisation of interfibrillar layers and thus increase the elastic load on the fibrils. These processes result in the appearance of free valences, translated with a low frequency to the narrow internal nanopores of the fibrils. Due to the narrowness of the pores and the high-elasticity tension of the polymer molecules in the fibrils, the peroxyl radicals formed under these conditions undergo mainly β-isomerisation to give epoxide rings and free hydroxyls. The hydroxyl and the epoxide, which are unable to separate widely in a narrow nanopore, react with each other; this gives rise to the non-hydroperoxide oxidation pathway leading to ketones (aldehydes) and acids





Rupture of an individual polymer molecule in the structure of an elastically stretched fibril affords fragments which relax independently to the most equilibrium conformation by transferring the mechanical load to the surrounding molecules and enhancing their tension. Thus, narrow nanopores having an increased length appear inside the fibrils; they serve simultaneously as the sites of accumulation of the oxygen molecules expelled from the neighbouring layers of the intrafibril sponge.

The subsequent reactions inside the newly arisen relaxation site of oxidation include the transfer of free valence over its surface in accordance with the above scheme. Under these conditions, carboxy and epoxy groups are formed in the vicinity of each other; they react to give ester groups. Thus, orientational drawing of IPP and HDPE creates conditions for the formation of esters in the relaxation intrafibril sites even at early oxidation stages, whereas in the case of isotropic polyethylene melts, esters are formed only after fairly extensive oxidative destruction has taken place (see Section IX).

An important feature of oxidation in the relaxation sites inside the fibrils is that the removal of fragments of macromolecules from these sites facilitates the arrival of free radicals at the intact polymer chains, which remain in the stretched state. As a consequence, the process propagates predominantly across the fibril, and the intermediate polymeric peroxyls participating in the process are rigidly fixed at the elastically stretched macromolecules; thus, they are mainly converted without the formation of POOH.

The continuous accumulation of structural damages inside the fibril and enhancement of the load on the remaining oriented chains should result sooner or later in the rupture of the fibril and in the abrupt relief of the elastic strain. The sharp increase in the beating mobility of a nanopore in the fibril fragments substantially increases the probability of intermolecular propagation of oxidation chains accompanied by the formation and simultaneous dissociation of POOH. In other words, upon the relief of mechanical stress, oxidation sharply accelerates becoming a local chemical outburst and efficiently influences the surrounding matrix both by transferring mechanical load and injecting chemically reactive species therein.

During further oxidation, fragmentation involves initially the separate macroscopic areas and then the whole oriented sample, whose ends are mechanically fixed. As a consequence, a backbone crack grows through the sample cross-section, which fractures the sample, and oxidation passes to the self-accelerated stage.[5]

The kinetic, structural and mechanical features of oxidation listed above have been observed in experiments with polyolefin films subjected to uniaxial orientational drawing. Commercial polymeric articles produced by extrusion, moulding and hose blowing have micellar structures. The structural lability of molecular spongy micelles and the ability of the crystalline framework to be reorganised account for the appearance of uncontrolled internal stresses and local deformations accompanied by fibrillation, taking place in these articles to one or another extent.

The structural and mechanical inhomogeneities introduced into the articles at the stage of processing of polymer ingredients are the reason for the change of the physical properties of articles during performance and storage.[91] Even minor external mechanical action (during cooling of the melt) induces the layer structural inhomogeneity of the material, caused by the relaxation mechanism of heat removal and non-uniform temperature distribution over the material thickness.[92]

This should lead to non-reproducibility of the quantitative results of kinetic studies, which is typical of these materials. This is illustrated by numerous experimental data (see Ref. 93 and references therein), which show that the durations of the induction periods and the amounts of accumulated products in the oxidation of IPP and LDPE vary over wide limits, depending on the previous history and thickness of samples manufactured by industrial technologies.

The diversity of factors which influence in one or another way the internal structure of polymeric articles makes very difficult the task of constructing a unified kinetic model of oxidation, which would provide a quantitative description for both laboratory specimens and commercial materials. However, we hope that the oxidation models proposed here would lay a more reliable foundation for the analysis of particular processes of ageing and stabilisation of polymers than liquid-phase models, which are not quite applicable to polymers.

XI. Conclusion

The purpose of this review is to demonstrate the principles of structure-kinetic modelling of chain oxidation reactions occurring in a non-crystalline polymeric matrix. A molecular spongy micelle, an important element in the framework structure of a noncrystalline polymer, was chosen as the morphological basis for modelling.

The kinetic model developed with allowance for the nanoscale micellar heterophase structure has already explained a series of specific features of free radical chain transformations which cannot be explained in terms of homogeneous reaction models.[15, 16, 18–22, 38, 94] This model was used to interpret the mechanisms of separate stages of the oxidation of polymers described by kinetic laws different in kind. These stages either replace one another during the process or are changed themselves due to the change in the thermomechanical state of the polymeric object.

The structure-mechanical reasons for the curious features of initiated oxidation, which do not fit in the homogeneous reaction models, were identified. The morphological and structure-kinetic models used here impart definite meaning to the concept of structure-mechanical modification of the chemical reactivity of species reacting in a molecular spongy matrix, which is considered as a process directly related to the molecular-segment lability and flickering mobility of nanopores.

It should be emphasised that the heterophase models considered here not only disclose the physical essence of each oxidation stage but also identify the relationship between the chemistry of transformations and the most important structural properties of the molecular spongy matrix, thus extending the morphological basis of the chemical physics of polymers.

References

1. V S Pudov, B A Gromov, E G Sklyarova, M B Neiman *Neftekhimiya* **3** 743 (1963)
2. V S Pudov, M B Neiman, in *Starenie i Stabilizatsiya Polimerov* (Ageing and Stabilisation of Polymers) (Ed. A S Kuz'minskii) (Moscow: Khimiya, 1966) p. 5
3. L Reich, S S Stivala *Autoxidation of Hydrocarbons and Polyolefins. Kinetics and Mechanisms* (New York: Marcel Dekker, 1969)
4. Yu A Shlyapnikov, S G Kiryushkin, A P Mar'in *Antiokislitel'naya Stabilizatsiya Polimerov* (Antioxidant Stabilisation of Polymers) (Moscow: Khimiya, 1986)
5. A A Popov, N Ya Rapoport, G E Zaikov *Okislenie Orientirovannykh i Napryazhennykh Polimerov* (Oxidation of Oriented and Stressed Polymers) (Moscow: Khimiya, 1987)
6. N M Emanuel', A L Buchachenko *Khimicheskaya Fizika Molekulyarnogo Razrusheniya i Stabilizatsii Polimerov* (Chemical Physics of Molecular Destruction and Stabilisation of Polymers) (Moscow: Nauka, 1988)
7. V A Roginskii *Fenol'nye Antioksidanty. Reaktsionnaya Ssposobnost' i Effektivnost'* (Phenol Antioxidants. Reactivity and Efficiency) (Moscow: Nauka, 1988)
8. E T Denisov *Okislenie i Destruktsiya Karbotsepnykh Polimerov* (Oxidation and Destruction of Carbon-Chain Polymers) (Leningrad: Khimiya, 1990)

9. J Vago, Z Fodor, T T Nagy, M Iring, T Kelen, F Tüdös *Polym. Bull.* **10** 559 (1983)
10. T Kelen, M Iring, F Tüdös *Eur. Polym. J.* **12** 35 (1976)
11. M Iring, T Kelen, F Tüdös *Makromol. Chem.* **175** 467 (1974)
12. E T Denisov *Usp. Khim.* **47** 1090 (1978) [*Russ. Chem. Rev.* **47** 572 (1978)]
13. N M Emanuel', A L Buchachenko *Khimicheskaya Fizika Stareniya i Stabilizatsii Polimerov* (Chemical Physics of Ageing and Stabilisation of Polymers) (Moscow: Nauka, 1982)
14. F Gugumus *Polym. Degrad. Stab.* **63** 525 (1999)
15. Yu A Mikheev, L N Guseva, G E Zaikov *Vysokomol. Soedin., Ser. B* **39** 1082 (1997) [a]
16. Yu A Mikheev, L N Guseva, G E Zaikov *Usp. Khim.* **66** 3 (1997) [*Russ. Chem. Rev.* **66** 1 (1997)]
17. Yu A Shlyapnikov *Khim. Fiz.* **14** (10) 48 (1995) [b]
18. Yu A Mikheev, L N Guseva *Khim. Fiz.* **6** 1259 (1987) [b]
19. Yu A Mikheev, L N Guseva, D Ya Toptygin *Vysokomol. Soedin., Ser. A* **31** 2544 **(**1989) [a]
20. Yu A Mikheev, L N Guseva *Khim. Fiz.* **11** 964 (1992) [b]
21. Yu A Mikheev, L N Guseva *Khim. Fiz.* **12** 1081 (1993) [b]
22. Yu A Mikheev *Khim. Fiz.* **18** (8) 40 (1999) [b]
23. T A Bogaevskaya, B A Gromov, V B Miller, T V Monakhova, Yu A Shlyapnikov *Vysokomol. Soedin., Ser. A* **14** 1552 **(**1972) [a]
24. T V Monakhova, T A Bogaevskaya, B A Gromov, Yu A Shlyapnikov *Vysokomol. Soedin., Ser. B* **16** 91 **(**1974) [a]
25. T A Bogaevskaya, T V Monakhova, Yu A Shlyapnikov *Vysokomol. Soedin., Ser. B* **20** 465 (1978) [a]
26. M Iring, Z Laszlo-Hedvig, F Tüdös, T Kelen *Polym. Degrad. Stab.* **5** 467 (1983)
27. N M Emanuel' *Vysokomol. Soedin., Ser. A* **27** 1347 **(**1985) [a]
28. Yu A Mikheev, L N Guseva, G E Zaikov *Vysokomol. Soedin., Ser. A* **41** 346 (1999) [a]
29. Yu A Mikheev, G E Zaikov *Vysokomol. Soedin., Ser. A* **41** 852 (1999) [a]
30. V S Pudov, Candidate Thesis in Chemical Sciences, Institute of Chemical Physics, Academy of Sciences, USSR, Moscow, 1963
31. T V Monakhova, Candidate Thesis in Chemical Sciences, Institute of Chemical Physics, Academy of Sciences, USSR, Moscow, 1976
32. G P Andrianova *Fizikokhimiya Poliolefinov* (Physical Chemistry of Polyolefins) (Moscow: Khimiya, 1974)
33. Yu A Mikheev, L N Guseva, L E Mikheeva, S V Kalantsova *Khim. Fiz.* **12** 528 (1993) [b]
34. Yu A Mikheev, L N Guseva *Khim. Fiz.* **15** (9) 131 (1996) [b]
35. L S Shibryaeva, S G Kiryushkin, G E Zaikov *Int. J. Polym. Mater.* **16** 71 (1992)
36. V B Aleskovskii, V G Korsakov *Fizikokhimicheskie Osnovy Ratsional'nogo Vybora Aktivnykh Materialov* (Physicochemical Foundations of Rational Choice of Active Materials) (Leningrad: Leningrad State University, 1980)
37. M Iring, T Kelen, Z Fodor, F Tüdös *Polym. Bull.* **7** 489 (1982)
38. Yu A Mikheev, G E Zaikov *Khim. Fiz.* **16** (11) 62 (1997) [b]
39. Yu A Mikheev, L N Guseva, G E Zaikov *J. Appl. Polym. Sci.* **67** 1693 (1998)
40. J Loftus, C N Satterfield *J. Phys. Chem.* **69** 909 (1965)
41. K Barabas, M Iring, S Laszlo-Hedvig, T Kelen, F Tüdös *Eur. Polym. J.* **14** 405(1978)
42. M Iring, S Laszlo-Hedvig, K Barabas, T Kelen, F Tüdös *Eur. Polym. J.* **14** 439 (1978)
43. K Barabas, M Iring, T Kelen, F Tüdös *J. Polym. Sci., Symp.* 65 (1976)
44. V M Yur'ev, A N Pravednikov, S S Medvedev *J. Polym. Sci.* **55** 353 (1961)
45. V L Antonovskii, E T Denisov, L V Solntseva *Kinet. Katal.* **7** 409 (1966) [c]
46. H C Beachell, D L Beck *J. Polym. Sci.* **3A** 457 (1965)
47. D L Faulkner *Polym. Eng. Sci.* **22** 466 (1982)
48. D Ryshavy, L Balaban, V Slavik, Ya Ruzha *Vysokomol. Soedin.* **3** 1110 (1961) [a]
49. H N Cheng, F C Schilling, F A Bovey *Macromolecules* **9** 363 (1976)
50. Z Manyasek, D Berek, M Michko, M Lazar, Yu Pavlinets *Vysokomol. Soedin.* **3** 1104 (1961) [a]
51. I G Latyshkaeva, T A Bogaevskaya, G P Belov, Yu A Shlyapnikov *Vysokomol. Soedin., Ser. B* **19** 531 (1977) [a]
52. V P D'yakonov *Spravochnik po Raschetam na Mikrokal'kulyatorakh* (Handbook for Calculations on Microcalculators) (Moscow: Nauka, 1986)
53. E M Antipov, Yu K Ovchinnikov, A V Rebrov, G P Belov, G S Markova, N F Bakeev *Vysokomol. Soedin., Ser. A* **20** 1727 (1978) [a]
54. M Iring, T Kelen, F Tüdös *Eur. Polym. J.* **11** 631 (1975)
55. M Iring, T Kelen, F Tüdös *Polym. Bull.* **15** 531(1986)
56. A V Tobolsky, P M Norling, N H Frick, H Yu *J. Am. Chem. Soc.* **86** 3925 (1964)
57. V M Gol'dberg, V N Esenin, I A Krasotkina *Vysokomol. Soedin., Ser. A* **19** 1720 (1977) [a]
58. L Dulog, K-H David *Makromol. Chem.* **145** 67 (1971)
59. I C McNeill *J. Chem. Biochem. Kinet.* **4** 129 (1998)
60. A B Mazaletskii, V G Vinogradova *Khim. Fiz.* **14** (10) 86 (1995) [b]
61. Ph Grosborne, J Seree de Roch, L Sajus *Bull. Soc. Chim. Fr.* 2020 (1968)
62. L Dulog, G Storck *Makromol. Chem.* **91** 50 (1966)
63. J Glastrup *Polym. Degrad. Stab.* **52** 217 (1996)
64. Z G Pikh, I I Yatchishin, D K Tolopko, in *Tez. Dokl. VII Vsesoyuz. Konf. po Khimii Organicheskikh Peroksidov* (Abstracts of Reports of the VIIth All-Union Conference on the Chemistry of Organic Peroxides) (Volgograd: Volgograd Polytechnic Institute, 1980) p. 111
65. Yu A Mikheev, L N Guseva, D Ya Toptygin *Kinet. Katal.* **28** 287 (1987) [c]
66. E T Denisov *Vysokomol. Soedin., Ser. A* **19** 2513 (1977) [a]
67. K Ingold *Chem. Rev.* **61** 563 (1961)
68. R V Kucher, P F Ivanenko, I P Shevchuk *Neftekhimiya* **10** 731 (1970)
69. E L Shanina, V A Roginskii, V B Miller *Vysokomol. Soedin., Ser. B* **20** 145 (1978) [a]
70. V V Lipes *Kinet. Katal.* **27** 1046 (1986) [c]
71. V V Lipes, V I Morozova *Khim. Fiz.* **5** 372 (1986) [b]
72. Zh D Chaplanova, Yu I Gudimenko, V E Agabekov *Vysokomol. Soedin., Ser. B* **29** 35 (1987) [a]
73. Zh D Chaplanova, Yu I Gudimenko, V E Agabekov *Vysokomol. Soedin., Ser. B* **29** 939 (1987) [a]
74. V E Agabekov, Zh D Chaplanova, Yu I Gudimenko *Int. J. Polym. Mater.* **13** 195 (1990)
75. A A Ivanov, A P Firsov, V D Grigoryan, A A Berlin *Vysokomol. Soedin., Ser. A* **11** 1390 (1969) [a]
76. N Ya Rapoport, L S Shibryaeva, V B Miller *Vysokomol. Soedin., Ser. A* **25** 831 (1983) [a]
77. N M Emanuel', E T Denisov, Z K Maizus *Tsepnye Reaktsii Okisleniya Uglevodorodov v Zhidkoi Faze* (Chain Reactions of Oxidation of Hydrocarbons in Liquid Phase) (Moscow: Nauka, 1965)
78. R N Abadzheva, R V Kucher *Neftekhimiya* **5** 528 (1965)
79. A E Shilov, in *Khimicheskaya Kinetika i Tsepnye Reaktsii. K Semidesyatiletiyu Akademika N N Semenova* (Chemical Kinetics and Chain Reactions. For the 70th Anniversary of Academician N N Semenov) (Ed. V N Kondrat'ev) (Moscow: Nauka, 1966) p. 229
80. Yu A Mikheev, L N Guseva *Khim. Fiz.* **10** 724 (1991) [b]
81. V V Dudorov *Kinet. Katal.* **4** 214 (1963) [c]
82. M Iring, S Laszlo-Hedvig, T Kelen, F Tüdös, L Füzes, G Samay, G Bodor *J. Polym. Sci., Symp.* 55 (1976)
83. N Ya Rapoport, L S Shibryaeva, G E Zaikov, M Iring, F Tyudesh, Z Fodor *Vysokomol. Soedin., Ser. A* **28** 842 (1986) [a]
84. A Holmström, E M Sörvik *J. Polym. Sci., Polym. Chem. Ed.* **16** 2555 (1978)
85. R A Bal'tenas, Ya Yu Bal'tenene, Z K Kevyalaitis *Vysokomol. Soedin., Ser. A* **23** 1466 (1981) [a]
86. F Gugumus *Polym. Degrad. Stab.* **65** 5 (1999)
87. Yu A Mikheev *Khim. Fiz.* **10** 715 (1991) [b]
88. A L Volynskii, G M Lukovkin, N F Bakeev *Vysokomol. Soedin., Ser. A* **19** 785 (1977) [a]
89. I I Barashkova, A M Vasserman, N Ya Rapoport *Vysokomol. Soedin., Ser. A* **21** 1683 (1979) [a]
90. A Valadez-Gonzalez, J M Cervantes-Uc, L Veleva *Polym. Degrad. Stab.* **63** 253 (1999)
91. A O Baranov, E V Prut, N S Enikolopyan *Vysokomol. Soedin., Ser. B* **28** 94 (1986) [a]
92. A M Ar'ev *Plast. Massy* 52 (1992)
93. F Gugumus *Polym. Degrad. Stab.* **62** 245 (1998)
94. Yu A Mikheev *Int. J. Polym. Mater.* **16** 237 (1992)

[a] — *Polym. Sci. (Engl. Transl.)*
[b] — *Russ. J. Chem. Phys. (Engl. Transl.)*
[c] — *Kinet. Catal. (Engl. Transl.)*